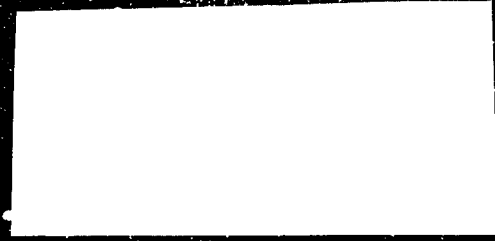
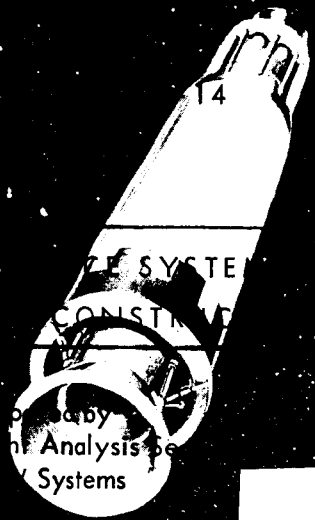


MSC-G-R-66-7
Supplemental Report 4



FF No. 602(D)

(THRU) 20
(CODE) 20
(CATEGORY) 20

(PAGES) 115
(NASA CR OR TMX OR AD NUMBER) CR 89428



Issued as: Supplemental Report 4
 To: Gemini Program Mission Report
 Gemini X
 MSC-G-R-66-7
 By: Gemini X Mission Evaluation Team
 National Aeronautics and Space
 Administration
 Manned Spacecraft Center
 Houston, Texas

MISSION PLANNING
 NATIONAL AERONAUTICS AND SPACE ADMINISTRATION
 MANNED SPACECRAFT CENTER

(NASA-CR-89428) GEMINI 10 INERTIAL GUIDANCE SYSTEM EVALUATION AND TRAJECTORY RECONSTRUCTION (TRW Systems, Redondo Beach, Calif.) 115 p N79-76296
 Unclas
 00/18 11032

TRW NOTE NO. 66 FMT-270

MSC-G-R-66-7

Supplemental Report 4

PROJECT GEMINI
TASK MSC/TRW G-14

C67-8752

GEMINI 10 INERTIAL GUIDANCE SYSTEM EVALUATION
AND TRAJECTORY RECONSTRUCTION (U)

Issued as:
Supplemental Report 4

3 JANUARY 1967

By:
Gemini X Mission Evaluation Team
National Aeronautics and Space
Administration
Manned Spacecraft Center
Houston, Texas

To:
Gemini Program Mission Report
Gemini X
MSC-G-R-66-7

Prepared for
MISSION PLANNING AND ANALYSIS DIVISION
NATIONAL AERONAUTICS AND SPACE ADMINISTRATION
MANNED SPACECRAFT CENTER
HOUSTON, TEXAS
NAS 9-4810

Approved by John R. Henson
J. R. Henson
Systems Analysis Branch
Guidance and Control Division
NASA/MSC

Approved by Robert J. Boyles
R. J. Boyles, Task Manager
TRW Systems

Approved by J. C. Harpold
J. C. Harpold
Mission Analysis Branch
Mission Planning Analysis Division
NASA/MSC

Approved by J. W. McCarthy
J. W. McCarthy, Manager
Systems Engineering Department
TRW Systems

Approved by R. R. Carley
R. R. Carley
Gemini Program Office
NASA/MSC

Approved by C. W. Pittman
C. W. Pittman, Acting Manager
Systems Analysis
Mission Trajectory Control Program
TRW Systems

TRW SYSTEMS
AN OPERATING GROUP OF TRW INC.

LIST OF CONTRIBUTORS

R. J. Boyles
R. G. Fierro
P. M. Jackson
P. D. Levine
A. M. Notkoff

ABSTRACT

This report contains a detailed evaluation of the Gemini 10 inertial guidance system accuracy during the ascent and reentry phases of the mission. An analysis of the external tracking instrumentation accuracy during ascent is also included. The results of the error analyses are used to construct a reference Gemini 10 trajectory for the ascent and reentry portions of the mission.

The reconstructed relative trajectory between the Gemini and Agena 10 vehicles is compared to the Gemini 10 onboard radar measurements and the residuals evaluated. The measurements of the altitudes of various stars by the astronaut, using a hand-held sextant, are compared to calculated values.

This TRW supplemental report, the IBM supplemental report, and the NASA/MSC Gemini 10 Mission final report represent the complete approved inertial guidance system analysis accomplished on this mission.

(Reverse of this page intentionally left blank.)

CONTENTS

	Page
1. INTRODUCTION AND SUMMARY	1-1
2. INERTIAL GUIDANCE SYSTEM PERFORMANCE ANALYSIS AND ASCENT TRAJECTORY RE-CONSTRUCTION	2-1
2.1 Inertial Guidance System Error	2-2
2.1.1 Free-Flight Fix	2-3
2.1.2 Insertion Conditions	2-5
2.2 Inertial Measurement Unit Error Analysis	2-5
2.2.1 Preflight Compensation	2-5
2.2.2 Residual IMU Error After Compensation	2-11
2.2.3 Error Coefficient Recovery	2-12
2.3 IGS Azimuth Update	2-16
2.4 Conclusions	2-17
2.5 Ascent Trajectory Reconstruction	2-18
3. REENTRY IGS PERFORMANCE EVALUATION AND TRAJECTORY RECONSTRUCTION	3-1
3.1 Introduction and Summary	3-1
3.2 Reentry Error Sources	3-1
3.2.1 Initial Conditions	3-4
3.2.2 Alignment Errors	3-6
3.2.3 IGS Error Sources	3-6
3.2.4 Unaccounted Error	3-7
3.3 Reentry Simulation	3-8
3.4 Conclusions	3-9
3.5 Reentry Trajectory Reconstruction	3-9
4. TRACKING SYSTEM PERFORMANCE	4-1
4.1 GE MOD III	4-1
4.1.1 GE MOD III Burroughs (TRW Reduction)	4-1
4.1.2 GE MOD III Burroughs (GE Processed)	4-3
4.2 MISTRAM	4-3
4.3 AFETR Best Estimate of Trajectory	4-4
4.4 Conclusions	4-4

CONTENTS (Concluded)

	Page
5. RENDEZVOUS RADAR EVALUATION	5-1
5.1 Introduction	5-1
5.2 Telemetry Data	5-1
5.3 Trajectory Reconstruction	5-2
5.3.1 Agena 10 Trajectory	5-2
5.3.2 Gemini 10 Trajectory Recon- struction	5-2
5.4 Analysis of Rendezvous Radar Output	5-2
5.5 Conclusions	5-5
6. ANALYSIS OF SEXTANT SIGHTINGS ON GEMINI 10. . .	6-1
6.1 Introduction	6-1
6.2 Horizon Bias	6-1
6.3 Sextant Measurements	6-1
6.4 Onboard Computations	6-3
APPENDICES	
A ASCENT TRAJECTORY	A-1
B REENTRY TRAJECTORY	B-1
C TRACKER CALIBRATION DATA	C-1
REFERENCES	R-1
Total Pages:	
115	

ILLUSTRATIONS

	Page
2-1 Sensed Velocity Comparison in Computer Coordinates.	2-19
2-2 Total Inertial Position Comparison in Computer Coordinates.	2-20
2-3 Total Inertial Velocity Comparison in Computer Coordinates.	2-21
2-4 Navigation Position Error	2-22
2-5 Navigation Velocity Error	2-23
2-6 Gyro Constant Drift Rate History	2-24
2-7 Gyro Spin Axis Unbalance Drift History	2-24
2-8 Gyro Input Axis Unbalance Drift History.	2-24
2-9 Sensed Velocity Comparison in Computer Coordinates with IGS Error Fit.	2-25
2-10 IGS/MOD III Comparisons (RAE)	2-26
2-11 IGS/MOD III Comparisons (Range Rate, \dot{R} , \dot{P} , and \dot{Q}).	2-26
2-12 IGS/MISTRAM I, 10K Comparisons (Range Rate, \dot{R} , \dot{P} , and \dot{Q}).	2-27
2-13 IGS/MISTRAM I, 100K Comparisons (Range Rate, \dot{P} and \dot{Q}).	2-27
3-1 Gemini Reentry Ground Trace	3-11
3-2 Uncorrected IGS/Radar Comparison in IGS Coordinates	3-12
3-3 Post Retro IGS Indicated Sensed Velocity	3-13
3-4 Corrected IGS/Radar Comparison in IGS Coordinates	3-14
3-5 Reentry Error Functions.	3-15
3-6 TRW BET - McDonnell Simulation Differences (IGS Coordinates).	3-16
3-7 Reentry Trajectory Parameters	3-17
3-8 IGS Measured Sensed Velocities and Accelerations.	3-18

ILLUSTRATIONS (Concluded)

	Page
4-1 Sensed Position Comparison in Computer Coordinates (MOD III)	4-5
4-2 Sensed Velocity Comparison in Computer Coordinates (MOD III)	4-6
4-3 Sensed Position Comparison in Computer Coordinates (MISTRAM)	4-7
4-4 Sensed Velocity Comparison in Computer Coordinates (MISTRAM)	4-8
4-5 Sensed Position Comparison in Computer Coordinates (BET and MF)	4-9
4-6 Sensed Velocity Comparison in Computer Coordinates (Range BET MF and MISTRAM Final)	4-10
5-1 Rendezvous Geometry	5-6
5-2 Radar Telemetered Parameters (On Board Radar Range)	5-7
5-3 Radar Telemetered Parameters (On Board Azimuth)	5-8
5-4 Radar Telemetered Parameters (On Board Radar Elevation)	5-9
5-5 Radar Residuals (Telemetered Range Minus TRW Calculated Range)	5-10
5-6 Radar Residuals (Telemetered Azimuth Minus TRW Calculated Azimuth)	5-11
5-7 Radar Residuals (Telemetered Elevation Minus TRW Calculated Elevation)	5-12
A-1 Sensed Acceleration in Computer Coordinates - Ascent	A-2
C-1 GE MOD III Refraction Corrections (Range and Elevation)	C-3
C-2 GE MOD III Refraction Corrections (Range Rate, P and Q)	C-4

TABLES

	Page
2-1 IGS Errors at SECO + 20 Seconds	2-3
2-2 Insertion Conditions (SECO + 20 Seconds)	2-5
2-3 IMU Error Compensation	2-6
2-4 TRW Estimates of Gemini IMU Errors at SECO + 20 Sec- onds With and Without Gyro Drift Error Compensation . .	2-7
2-5 IMU Error Coefficients	2-9
2-6 Expected IGS Error from Postflight Calibrations	2-10
2-7 TRW Estimates of Gemini Timing Errors	2-10
2-8 IGS Error Source Summary	2-13
2-9 TRW Proposed Error Model	2-14
2-10 History of Azimuth Alignment Correction	2-17
3-1 Gemini 10 Reentry Trajectory Summary	3-2
3-2 Reentry Error Summary	3-2
3-3 Effects of Error at Guidance Termination (76,000 Feet) in IGS Coordinates	3-3
3-4 Gemini 10 Reentry Retrofire Vector Summary (21 July 20 ^h , 30 ^m , 51 ^s GMT)	3-5
3-5 Retrofire Maneuver Summary	3-5
4-1 Recovered Tracking Error Coefficients	4-2
5-1 Average Magnitude of Residents (Radar-Calculated)	5-6
6-1 Horizon Bias	6-2
6-2 Star Altitude Measurement Comparison	6-2
6-3 Star Altitude Residual Comparison	6-4
A-1 Sensed Trajectory for the Ascent Flight Phase	A-3
A-2 Reconstructed Ascent Trajectory, ECI Coordinates	A-5

TABLES (Concluded)

	Page
A-3a, b Reconstructed Ascent Trajectory, Special Parameters	A-7
B-1 Reconstructed Reentry Trajectory, ECI Coordinates	B-2
B-2a, b Reconstructed Reentry Trajectory, Special Parameters	B-6

~~CONFIDENTIAL~~

1. INTRODUCTION AND SUMMARY

The Gemini 10 flight was launched on 18 July 1966 from Complex 19 at Cape Kennedy, Florida. This report, which has been prepared for the NASA Manned Spacecraft Center by TRW Systems in response to Task MSC/TRW G-14 of the Gemini Mission Trajectory Control Program, presents TRW's best estimate of the inertial guidance system (IGS) accuracy performance during the ascent, orbit and reentry phases of its operation on the Gemini 10 flight. Also presented are analysis results of the rendezvous radar performance and sextant sightings taken during the mission. This report constitutes an addendum to the Gemini 10 NASA/MSC Gemini Program Mission Report, Reference 6.

The basic data reduction and techniques of analysis used to obtain the conclusions in this report are defined in detail in the TRW Analysis Plan and Accuracy Prediction reports, References 1 and 2 respectively. The following is a brief summary of the analysis results.

- a) The TRW estimate of total IGS error at SECO + 20 seconds is:

$\Delta x = 1380 \pm 200 \text{ ft}$	$\Delta \dot{x} = -0.3 \pm 1 \text{ ft/sec}$
$\Delta y = 1810 \pm 500$	$\Delta \dot{y} = 13.5 \pm 3$
$\Delta z = 450 \pm 300$	$\Delta \dot{z} = 3.9 \pm 3$

The uncertainties are engineering judgments and equivalent to one sigma error estimates.

- b) A set of IGS and tracking system error source coefficients was derived from analysis of position and velocity comparisons between IGS telemetry and tracking system data. Recovered IGS error sources that contributed significantly to the explanation of the observed differences were:

~~CONFIDENTIAL~~

<u>Error source</u>	<u>Coefficient</u>	<u>Velocity error contribution in IGS coordinates at SECO + 20 sec (ft/sec)</u>
<u>x-axis</u>		
No significant contributor		
<u>y-axis</u>		<u>$\dot{\Delta y}$</u>
X accelerometer bias	46.6 ± 10 ppm g	-1.2
Z accelerometer bias	76.9 ± 10 ppm g	0.9
Z accelerometer scale factor	-451 ± 66 ppm g	3.1
Y gyro constant drift rate	0.35 ± 0.16 °/hr	9.3
Y gyro input axis unbalance	-0.044 ± 0.08 °/hr/g	-1.2
Platform misalignment about Y accelerometer axis	17 ± 31 $\widehat{\text{sec}}$	2.0
<u>z-axis</u>		<u>$\dot{\Delta z}$</u>
X gyro input axis unbalance	-0.41 ± 0.12 °/hr/g	5.0
X gyro spin axis unbalance	0.14 ± 0.14 °/hr/g	-1.3
Z gyro constant drift rate	0.20 ± 0.13 °/hr	2.8
Z gyro input axis unbalance	-0.038 ± 0.074 °/hr/g	-1.3
Platform misalignment about X accelerometer axis	36 ± 13 $\widehat{\text{sec}}$	-3.9
IGS azimuth misalignment	19.8 ± 10 $\widehat{\text{sec}}$	2.4

~~CONFIDENTIAL~~

c) Significant tracking system bias errors recovered from the analysis were:

<u>MISTRAM I</u>	<u>Coefficient</u>	<u>Velocity error contribution in IGS coordinates at SECO + 20 sec (ft/sec)</u>
P_{100K} bias	-0.50 ± 0.10 ft	$\Delta y = 6.5$
<u>GE/MOD III</u>		
Refraction	-4.4 ± 2.2 n units	$\Delta y = 4.4$

d) The TRW estimate of the IGS error during reentry at guidance termination (76, 000 ft) is:

- 0 ± 0.3 n.mi.downrange
- -4.9 ± 0.3 n.mi.crossrange (south)
- -3.3 ± 0.3 n.mi.altitude (low)

Approximately 80 percent of the apparent IGS error is estimated to be due to initial platform misalignment at retrofire.

e) The TRW estimate of the reentry trajectory miss from the intended splashdown point is:

- 5.1 ± 0.5 n.mi.downrange (long)
- 2.9 ± 0.5 n.mi.crossrange (north)

f) The following conclusions were reached as a result of the rendezvous radar evaluation:

- During the radar tracking interval preceding platform alignment (208 to 224 minutes GET) radar/platform angle error trends of up to 3 degrees were evident. The error was most likely in the radar measurement.
- During platform alignment, the azimuth angle residuals showed excursions of ± 3 degrees, indicating possible problems in alignment. [MSC analysis indicated the platform was momentarily torqued out of alignment due to a spacecraft roll error.]

~~CONFIDENTIAL~~

- After platform alignment, there is an indicated platform/radar system misalignment: yaw/azimuth misalignment = $-1.9 \pm 0.5^\circ$, pitch/elevation misalignment = $-0.6 \pm 0.5^\circ$.
- No radar range error is evident to within the accuracy of the trajectory reconstruction, 1000 to 3000 feet.

Sections 2 and 3 contain details of the ascent and reentry IGS analysis and trajectory reconstruction. The trajectory listings are contained in Appendixes A and B. An analysis of the quality of the external tracking data obtained during ascent is contained in Section 4, and includes plots of the residuals of each tracking system compared to the reconstructed trajectory. A discussion of tracking system calibration data is contained in Appendix C. Section 5 discusses the comparison made between telemetered rendezvous radar measurements and TRW calculated values. Sextant sighting measurements are compared to calculated values in Section 6.

~~CONFIDENTIAL~~

2. INERTIAL GUIDANCE SYSTEM PERFORMANCE ANALYSIS AND ASCENT TRAJECTORY RECONSTRUCTION

This section provides an evaluation of the performance of the IGS during the Gemini 10 ascent flight phase. The evaluation was accomplished by making comparisons of telemetered IGS quantities and external tracking data and conducting visual and regression analyses on the residuals of the comparisons.

Cartesian comparisons (sensed, total, and delta-delta) were made for display and visual analyses. These were referenced to the IGS computer coordinate system which is an inertial, orthogonal right-handed system referenced to the center of the earth. The x and z axes lie in a plane parallel to the geodetic tangent plane at the launch site at platform release time, with the x axis defined by the launch azimuth (actually the misaligned azimuth) positive down range. The y axis is positive down along the geodetic vertical, and the z axis is directed so as to complete the right-handed x, y, z set.

Sensed comparisons (Figure 2-1) were generated by scaling and biasing accumulated accelerometer count data and comparing the result with external tracking data adjusted for gravity and transformed to IGS coordinates. The Gemini 10 IGS measured quantities were compensated in flight with preflight measured IMU error sources; therefore, postflight IGS/tracker comparisons were generated with similarly compensated IGS sensed velocities. Section 2.2.1 provides a discussion of the compensations and their effects. The differences of the sensed coordinate IGS/tracker comparisons are attributable to residual uncompensated IMU errors, external tracking system errors, and initial alignment errors.

Total inertial comparisons, Figures 2-2 and 2-3, were generated by differencing telemetered total position and velocity outputs from the airborne computer with external tracking data. In addition to IMU, tracking data, and alignment errors, these comparisons include airborne computer navigation errors. These are caused by gravity computation errors, which result from numerical approximations and IMU position errors, and by computational errors due to truncation, etc. The navigation errors were

~~CONFIDENTIAL~~

extracted by differencing the sensed and inertial comparison sets to form delta-delta comparisons (Figures 2-4 and 2-5).

Position and velocity comparisons were also made in the external tracking system measurement coordinates. These were made for the purpose of isolating uncompensated IGS and tracking system error source coefficients by performing visual and computer regression analyses of the differences. External tracking data used in the evaluation included Quick-Look MISTRAM I 10K and 100K and GE/MOD III. Tracking data constants and corrections are presented in Appendix C.

External tracking data used for complementary analyses included MISTRAM Final and AFETR Final BET data. The results of analysis of these data sources are presented in Table 4-1 of Section 4.

Support in the estimation of the total IGS error was obtained from a comparison of the IGS position and velocity vector at SECO +20 seconds with a similar vector derived from an orbital BET propagated back to SECO +20. The details of this comparison are given in Section 2.1.1.

All ascent-phase plots enclosed are referenced to liftoff time (22h 20m 26.648s GMT), which occurred 3.260 seconds after IGS platform release.

2.1 INERTIAL GUIDANCE SYSTEM ERROR

The estimated IGS errors following the end of the powered ascent phase (SECO+20 seconds, 360 seconds from liftoff) are contained in Table 2-1. The column headed "IMU and Alignment Error" represents the error contributed by the accelerometer, gyro, and initial platform alignment sources; the column titled "Navigation Error" is the contribution of various approximations within the airborne computer as observed from the delta-delta comparisons; and the "Total IGS Error" column is the sum of the two and represents the total IGS error. The column titled "TRW Orbit 1 Reconstruction" is the guidance error estimated from a comparison at SECO +20 seconds between the IGS data and the free flight reconstruction of Revolution 1 propagated back to insertion. Details of the reconstructed trajectory are given in Section 2.2.1. An additional column titled "NASA 30-Day Report" lists the values representing the NASA/MSC estimates of IGS errors. The \pm numbers listed are one-sigma uncertainty

~~CONFIDENTIAL~~

estimates. They are the result of the analysis of the MOD III, MISTRAM and free flight trajectory estimations, and the statistical error regression.

Table 2-1. IGS Errors at SECO +20 Seconds

Observation	TRW Ascent Data Analysis			TRW orbit 1 reconstruction	NASA 30-day report
	IMU and alignment error	Navigation error	Total IGS error	Total IGS error	Total IGS error
\dot{X} ft/sec	0.3±1.0	-0.6±0.1	-0.3±1.0	-0.3±2.0	0±1.0
\dot{Y} ft/sec	13.3±4.0	0.2±0.1	13.5±4.0	16.0±3.0	15.5±3.0
\dot{Z} ft/sec	4.3±2.0	-0.4±0.1	3.9±3.0	6.9±3.0	5.4±2.0
X ft	1280±200	95±5	1375±200	918±300	545±100
Y ft	1860±500	-48±5	1812±500	2020±600	2450±100
Z ft	460±300	-9±5	451±300	308±600	440±50

2.1.1 Free-Flight Fix

A comparison between the IGS position/velocity vector at SECO +20 seconds and a position/velocity vector derived from a trajectory reconstruction of the flight interval from insertion to first rendezvous was made to support the total IGS error estimation. This comparison point is indicated by a large X on Figures 2-1, 2-2, 2-3 and 2-9 at 360 seconds. (The position and velocity comparisons presented in this report were generated excluding a timing error of 0.0485 second in the IGS data. This timing error causes a position error at SECO +20 seconds of 1200, -330, 10 feet in IGS coordinates. The "TRW ascent data analysis" in Table 2-1 includes this error but the plotted "TRW orbit 1 reconstruction" comparison does not, so as to make it consistent with the "ascent" comparison plots.) This orbit reconstruction utilized tracking data for spacecraft revolutions 1 through 3 and IGS sensed velocity measurements of maneuvers executed during this flight phase. The trackers, which follow, provided C-band tracking data consisting of range, azimuth, and elevation observations.

CONFIDENTIAL

<u>Station</u>	<u>Revolutions</u>
Antigua	1, 2
Ascension	1, 2
Pretoria	1, 3
Carnarvon	1, 2
California	1, 2, 3
Hawaii	1, 2, 3
White Sands	1, 2
Eglin	1
Merritt	1
Grand Bahama	2
Grand Turk	3

The following IGS measured maneuver parameters were considered in the reconstruction.

Maneuver	Burn initiation time (GET) (hr:min:sec)	Velocity Increment in IGS coordinates			Burn duration (sec)
		$\Delta\dot{X}$ (ft/sec)	$\Delta\dot{Y}$ (ft/sec)	$\Delta\dot{Z}$ (ft/sec)	
Separation	00:06:11	1.5	0.6	-0.8	19
IVAR	00:06:47	26.2	-0.62	0.5	36
Phase adjust	02:18:08	55.2	-1.2	1.2	77
Plane change	02:30:46	0.4	-0.5	-11.0	12
Coelliptical	03:47:35	47.1	-5.9	-0.3	93.9
Terminal phase initiation (TPI)	04:33:42	37.1	-20.0	0.2	60

The TRW reconstructed state vector at SECO +20 seconds (361.5 seconds GET) in IGS coordinates was:

$$\begin{aligned}
 X &= 3,974,910 \text{ ft} & \dot{X} &= 25,265.64 \text{ ft/sec} \\
 Y &= -21,066,644 \text{ ft} & \dot{Y} &= 4,763.24 \text{ ft/sec} \\
 Z &= -94,789 \text{ ft} & \dot{Z} &= -81.14 \text{ ft/sec}
 \end{aligned}$$

The uncertainty associated with the orbit reconstruction vector, in Table 2-1, is an engineering estimate based on an examination of the radar residuals to the TRW BET and the uncertainty associated with integrating the BET from the free-flight phase back through the IVAR and Separation maneuvers. Further details of the orbit reconstruction can be found in Reference 3.

CONFIDENTIAL

2.1.2 Insertion Conditions

The IGS error magnitudes indicated in Table 2-1 under "TRW ascent data analysis" give the following trajectory referenced errors:

Velocity magnitude error = 1.8 ft/sec (IGS too large)

Flight path angle error = -0.024 deg (IGS velocity vector below trajectory)

Out-of-plane velocity error = 3.9 ft/sec (IGS left of trajectory).

Estimates of insertion conditions as determined from real time MISTRAM and GE tracking data are presented in Table 2-2. For comparison, the values derived from the TRW BET are also presented.

Table 2-2. Insertion Conditions (SECO +20 Seconds)

Observation	TRW BET	IGS	MISTRAM		GE MOD III	
			Real time	Final	Real time	Final
Velocity magnitude (ft/sec)	25711.8	25713.6	25716	25712	26693	25707
Flight path angle (deg)	-0.001	-0.025	-0.07	-0.035	+0.14	-0.021

2.2 INERTIAL MEASUREMENT UNIT ERROR ANALYSIS

2.2.1 Preflight Compensation

The Gemini 10 IMU measured quantities were compensated inflight analytically with preflight measured gyro drift error coefficients. The drift errors used for compensation and their contributions to the total IGS compensation are listed in Table 2-3. Also presented are the total observed error and the error which would have been present without compensation. The gyro preflight calibration history plots, Figures 2-6 through 2-8, suggest that a logical set of gyro drift coefficients was chosen and no logical process for deriving a better preflight compensation set based upon the calibration histories is apparent. Two postflight gyro coefficient calibrations are also plotted in these figures.

CONFIDENTIAL

Table 2-3. IMU Error Compensation

Error Source	Units	Coefficient	Contribution to IGS error compensation at SECO +20 seconds		
			\dot{X} (ft/sec)	\dot{Y} (ft/sec)	\dot{Z} (ft/sec)
X gyro constant drift rate	°/hr	0.17	-0.02	0.00	-1.63
Y gyro constant drift rate	°/hr	-0.24	-0.21	-6.45	0.00
Z gyro constant drift rate	°/hr	-0.06	0.00	0.00	-0.83
X gyro input axis unbalance	°/hr/g	0.29	-0.04	-0.05	-3.58
Y gyro input axis unbalance	°/hr/g	0.10	0.35	2.75	0.00
Z gyro input axis unbalance	°/hr/g	-0.29	0.09	0.00	-10.05
X gyro spin axis unbalance	°/hr/g	-0.55	0.04	-0.11	5.05
Y gyro spin axis unbalance	°/hr/g	0.06	0.00	0.07	0.00
Z gyro spin axis unbalance	°/hr/g	-0.29	-0.01	0.00	2.18
Total compensation			+0.20	-3.79	-8.86
Error with compensation			+0.3	+13.3	+4.3
Error without compensation			+0.50	+9.5	-4.6

Table 2-4 contains the TRW estimate of IMU error on Gemini flights 6 through 10, and provides an indication of the effect preflight gyro drift error compensation would have had on these flights if it had been utilized. Gemini 10 was the first flight to incorporate the ability to compensate inflight for preflight estimated gyro drift errors. The summary indicates no significant reduction of errors would have been achieved by compensation with the NASA/Honeywell preflight estimated coefficients. However, the preflight coefficients estimated for flights 6 through 9 were based primarily on single platform calibrations prior to flight, whereas the

CONFIDENTIAL

Table 2-4. TRW Estimates of Gemini IMU Errors at SECO +20 Seconds With and Without Gyro Drift Error Compensation

Flight No.	TRW Estimates of IMU Error at SECO +20 Seconds			
	\dot{X} (ft/sec)	\dot{Y} (ft/sec)	\dot{Z} (ft/sec)	\dot{Z}' (ft/sec)**
6 As flown	-1.81	9.7	-1.92	-0.22
Honeywell				
Preflight value	-0.87	-6.6	+0.54	+0.54
With compensation	-0.94*	16.3	-2.46	-0.76
7 As flown	+5.6	+9.9	+0.2	-2.4
Honeywell				
Preflight value	+0.7	+4.1	-6.2	-6.2
With compensation	+4.9*	+5.8*	+6.8	+3.8
8 As flown	+5.18	-4.86	+11.35	+4.34
Honeywell				
Preflight value	+0.03	-0.55	+7.65	+7.65
With compensation	+5.15*	-4.31*	+3.70*	-3.31*
9 As flown***	+8.60	-1.63	8.31	2.54
Honeywell				
Preflight value	+0.39	+3.43	-1.29	-1.29
With compensation	+8.21*	-5.06	9.60	3.83
10 Without compensation	+0.50	+9.5	-4.6	-7.0
Compensation	0.20	-3.79	-8.86	-8.86
With compensation (as flown)	+0.3*	+13.3	+4.3*	+1.9*

*Error improved or unaffected by compensation

**Z' = Crossrange error with the effects of IGS/Burroughs azimuth alignment update error removed

***Gemini 9 error listed assumes IGS/Burroughs inflight azimuth update was successfully completed. Actual error was 166 f.p.s. in Z.

actual compensations used for Gemini 10 were based upon the complete history of Gemini 10 platform calibrations.

It is observed that the crossrange (\dot{Z}') error, adjusted for the Burroughs azimuth update error, is generally smaller than the vertical (\dot{Y}) error. There is no apparent reason for this difference based on the gyro drift error propagations. It could be explained by assuming that initial platform misalignment was the major system error source, since the

CONFIDENTIAL

azimuth update procedure nulls out the crossrange component of this error source but not the downrange component. Accelerometer scale factor error also is a contributor to the vertical error but not the crossrange error.

Table 2-5 provides a comparison of the TRW proposed Gemini 10 total IMU errors (compensation + residuals) with error magnitudes derived from both preflight and postflight calibration data. As noted from Table 2-4, there has not been consistent agreement between preflight IMU calibration data and TRW postflight error estimation based on the apparent flight performance. Generally, there has not been a postflight IMU calibration to check on instrument stability.

Table 2-6 shows the velocity error propagation of the differences between the September 23 postflight calibration and the preflight estimated (and flown) coefficients. The shift in the Y gyro constant drift rate (YGCDR) term is 0.22 deg/hr, equivalent to 6 ft/sec y velocity error at SECO. This shift is in remarkably good agreement with the 0.35 deg/hr shift indicated by the TRW regression as the cause of the observed flight error in the vertical direction (see Table 2-8).

This correlation does not show up so obviously for the other large gyro coefficient shift called for by the postflight regression: X gyro input axis unbalance equal to -0.41 deg/hr/g. There are, however, sizeable shifts evident in the postflight X gyro calibrations for the constant drift (-0.2 deg/hr) and spin axis unbalance drift (0.1 deg/hr/g).

If sizeable and unpredictable coefficient shifts are measured across the flight test, it would seem conceivable that different and even larger shifts might be apparent during the very dynamic flight test. This is not to contend that the postflight statistical regression on the IGS/tracker residuals gives absolutely reliable results. In fact, the error separation is very seriously limited by the high correlation among the velocity error propagations of the possible error sources. However, the regression does select a statistically "best" fit when given the available data, error model, and related statistics. The most that can be hoped for from the flight profile of Gemini 10 is a reasonable indication of the likely error sources.

CONFIDENTIAL

CONFIDENTIAL

Table 2-5. IMU Error Coefficients

Error sources (TRW symbols)	Units	Preflight Platform Calibrations										Flight Compensation			Postflight platform calibrations	
		24 Feb	14 June	15 June	16 June	17 June	20 June	29 June	15 July	Preflight average	NASA/Honeywell preflight estimated	TRW postflight estimated	23 Sept	26 Sept		
XGDDR	*/hr	0.135	0.185	0.163	0.19	0.14	0.207	0.15	0.111	0.160	0.17	0.157 ± 0.19	-0.025	-0.023		
XGIAU	*/hr/g	0.23	0.253					0.287	0.293	0.265	0.29	-0.126 ± 0.12	0.341	0.348		
XGSAU	*/hr/g	-0.24	-0.485	-0.52	-0.592	-0.508	-0.567	-0.55	-0.561	-0.502	-0.55	-0.412 ± 0.14	-0.449	-0.452		
YGDDR	*/hr	-0.135	-0.222					-0.244	-0.251	-0.213	-0.24	0.107 ± 0.16	-0.02	-0.01		
YGIAU	*/hr/g	-0.07	-0.025					0.136	0.102	0.036	0.10	0.056 ± 0.08	0.122	0.042		
YGSAU	*/hr/g	0.14	-0.003					0.114	-0.009	0.06	0.06	0.071 ± 0.20	-0.125	-0.184		
ZGDDR	*/hr	-0.014	-0.0611					-0.048	-0.041	-0.041	-0.06	0.14 ± 0.13	-0.008	0.004		
ZGIAU	*/hr/g	0.06	-0.273					-0.3	-0.251	-0.191	-0.29	-0.33 ± 0.07	-0.278	-0.278		
ZGSAU	*/hr/g	-0.06	-0.286					-0.308	-0.176	-0.208	-0.29	-0.36 ± 0.09	-0.221	-0.223		
Deviation from loaded value																
XSF	ppm	-31	0					-23	-103	-39	(1)	-46 ± 114				
YSF	ppm	-30	0					130	-117	-4.3	(1)	(1)				
ZSF	ppm	-240	0					78	18	-36	(1)	-451 ± 65				
BX	ppm g	38	0							19	(1)	46 ± 20				
BY	ppm g	57	-3							28	(1)	0 ± 20				
BZ	ppm g	-30	12							-9	(1)	77 ± 20				

(1) No change made from previously loaded values.

CONFIDENTIAL

CONFIDENTIAL

Table 2-6. Expected IGS Error From Postflight Calibrations

Error source	Units	Postflight minus preflight	Error at SECO + 20 seconds		
			$\Delta\dot{x}$ (ft/sec)	$\Delta\dot{y}$ (ft/sec)	$\Delta\dot{z}$ (ft/sec)
XGCDR	o/hr	-0.195	0.02		1.88
XGLAU	o/hr/g	0.051	-0.008	-0.008	-0.642
XGSAU	o/hr/g	0.101	-0.007	0.02	-0.93
YGCDR	o/hr	0.22	0.19	5.9	
YGLAU	o/hr/g	0.022	0.08	0.6	
YGSAU	o/hr/g	-0.185	-0.16	-0.2	
ZGCDR	o/hr	0.052	-0.007		0.73
ZGLAU	o/hr/g	0.012	-0.004		0.42
ZGSAU	o/hr/g	0.069			-0.52
Total			0.11	6.3	0.94

Table 2-7. TRW Estimates of Gemini Timing Errors

Flight No.	Time correlation (sec)	IGS clock drift (ppm)
3	-0.005	0
4	-0.002	30
5	0.014	-60.5
6	0.015	-63
7	0	-32.2
8	0.025	-90
9	0.017	-63
10	0.006*	-85
	Mean	+0.009

*0.0485 second known TRS bias removed.

CONFIDENTIAL

~~CONFIDENTIAL~~

2.2.2 Residual IMU Error After Compensation

Recovery of the IMU error source coefficients, which existed after compensation, was accomplished by visual analysis and by performing computer statistical regressions on IGS/tracker residuals. Figure 2-1 presents sensed velocity comparisons compensated for preflight estimated IMU errors, and a 0.0485 second TRS bias error. The IMU error source coefficients recovered as a result of the analysis are presented in Table 2-8.

2.2.2.1 Timing Error

The first set of velocity comparisons generated showed -5.3 and -5.6 ft/sec jumps in the x velocity residual at booster engine cutoff (BECO) and sustainer engine cutoff (SECO). This error trend indicated large IGS timing errors. Conversations with NASA MSC personnel revealed that 0.0485 second of the observed time correlation error was explained by a known time reference system (TRS) bias. The majority of the time correlation error was therefore identified; however, the remaining trend, obvious in Figure 2-1 from the small jumps at BECO and SECO, called for an additional 0.006 m sec time correlation error and an 85 part per million (ppm) clock drift error. Although the timing error results in zero sensed velocity error after SECO, where the thrust acceleration goes to zero, a relatively large x total position error of 1000 feet does remain after burnout. The Gemini 10 time correlation and clock drift error are compared with timing errors recovered from previous Gemini flights in Table 2-7. The summary indicates that the Gemini 10 timing errors are consistent with timing errors observed on previous flights. The clock drift is large however.

2.2.2.2 Accelerometer Bias Error

Accelerometer bias errors were determined from plots of IGS sensed velocities during free flight intervals of Revolution 4 and later during the free flight period after retrofire. The following bias errors were determined:

~~CONFIDENTIAL~~

~~CONFIDENTIAL~~

	<u>Revolution 4</u>	<u>Post Retrofire</u>
X accelerometer bias	46.6 ± 10 ppm g	6.2 ± 10 ppm g
Y accelerometer bias	0 ± 10 ppm g	43.6 ± 10 ppm g
Z accelerometer bias	76.9 ± 10 ppm g	46.9 ± 10 ppm g

The values calculated from Revolution 4 were used for the ascent phase analysis and those recovered from the post retrofire data were used for the reentry analysis.

2.2.3 Error Coefficient Recovery

The IMU error source coefficients presented in Table 2-8 were recovered by first determining accelerometer bias errors, compensating the IGS/tracker comparisons for these, and then performing statistical regression analysis on the residuals of the comparisons. The regression domain chosen was the following:

10K MISTRAM \dot{P} , \dot{Q} , \dot{R}_{SUM}

100K MISTRAM \dot{P} , \dot{Q}

GE MOD III (GE processed) R, A, E, \dot{R} , \dot{P} , \dot{Q}

The error model presented in Table 2-9 was selected to recover coefficients for most of the IMU error sources estimated by platform ground calibration tests. The terms preceded by an asterisk were recovered visually and were consequently not solved in the regression solution. However, the estimated uncertainty in their determination was statistically accounted for in the output coefficient uncertainties.

Several variations or combinations of error terms were considered in initial regression attempts which considered accelerometer and platform misalignments as being dominant error sources rather than gyro drift errors. None of these provided satisfactory fits to the IGS/tracker residuals, however. Satisfactory explanations of the residuals were achieved only when pitch-drift type error sources were included in the total error model.

~~CONFIDENTIAL~~

Table 2-8. IGS Error Source Summary

IMU error source	Units	TRW Analysis			NASA 30-day Report							
		Coefficient	1 sigma uncertainty	Velocity error contribution at SECO +20 seconds		Coefficient (Fit 1)	Velocity error contribution at SECO +20 seconds					
				$\Delta\dot{X}$ (ft/sec)	$\Delta\dot{Y}$ (ft/sec)		$\Delta\dot{Z}$ (ft/sec)	$\Delta\dot{X}$ (ft/sec)	$\Delta\dot{Y}$ (ft/sec)	$\Delta\dot{Z}$ (ft/sec)		
I Accelerometer												
X accelerometer bias	ppm g	46.6	10	0.22	-1.15	50	0.2	-1.3	N	N		
Y accelerometer bias	ppm g	0	10			N			N	N		
Z accelerometer bias	ppm g	76.9	10		0.89	80		0.9	80	80	0.9	
X accelerometer scale factor	ppm	-46	114	-1.15		-50	-1.2		N	N		
Z accelerometer scale factor	ppm	-451	66		3.06	-400		2.7	N	N	2.0	
X accelerometer misalignment toward Z	sec	-14	33	0.46		N			N	N		
Z accelerometer misalignment toward X	sec	+2.5	39		0.30	-17.5		-2.1	90	90	10.8	
II Pitch Drift												
Y gyro constant drift rate	o/hr	+0.35	0.16	0.31	9.32	N			N	N		
Y gyro input axis unbalance	o/hr/g	-0.044	0.08	-0.15	-1.21	+0.56	1.9	15.3	N	N		
Y gyro spin axis unbalance	o/hr/g	+0.011	0.20		0.01	N			N	N		
III Roll and Azimuth Drift												
X gyro constant drift rate	o/hr	-0.013	0.19			N			N	N		
X gyro input axis unbalance	o/hr/g	-0.41	0.12	0.06	0.06	5.04			N	N		
X gyro spin axis unbalance	o/hr/g	+0.14	0.14	-0.01	0.03	-1.28			N	N		
Z gyro constant drift rate	o/hr	+0.20	0.13	-0.03		2.78			N	N		
Z gyro input axis unbalance	o/hr/g	-0.038	0.074	0.01	-1.34	+0.10		3.40	0.10	0.10	3.4	
Z gyro spin axis unbalance	o/hr/g	-0.066	0.093		0.50	N			N	N		
IV System												
Platform misalignment about X accelerometer axis	sec	36	13	-0.05	-0.04	-3.90			N	N		
Platform misalignment about Y accelerometer axis	sec	17	31	0.56	2.04	N			N	N		
Platform azimuth misalignment	sec	19.8	10	0.06		2.37		2.4	+20	+20	2.4	
IGS time correlation	sec	0.0546	10			+0.0556	0	0	0	0	0	
IGS time scale factor	ppm	-84.9	65			-92	0	0	-92	-92	0	
TOTAL				0.29	13.31	4.30	0.6	15.3	5.8	0	13.7	5.8

*N represents negligible coefficient.

~~CONFIDENTIAL~~

Table 2-9. TRW Proposed Error Model

Symbol	Error source	Units	1 σ a priori uncertainty
* VOZ	Z accelerometer initialization	ft/sec	0.2
DT	Time correlation	sec	0.01
TSF	Time scale factor	ppm	20
* BX	X accelerometer bias	ppm g	10
* BY	Y accelerometer bias	ppm g	10
* BZ	Z accelerometer bias	ppm g	10
XSF	X accelerometer scale factor	ppm	160
ZSF	Z accelerometer scale factor	ppm	160
POX	Position bias - X computer axis	ft	50
POY	Position bias - Y computer axis	ft	50
POZ	Position bias - Z computer axis	ft	50
XZMSL	X accelerometer misaligned toward Z	arc sec	50
ZXMSL	Z accelerometer misaligned toward X	arc sec	50
XGCDR	X gyro constant drift rate	$^{\circ}$ /hr	0.2
YGCDR	Y gyro constant drift rate	$^{\circ}$ /hr	0.2
ZGCDR	Z gyro constant drift rate	$^{\circ}$ /hr	0.2
XGSAU	X gyro spin axis unbalance	$^{\circ}$ /hr/g	0.2
YGSAU	Y gyro spin axis unbalance	$^{\circ}$ /hr/g	0.2
ZGSAU	Z gyro spin axis unbalance	$^{\circ}$ /hr/g	0.2
XGLAU	X gyro input axis unbalance	$^{\circ}$ /hr/g	0.2
YGLAU	Y gyro input axis unbalance	$^{\circ}$ /hr/g	0.2
ZGLAU	Z gyro input axis unbalance	$^{\circ}$ /hr/g	0.2
PHIX	Platform alignment about X accelerometer axis	arc sec	50
PHIY	Platform alignment about Y accelerometer axis	arc sec	50
PHIZ	IGS azimuth alignment	arc sec	10
A4(1)	MISTRAM I refraction - central site	n-units	2.0
CO(3)	GE MOD III range bias	ft	10

* Not solved for in regression. (See Subsection 2.2.3.)

~~CONFIDENTIAL~~

Table 2-9. TRW Proposed Error Model (Concluded)

Symbol	Error source	Units	1σ a priori uncertainty
C2(3)	GE MOD III timing	sec	0.001
C4(3)	GE MOD III refraction	n-units	2.0
C5(3)	GE MOD III survey (east)	ft	3.0
C6(3)	GE MOD III survey (north)	ft	3.0
C7(3)	GE MOD III survey (up)	ft	1.0
DO(3)	GE MOD III azimuth bias	millirad	0.2
FO(3)	GE MOD III elevation bias	millirad	0.2

The results of the final regression solution have been presented in part in Table 2-8. Also recovered were the following tracking system and IGS position bias errors along with their one sigma uncertainties.

- MISTRAM I refraction = -0.48 ± 2.0 n-units
- GE MOD III range bias = -23 ± 3.8 ft
- GE MOD III timing bias = -0.61 ± 0.22 millisec
- GE MOD III refraction = -4.44 ± 2.22 n-units
- GE MOD III azimuth bias = -2.7 ± 15 μrad
- GE MOD III elevation bias = $+44 \pm 11$ μrad
- X computer axis position bias = -3.9 ± 4.0 ft
- Y computer axis position bias = $+20.2 \pm 5.2$ ft
- Z computer axis position bias = -19.6 ± 7.8 ft

IGS data position bias errors are considered to result from postflight data reduction errors rather than the IMU. The effect of tracking data errors on IGS/tracking data comparisons is discussed in Section 4.

The ability of the regression to fit the residuals is graphically displayed by heavy lines drawn upon the tracker coordinate position and velocity residuals in Figures 2-10 through 2-13. These lines represent the total error contribution of the recovered coefficients. It can be seen that the residuals between the lines and the respective data points are for

CONFIDENTIAL

the most part unbiased and the indicated line closely approximates the apparent position and velocity errors.

The degree to which the recovered IMU error sources explain the IGS/tracker residuals in guidance coordinates is indicated in Figure 2-9 by a heavy line. The x-axis residuals are explained by the IMU functions to within the data noise; however, unexplained residuals remain in the y and z axes. These residual differences are attributed to a MISTRAM P_{100K} bias of -0.5 ft and a GE MOD III refraction error of -4.4 n-units. On the other hand, the IMU functions accounted for nearly all of the IGS/MISTRAM 10K residuals suggesting that the MISTRAM 10K bias errors were smaller than those of the 100K data (see Figures 4-3 and 4-4 of Section 4).

Recovery of the MISTRAM I position bias errors was accomplished by compensating the IMU/tracker position domain residuals with the errors recovered in the regression analysis and estimating the bias levels from the remaining position errors (Section 4).

2.3 IGS AZIMUTH UPDATE

The IGS azimuth alignment update corrections were successfully accomplished on this flight. The initial alignment correction was obtained, during the first pass through the navigation equations, by comparing the actual platform roll gimbal angle after platform release with the desired value. Additional azimuth corrections were made at 100 and 140 seconds after liftoff. These were calculated by comparing the crossrange (z direction) velocity as measured by GE/Burroughs with that derived from the airborne system and attributing the residual to a platform misalignment about the vertical axis.

Table 2-10 compares the initial IGS alignment correction, total inflight update obtained, and residual alignment error on Gemini 10 with those obtained on previous Gemini missions. This summary shows that the Gemini 10 corrections are consistent with those obtained on previous flights. The residual azimuth misalignment on this flight was considerably smaller than rendezvous flights 6, 8, and 9.

CONFIDENTIAL

Table 2-10. History of Azimuth Alignment Correction

Flight No.	Initial alignment correction (deg)	Inflight update (deg)	Total Alignment Correction (deg)	Residual azimuth error (arc sec)
2	-0.07	-0.22	-0.29	0
3	+0.01	-0.53	-0.52	0
4	+0.03	-0.15	-0.12	0
5	+0.05	-0.32	-0.27	0
6	+0.06	-0.59	-0.53	-40
7	-0.01	-0.47	-0.48	0
8	+0.11	-0.21	-0.10	+57
9	+0.17	-0.40*	-0.23*	+48
10	-0.09	-0.13	-0.22	+20
Mean	+0.03	-0.34	-0.31	
		NASA/Honeywell Specification	0.75	

* Simulated

2.4 CONCLUSIONS

- a) The IGS vertical (y) velocity error of over 13 ft/sec was larger than expected. Error in the x and z coordinates was nominal.
- b) The net effect of the inflight gyro compensation was to increase the IGS y coordinate error by 4 ft/sec and leave the z coordinate error magnitude unchanged. However, the compensation would have significantly reduced (5 ft/sec) the z coordinate error magnitude if the Burroughs' azimuth update correction had been accurate. Available preflight gyro calibration data indicate that a logical set of preflight compensation coefficients was selected.
- c) A very large IGS time correlation error of 0.055 seconds was observed; however, the major portion, 0.049 seconds, is attributable to a known TRS bias. The clock drift of 85 parts per million was also large, but is consistent with that observed on previous flights.

CONFIDENTIAL

- d) Inflight updating of the IGS azimuth alignment was successfully accomplished, though a residual azimuth error equivalent to 20 $\widehat{\text{sec}}$ remained after updating. The residual error is one-half or less than that observed on any other rendezvous flight.
- e) Accelerometer bias errors recovered on this flight were nominal though apparent shifts occurred between ascent and reentry.

2.5 ASCENT TRAJECTORY RECONSTRUCTION

The ascent trajectory reconstruction consists of IGS data corrected for the alignment errors and IMU error sources presented in Table 2-8. A listing of this reference trajectory is provided in Appendix A.

The trajectory is given in an earth-centered inertial coordinate system. The z axis is aligned with the earth's rotational axis, positive north, and the x-y plane is the equatorial plane with the x-z plane containing the Greenwich meridian at platform release time. The time is referenced to liftoff, 3.260 seconds after platform release. Trajectory parameters such as velocity magnitude, altitude, flight path angle, heading, latitude and longitude are also printed.

CONFIDENTIAL

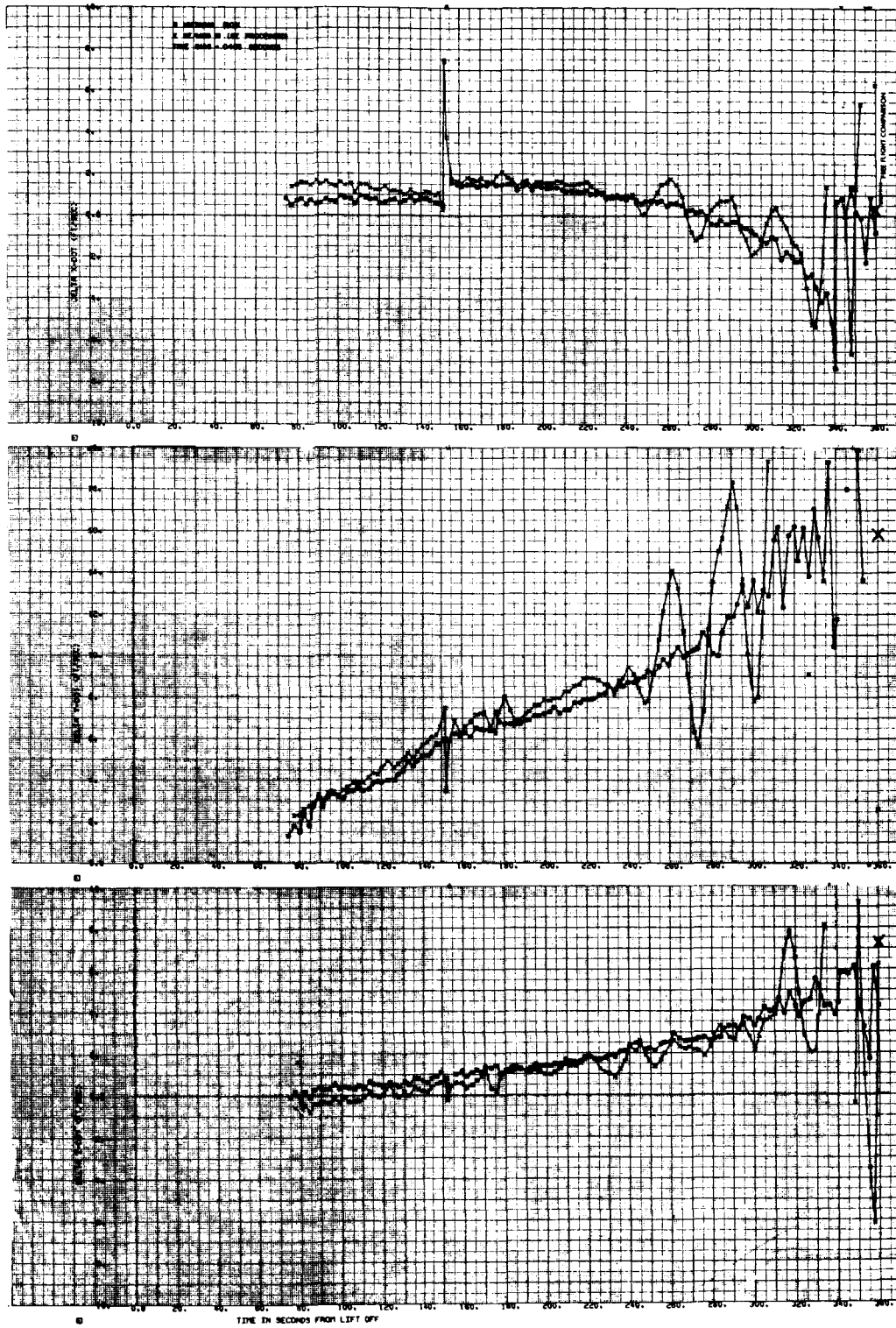


Figure 2-1. Sensed Velocity Comparison in Computer Coordinates

~~CONFIDENTIAL~~

~~CONFIDENTIAL~~

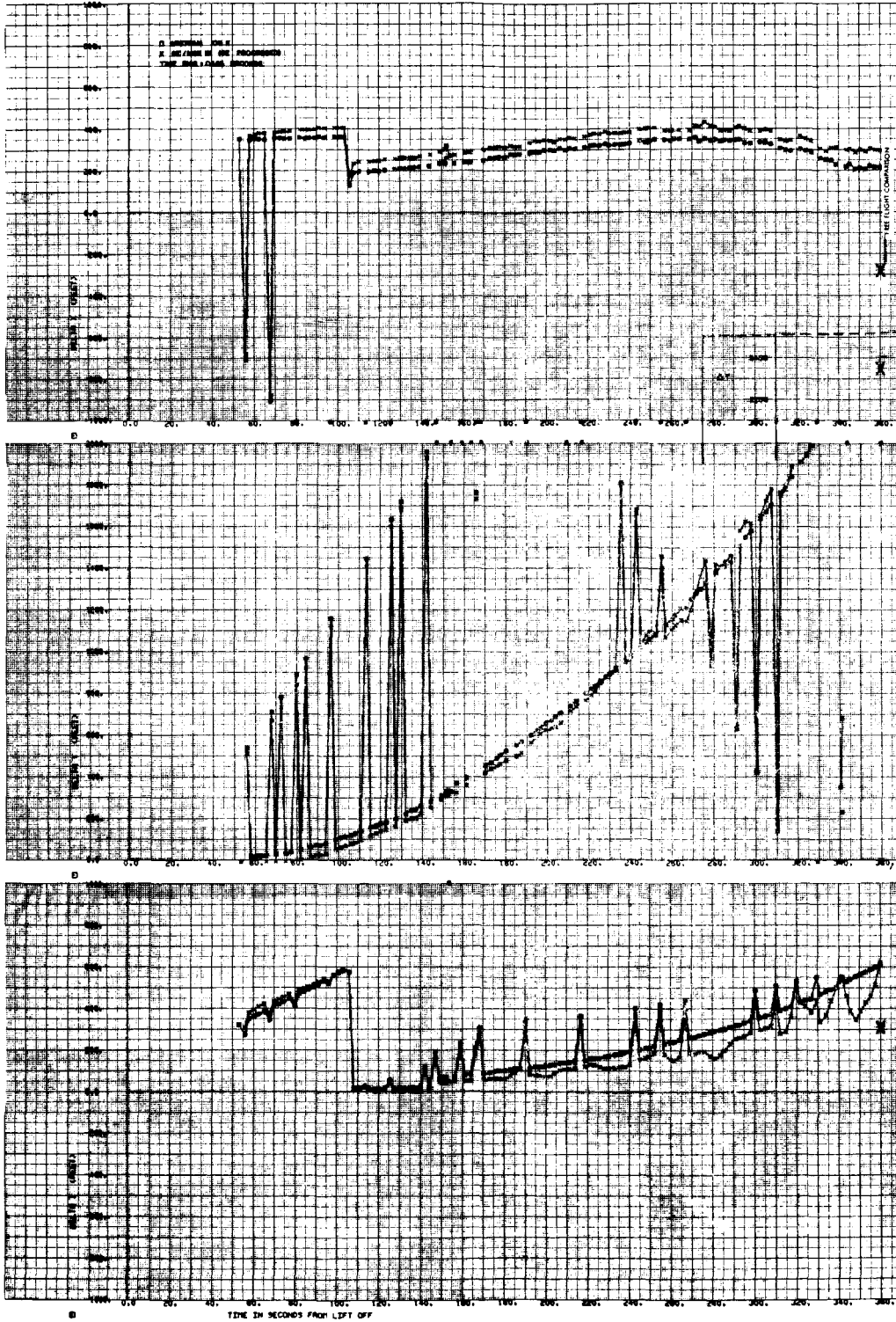


Figure 2-2. Total Inertial Position Comparison
in Computer Coordinates

~~CONFIDENTIAL~~

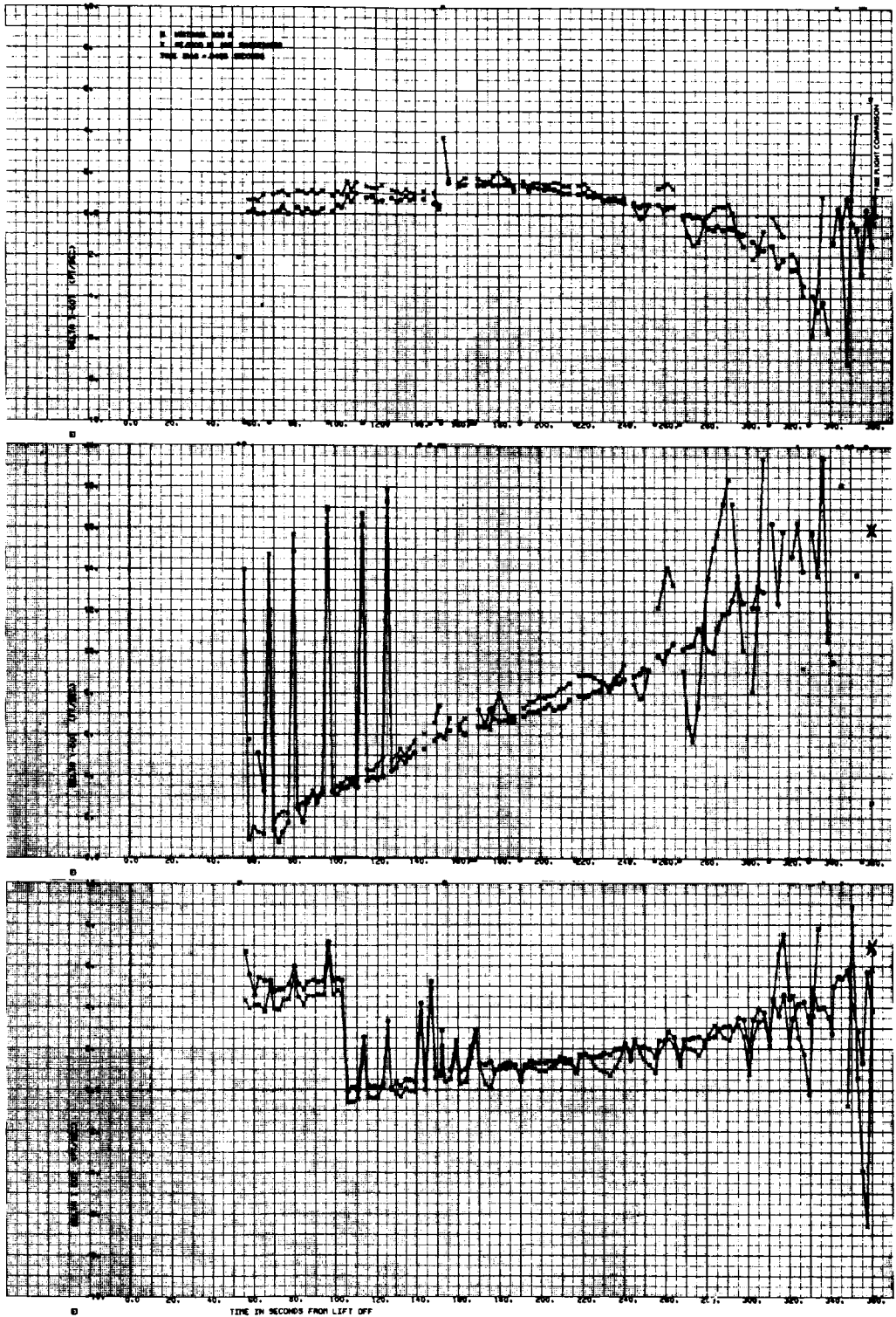


Figure 2-3. Total Inertial Velocity Comparison in Computer Coordinates

~~CONFIDENTIAL~~

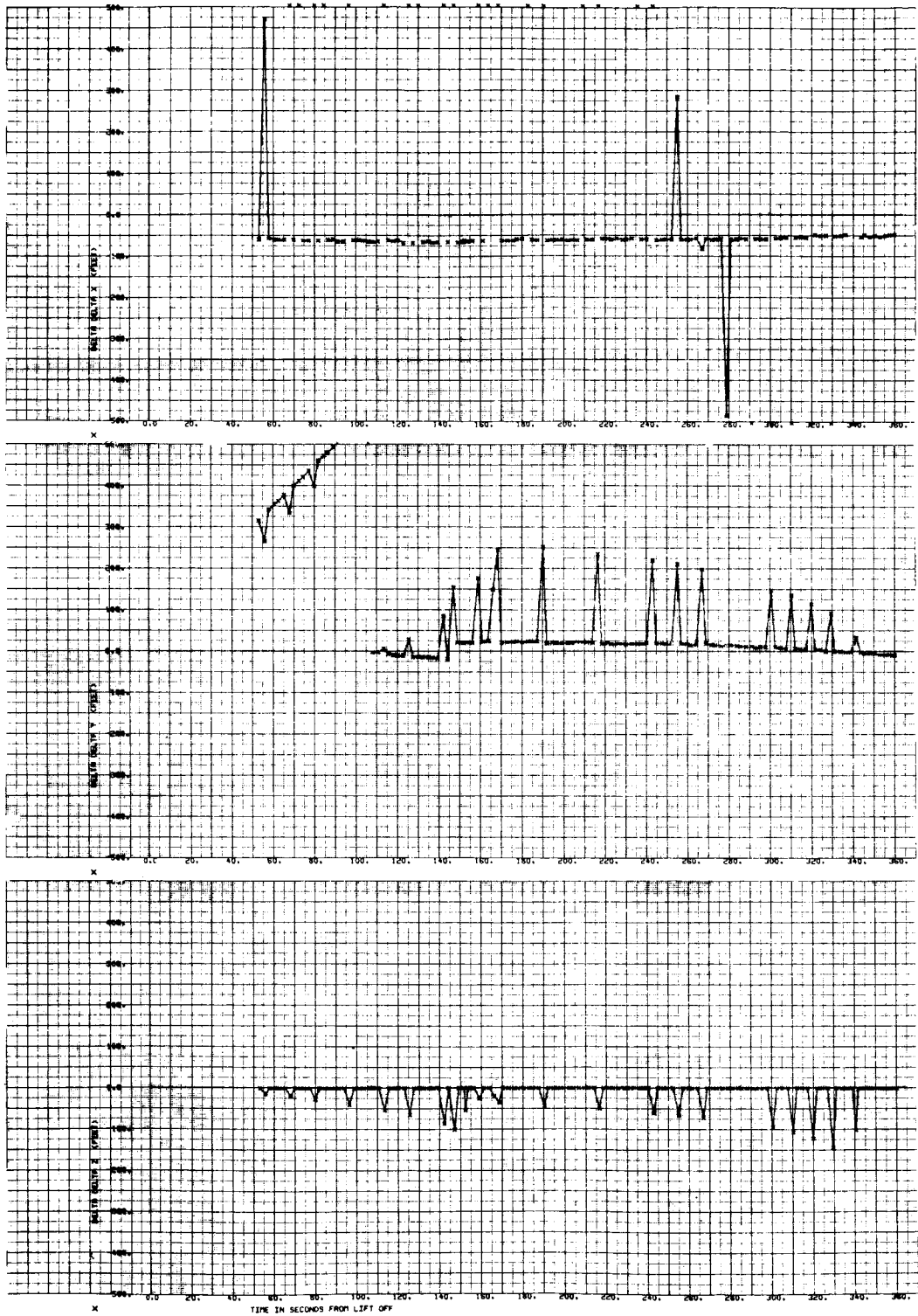


Figure 2-4. Navigation Position Error

~~CONFIDENTIAL~~

~~CONFIDENTIAL~~

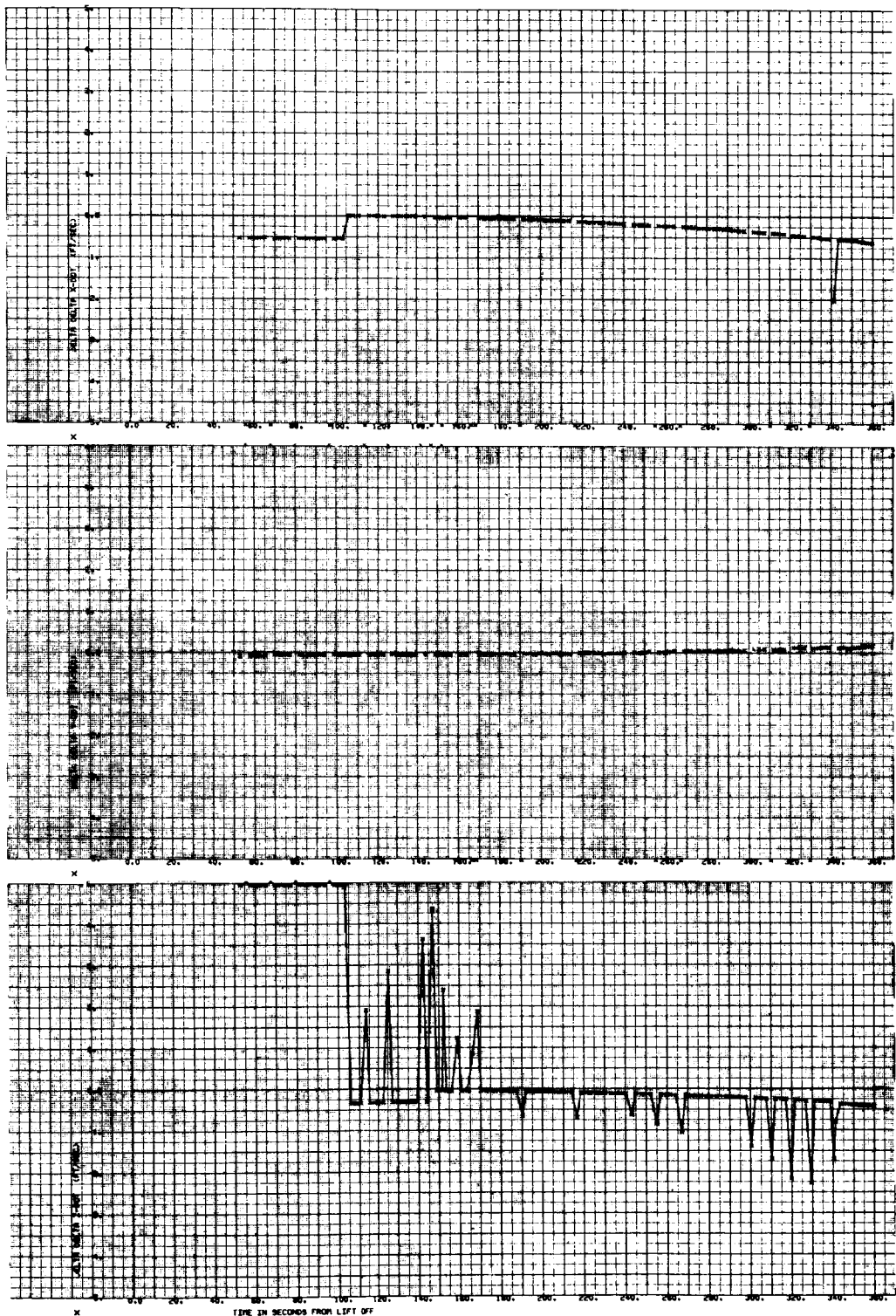


Figure 2-5. Navigation Velocity Error

~~CONFIDENTIAL~~

CONFIDENTIAL

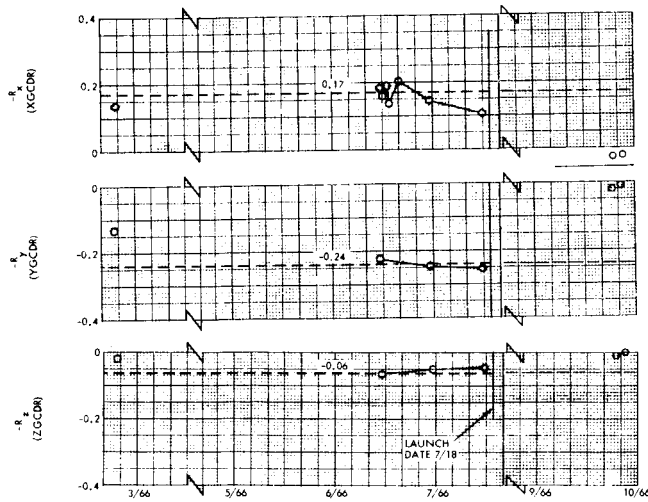


Figure 2-6. Gyro Constant Drift Rate History

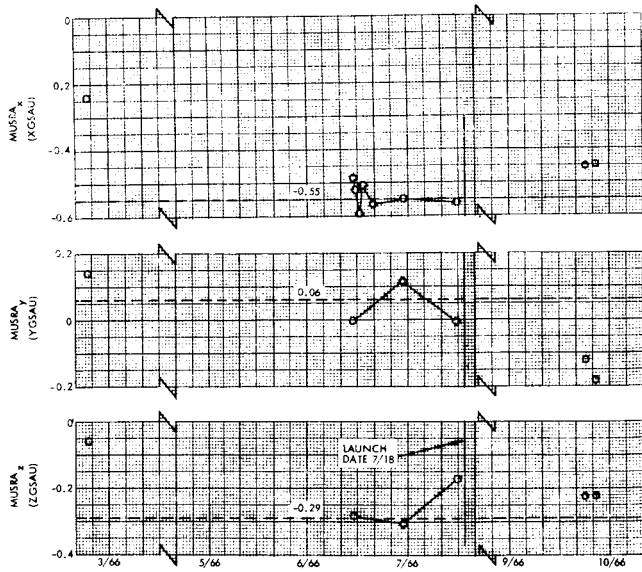


Figure 2-7. Gyro Spin Axis Unbalance Drift History

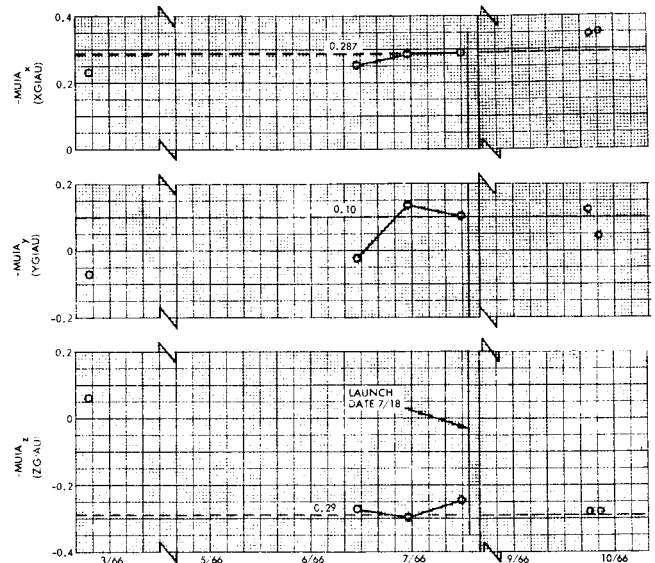


Figure 2-8. Gyro Input Axis Unbalance Drift History

CONFIDENTIAL

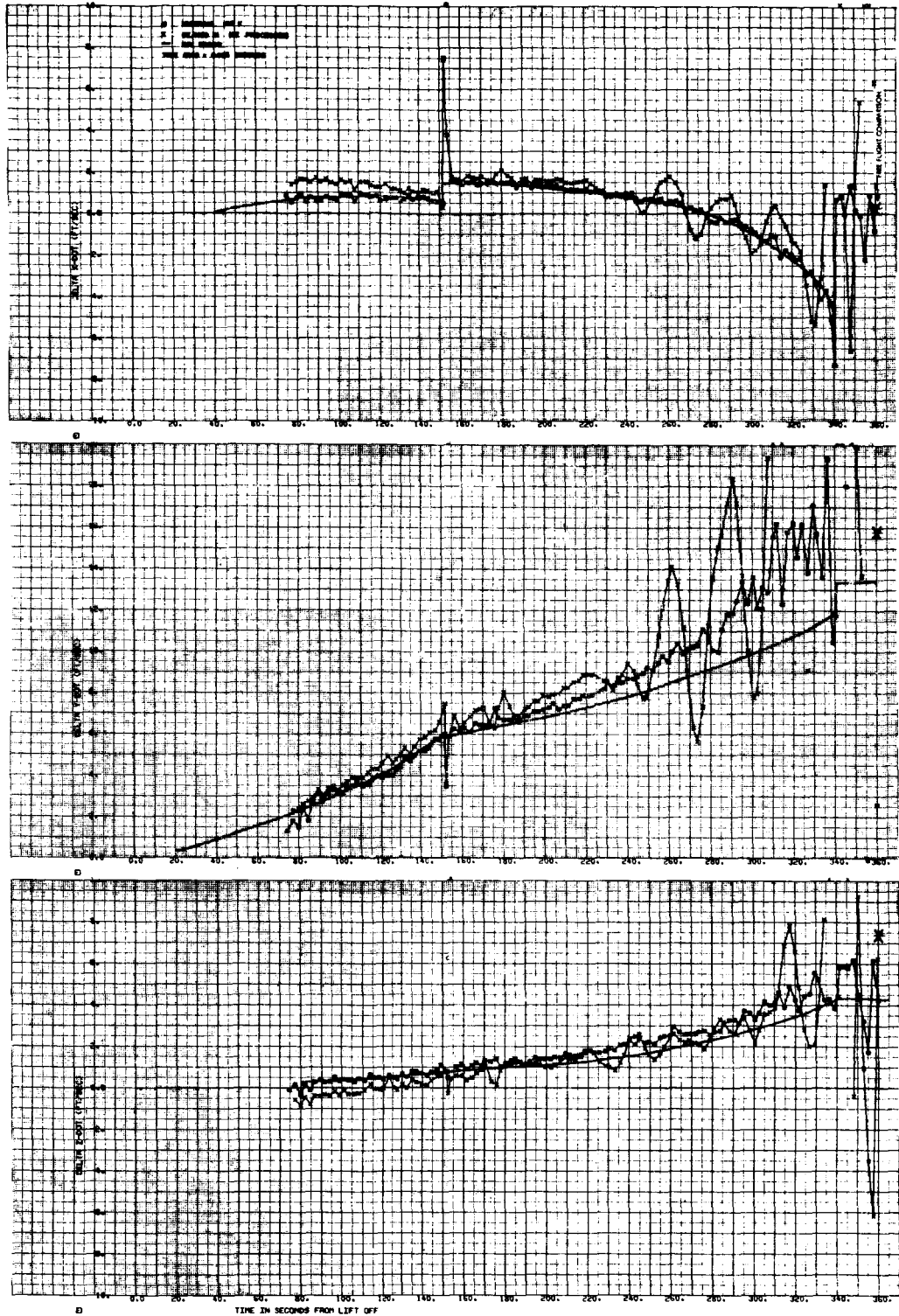


Figure 2-9. Sensed Velocity Comparison in Computer Coordinates with IGS Error Fit

CONFIDENTIAL

CONFIDENTIAL

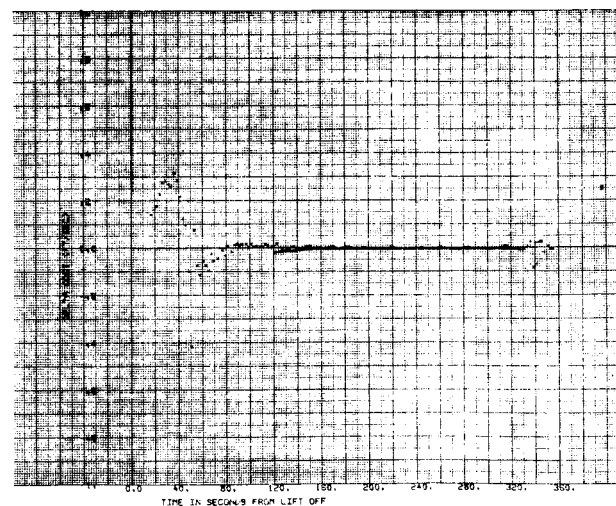
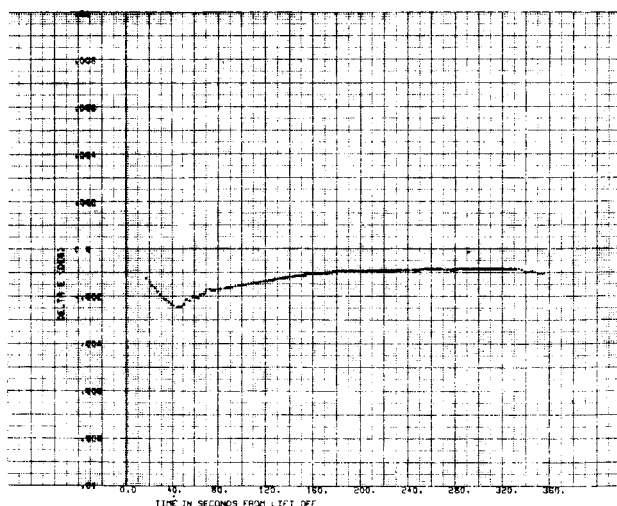
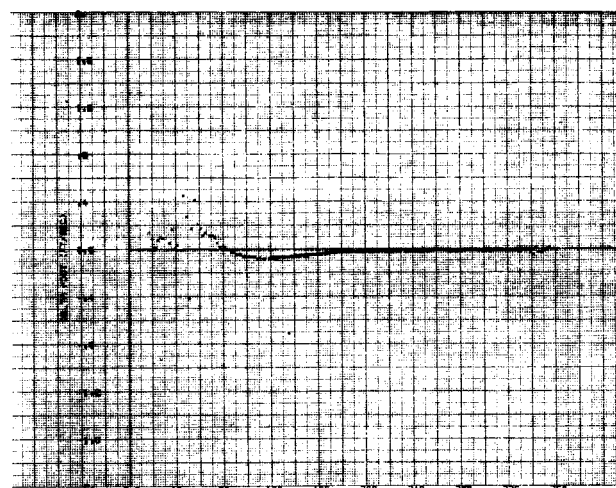
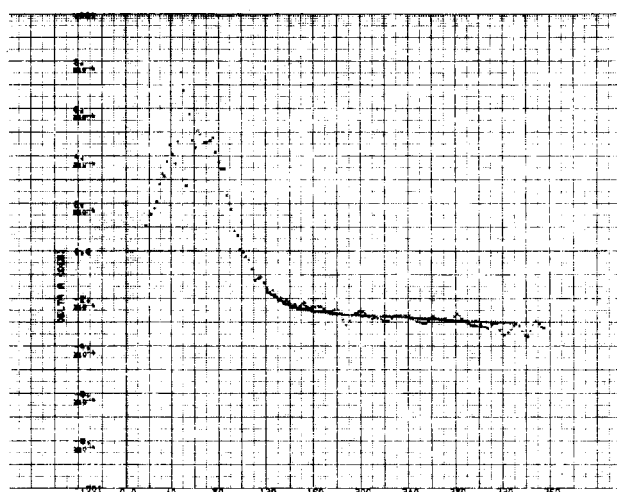
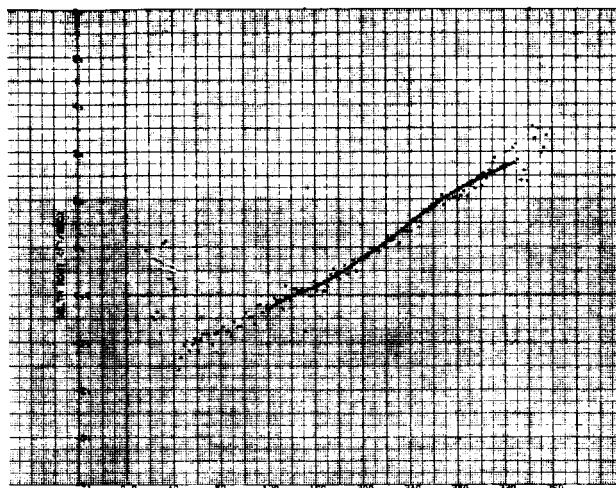
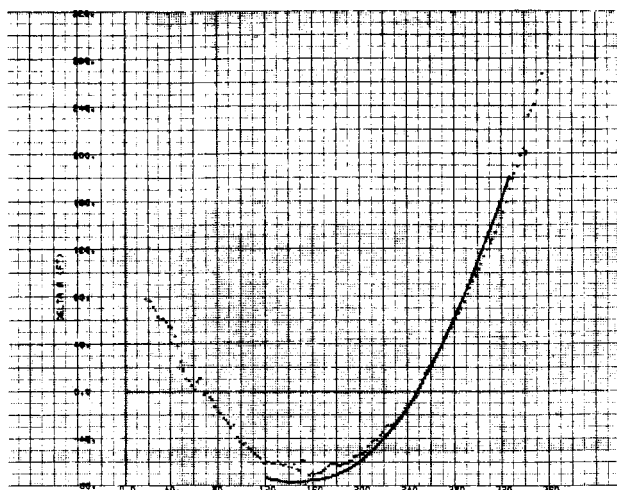


Figure 2-10. IGS/Mod III Comparisons (RAE)

Figure 2-11. IGS/Mod III Comparisons (Range Rate, \dot{R} , \dot{P} , and \dot{Q})

CONFIDENTIAL

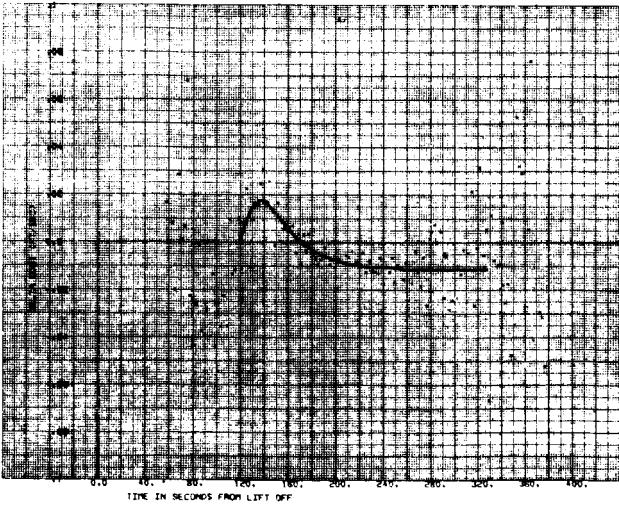
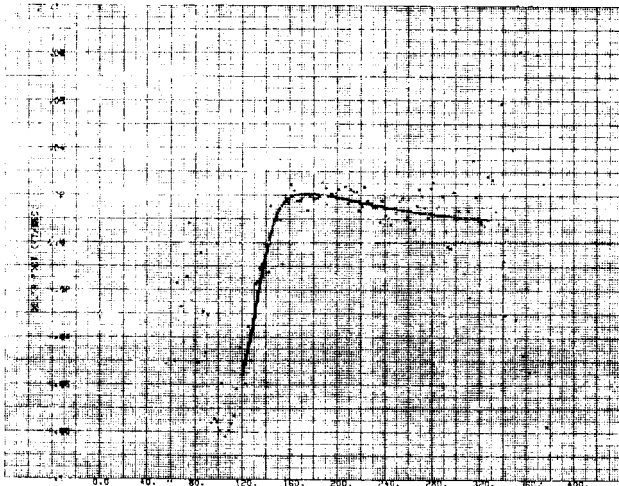
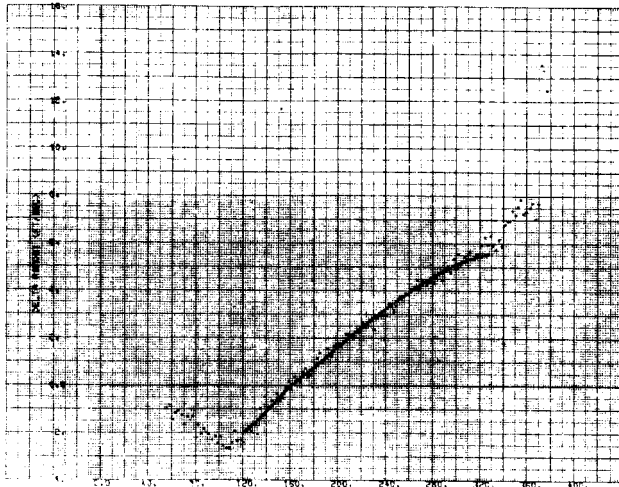


Figure 2-12. IGS/MISTRAN I, 10K
Comparisons (Range Rate,
 \dot{R} , \dot{P} , and \dot{Q})

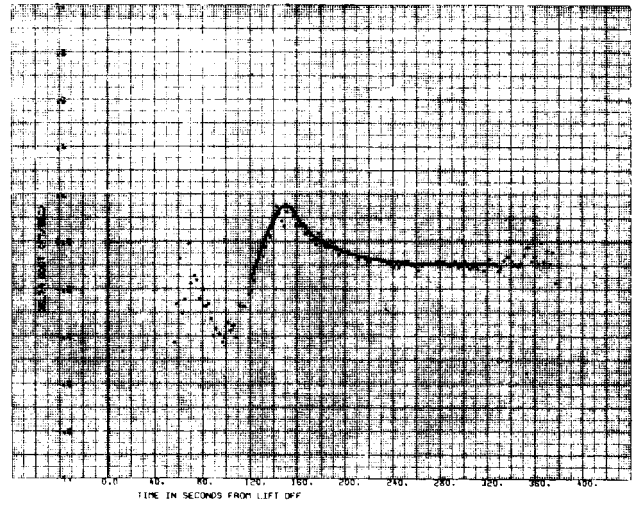
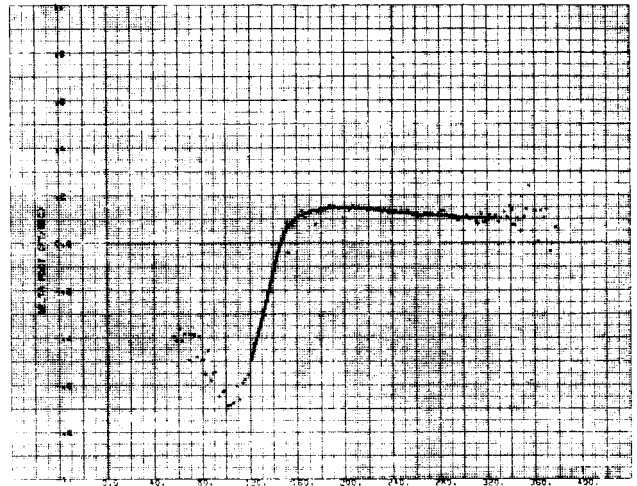


Figure 2-13. IGS/MISTRAN I, 100K
Comparisons (Range
Rate, \dot{P} and \dot{Q})

(Reverse of this page is
intentionally blank)

3. REENTRY IGS PERFORMANCE EVALUATION AND TRAJECTORY RECONSTRUCTION

3.1 INTRODUCTION AND SUMMARY

This section presents an evaluation of the IGS performance during the reentry flight phase. The evaluation was accomplished by comparing telemetered IGS quantities with external tracking data and with nominal terminal phase conditions, and estimating the most likely error sources from the residual trends.

The following C-band radar and telemetry were available for the analysis:

<u>Data Source</u>	<u>Interval (sec from retrofire)</u>
19:18, Merritt Isl.	1550 to 1747
0:18, Patrick AFB	1550 to 1750
3:18, Grand Bahama Isl.	1558 to 1757
7:18, Grand Turk Isl.	1721 to 1815
PCM Telemetry	0 to 2062

Table 3-1 provides various estimates of the spacecraft location at the times of significant events during the latter part of reentry. This same information is graphically displayed in Figure 3-1 along with the ground trace of the spacecraft as given by a TRW reconstruction of the spacecraft trajectory, uncorrected IGS data, and the last part of Grand Turk radar tracking. Table 3-2 summarizes the TRW estimate of guidance and control error on this flight. It is noted that very little of the indicated downrange miss can be attributed to IGS measurement error. The crossrange miss may be partially explained by the indicated IGS error. If the IGS is in error to the south, it would be expected that the spacecraft would be steered to the north of the intended target.

3.2 REENTRY ERROR SOURCES

Table 3-3 presents a summary of recovered error sources which provide an explanation for the apparent IGS error at guidance termination. To extract error sources from the available data the telemetered IGS trajectory was reconstructed using the RTCC retrofire position/velocity

CONFIDENTIAL



Table 3-1. Gemini 10 Reentry Trajectory Summary

Source of Data	Altitude (1000 ft)	Latitude (deg N)	Longitude (deg W)	Difference from target (n mi)	
				North	East
Guidance Termination (t* = 1815)					
IGS (uncorrected)	56	26.682	71.992	-2.0	0.43
TRW BET	76	26.764	71.986	2.9	0.75
Drogue Deployment (t* = 1870)					
TRW BET	37	26.768	71.902	3.2	5.2
IGS**	2	26.633	71.915	-4.9	4.6
Main Chute Deployment (t* = 1951)					
TRW BET	7	26.764	71.894	2.9	5.7
IGS**	-50	26.558	71.940	-9.4	2.3
Splashdown					
Target	0	26.715	72.00	0	0
Ship measurement	0	26.745	71.95	1.8	2.7
TRW BET (final telemetry point, t* = 2062)	2	26.756	71.888	2.5	6.0
IGS (final telemetry point)**	-90	26.456	71.991	-16.0	0.5

*Time from retrofire in seconds.
 **Differences between the IGS and true trajectories at times after "guidance termination" do not affect trajectory accuracy, but are useful for identification of error sources.

Table 3-2. Reentry Error Summary

Direction of error*	Value of IGS error at guidance ter- mination (76,000 ft) (n mi)	Spacecraft miss distance from intended target at impact (n mi)
Downrange	0 ± 0.3	5.1 ± 0.5 (long)
Crossrange	-4.9 ± 0.3 (south)	2.9 ± 0.5 (north)
Vertical	-3.3 ± 0.3 (low)	

*Downrange/crossrange error estimates are based on an approach azimuth of 94° from North.



Table 3-3. Effects of Error at Guidance Termination (76,000 Feet) in IGS Coordinates

Error source	Unit	Coefficient	X (ft)	Y (ft)	Z (ft)	\dot{X} (ft/sec)	\dot{Y} (ft/sec)	\dot{Z} (ft/sec)
X accelerometer bias	μg	6.23 ± 10	317			0.2		
Y accelerometer bias	μg	43.58 ± 10			-2,221			-1.7
Z accelerometer bias	μg	46.69 ± 10		2,469			2.7	
Platform roll alignment	arc sec	$-2,337 \pm 150$		56	-21,683		-1.0	-226.5
Platform pitch alignment	arc sec	$-2,000 \pm 300$	-18,556	-5,902		-199	-117	
Platform yaw alignment	arc sec	$-1,565 \pm 150$	-37		-4,618	0.7		-91.7
Y gyro input axis unbalance	o/hr/g	-0.715 ± 0.4	-1,422	-855		-21.5	-14.9	
Timing scale factor	ppm	-86 ± 65	-1,832	2,952	-14	-9.4	6.6	0.2
X accelerometer scale factor	ppm	-46 ± 113	33			-0.64		
Z accelerometer scale factor	ppm	-451 ± 64		876			9.2	
Initial conditions	ft, ft/sec	(See table 3-4)	-280	1,200	290	-0.9	-0.8	1.3
Unexplained position	ft		1,500	2,000	2,000			
		Total	-20,300	2,800	26,200	-230.0	-115.0	-318.0

~~CONFIDENTIAL~~

(state) vector, the telemetered time from retrofire, and properly scaled and biased accelerometer count data. The reconstructed IGS trajectory was then compared to the radar-determined trajectory (see Figure 3-2). A visual analysis was made in which probable error sources were combined to provide an explanation for the observed IGS/radar residuals.

In addition to providing an explanation (or fit) of the IGS radar residuals, the recovered error sources were constrained to provide explanations for differences between the IGS and nominal estimates of spacecraft main chute deployment altitude, descent rate, and available wind velocity data. The altitude rate was fit to approximately 30 feet per second during main chute descent. However, analysis showed that the drogue chute altitude could not be fit to an assumed 50,000-foot nominal value. After removal of the drogue altitude constraint, the analysis showed an estimate for the actual drogue chute deployment to be 37,000 feet (which was later substantiated by NASA's determination of a 38,000-foot drogue altitude).

The following sections provide discussions of the recovered reentry error sources listed in Table 3-3.

3.2.1 Initial Conditions

Reentry initial conditions input into the IGS were computed by the real time computer complex (RTCC), using the Carnarvon, Revolution 42 update, approximately one orbit prior to retrofire. The RTCC initial position/velocity vector is presented in Table 3-4 and compared with TRW estimates of the retrofire position/velocity vector. The TRW vector was derived from the postflight orbit reconstruction program (ESPOD) by fitting pre-retrofire and post-retrofire free flight tracking data while including a solution for the retrofire maneuver.

The agreement between the RTCC and TRW (ESPOD) vectors is well within 1000 feet and 1 foot/second, and is considerably smaller than has been noted on previous flights.

It is interesting to investigate the ESPOD solution for the retrofire maneuver. Table 3-5 gives the indicated IGS retrofire maneuver and small additional impulse apparently resulting from the retrosection

~~CONFIDENTIAL~~

Table 3-4. Gemini 10 Reentry Retrofire Vector Summary
(21 July 20^h30^m51.0^s GMT)

[Coordinates are those used in the MSC RTCC - ECI, X through Greenwich at 0 hours day of launch (18 July).]

Vector	IGS (RTCC)	TRW (ESPOD)	RTCC - TRW
X (ft)	-13,815,300	-13,814,853	-447
Y (ft)	17,301,300	17,302,284	-984
Z (ft)	-746,400	-747,096	+696
\dot{X} (ft/sec)	-17,381.1	-17,380.9	-0.2
\dot{Y} (ft/sec)	-13,556.7	-13,555.9	-0.8
\dot{Z} (ft/sec)	12,137.7	12,137.7	0

Table 3-5. Retrofire Maneuver Summary

Impulse source	$\Delta\dot{x}$ (ft/sec)	$\Delta\dot{y}$ (ft/sec)	$\Delta\dot{z}$ (ft/sec)
IGS indicated retrofire	-303.0	118.7	-5.0
Retro jettison	<u>-0.3</u>	<u>0.3</u>	<u>0</u>
Total indicated impulse	-303.3	119.0	-5.0
IGS misalignment error	<u>1.1</u>	<u>2.9</u>	<u>3.6</u>
Corrected retrofire impulse	<u>-304.4</u>	<u>116.1</u>	<u>-8.6</u>
ESPOD (free flight reconstruction)	-304.5	117.4	-9.7

jettison (retrofire plus 55 seconds) as obtained from telemetered IGS data (see sensed velocity plots Figure 3-4). Subtracted from the indicated maneuver is the net error in the IGS measurement resulting from the estimated platform misalignment. The ESPOD reconstruction value can then be compared with this adjusted IGS value. The agreement is very good and within the uncertainty generally associated with the trajectory reconstruction. The IGS platform misalignment errors were deduced from atmospheric IGS/tracking comparisons and terminal position/velocity criteria as described in paragraph 3.2.2. Large changes

CONFIDENTIAL

would be required in the IGS misalignment error estimates during atmospheric reentry to significantly change the indicated IGS retrofire measurement error shown in Table 3-5. This comparison, therefore, supports the validity of the ESPOD maneuver solution.

3.2.2 Alignment Errors

The primary assumption in attempting to extract IGS error sources during reentry was that platform alignment errors were most likely the dominant sources. Using this guideline, a set of alignment errors were determined which removed the error trend indicated in the IGS/tracker position comparisons of Figure 3-2. (Analysis could not be conducted in the velocity domain because of the very high noise on the differentiated radar position measurements.) Some tradeoff with gyro-drift type errors was required to satisfy both the radar tracking data and expected terminal phase conditions.

The platform alignment error coefficients recovered are consistent with those recovered on previous flights and provide an explanation for the major portion of the IGS trajectory error. This is evident in Table 3-3 which shows that the contributions of the misalignment errors are within 17 and 20 percent of total IGS trajectory x and z position errors respectively. The y axis contribution, although also large, had an approximate magnitude equal to the combination of all other contributors, but was in the opposite direction such that the total y error was quite small.

3.2.3 IGS Error Sources

The accelerometer bias errors listed in Table 3-3 were obtained from post retrofire IGS accelerometer output during free-flight. The X and Z accelerometer and timing scale factor errors were recovered during the ascent IGS analysis, as described in Section 2. These were included in the corrections to the IGS indicated reentry trajectory; however, the accelerometer scale factor errors do not contribute significantly to the fit.

The pitch gyro drift error was recovered after initial attempts to explain IGS/tracker differences with only platform alignment errors successfully nulled the IGS/radar differences, but a trajectory was produced which went down to a 20,000-foot altitude and then began

CONFIDENTIAL

climbing again. A more satisfactory trajectory resulted when the Y gyro input axis unbalance term (YGIAU) was substituted for part of the misalignment error used in the original fit. The position error propagations during reentry of a Y gyro input axis unbalance error (YGIAU) and a pitch misalignment (PHIY) are shown in Figure 3-5. It is noted that though their propagation is similar during the interval of radar tracking (1550 to 1820 seconds), the gyro drift error grows much faster than the misalignment error during the terminal phase of flight (1870 seconds and



The difference is undoubtedly due to a combination of error sources which were not identified in the analysis. Among these are:

- a) Small error in the assumed (ESPOD) initial conditions. This source is particularly sensitive since it propagates for 1500 seconds before being "observed" in the reentry radar comparison data.
- b) Incorrect selection of IGS error sources which, though they explain the very large error trends (over 25,000 feet and 200 feet/second), do not generate a completely consistent trajectory from retrofire to splashdown.
- c) Inadequate error modeling to account for the error in the calculation of gravity resulting from the IGS errors.
- d) Undiscovered systematic biases in the radar measurements.

Since the main goal of the analysis was to generate the most accurate trajectory reconstruction possible during atmospheric reentry, the apparent position bias was removed in the trajectory published here by arbitrarily altering ESPOD initial conditions as indicated below (ESPOD-BET).

$$\begin{aligned}\Delta x &= 705 \text{ ft} \\ \Delta y &= 600 \text{ ft} \\ \Delta z &= 2104 \text{ ft} \\ \Delta \dot{x} &= -0.8 \text{ ft/sec} \\ \Delta \dot{y} &= 0.2 \text{ ft/sec} \\ \Delta \dot{z} &= 3.7 \text{ ft/sec}\end{aligned}$$

3.3 REENTRY SIMULATION

A six-degree of freedom simulation of the Gemini 10 reentry was conducted by McDonnell Aircraft. The simulation was initialized with the RTCC retrofire position/velocity vector which initialized the IGS, assumed preflight aerodynamic characteristics, and the best postflight estimate of the spacecraft center of gravity. Comparisons of the simulation results with the TRW BET (Figure 3-6) show residuals of -6300, 9083, and -9446 in the IGS x, y, and z axes, respectively, at 1400 seconds. Similar differences were noted between the simulation and a reconstruction of the post retrofire free-flight interval prior to atmospheric reentry derived from the orbit reconstruction program (ESPOD).

CONFIDENTIAL

The available data were not sufficient for determination of the apparent simulation error which caused a large residual even before atmospheric reentry. However, the error could not have been due only to the initial vector, since the ESPOD and RTCC vectors were relatively close (see Table 3-4), but may be associated with the incorporation of the incorrect retrofire maneuver in the simulation.

During atmospheric reentry the error became an order of magnitude worse, since the computations probably used erroneous drag acceleration derived from simulation computed spacecraft altitude. The (simulation-BET) residuals steadily increased from the values at 1400 seconds to approximately 119,000, -222,000 and 29,000 feet in x, y and z at the last telemetry data point (t = 2062).

No comparison was made between the TRW reconstruction and the reentry trajectory presented in the MSC Final Report (Reference 6).

3.4 CONCLUSIONS

- a) The IGS computed trajectory was approximately 3.9 n. mi. south and 0.36 n. mi. west of the actual trajectory at guidance termination. The actual trajectory was approximately 2.5 n. mi. north and 6.0 n. mi. east of the intended target at splashdown.
- b) Approximately 80 percent of the apparent IGS error is attributable to platform alignment error of approximately 0.6 degree at retrofire.
- c) MSC real-time (RTCC) and TRW postflight (ESPOD) estimates of the retrofire position/velocity vector were within expected tolerances. However, the final TRW BET indicates the possibility of cross-range (z) differences of approximately 3000 feet and 3.7 feet per second.
- d) Large differences exist between a McDonnell simulated reentry trajectory and both the TRW reconstructions during the post-retrofire free-flight interval and the atmospheric reentry BET. The major source of the difference is in the simulation.

3.5 REENTRY TRAJECTORY RECONSTRUCTION

The reentry trajectory reconstruction consists of the IGS data corrected for initial conditions, initial platform misalignment, and IMU error sources as presented in Table 3-3. A listing of the BET is provided in Appendix B.

CONFIDENTIAL

CONFIDENTIAL

The data are provided in an earth-centered inertial coordinate system. The z axis is aligned with the earth's rotational axis, positive north, and the x-y plane is the equatorial plane with the x-z plane containing the Greenwich meridian at retrofire time. Trajectory parameters such as velocity magnitude, altitude, flight path angle, heading, latitude and longitude are also printed. Time is referenced to retrofire.

Figure 3-7 is a plot of reentry relative velocity, flight path angle, and altitude versus time from retrofire. The uncorrected sensed acceleration and velocity are plotted in Figure 3-8.

CONFIDENTIAL



Figure 3-1. Gemini Reentry Ground Trace

CONFIDENTIAL

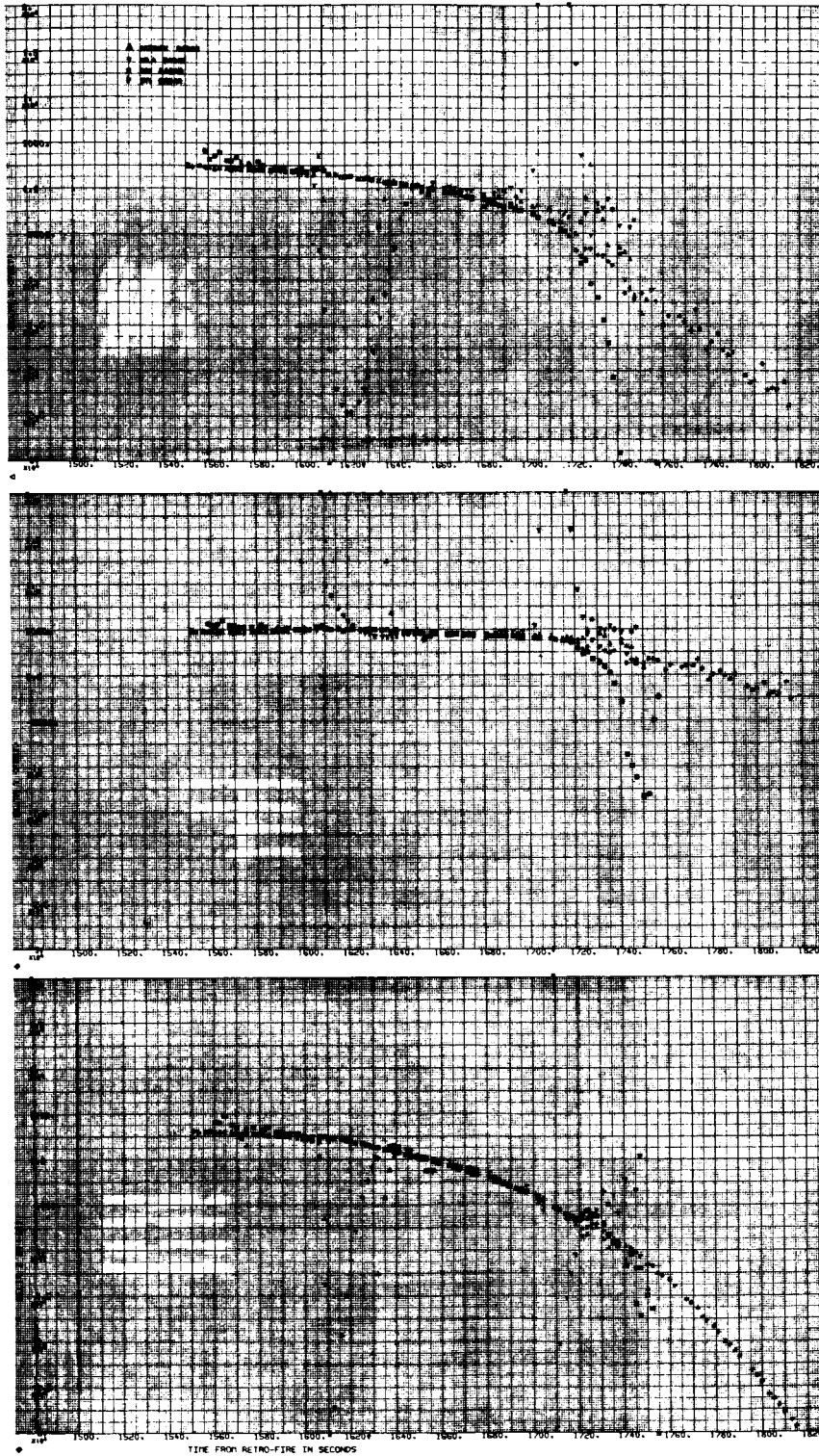
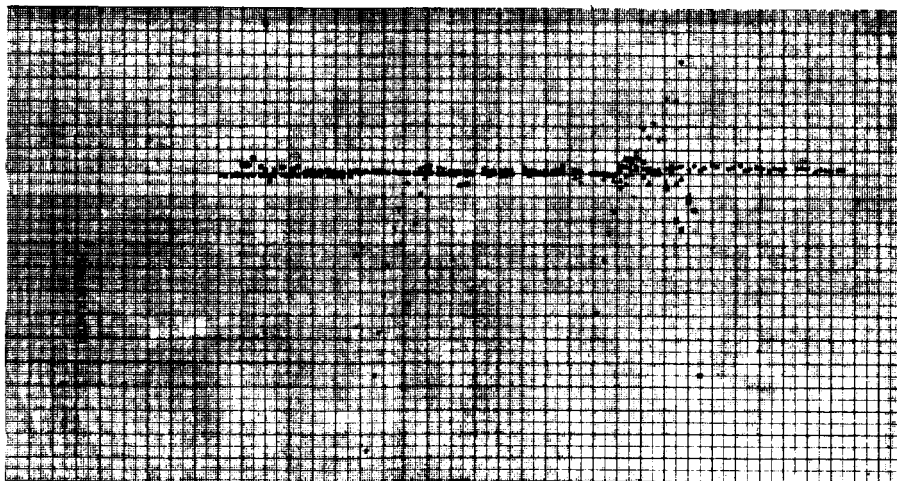
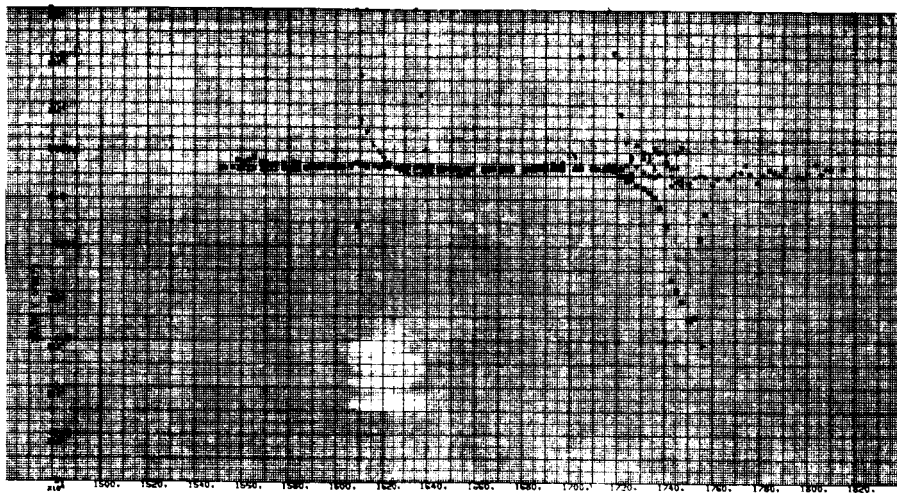
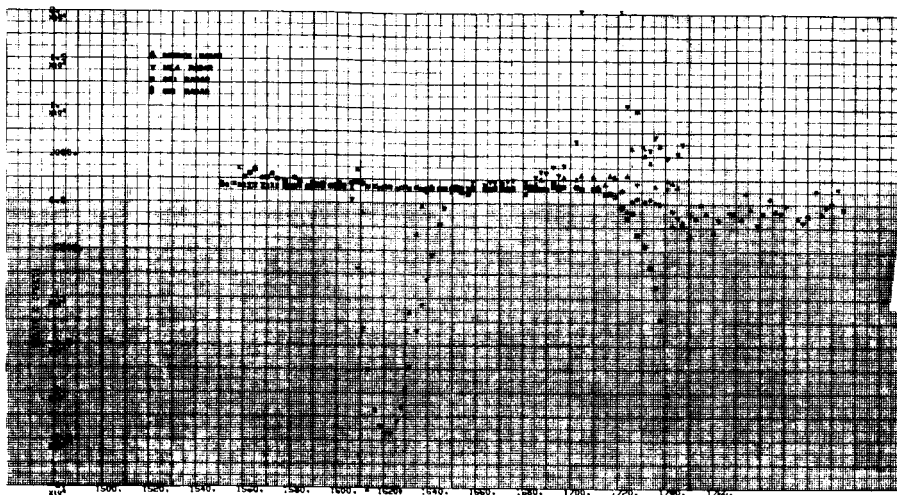


Figure 3-2. Uncorrected IGS - Radars in IGS Coordinates

CONFIDENTIAL



TIME FROM METRIC-FINE IN SECONDS

Figure 3-3. Corrected IGS - Radars in IGS Coordinates

CONFIDENTIAL

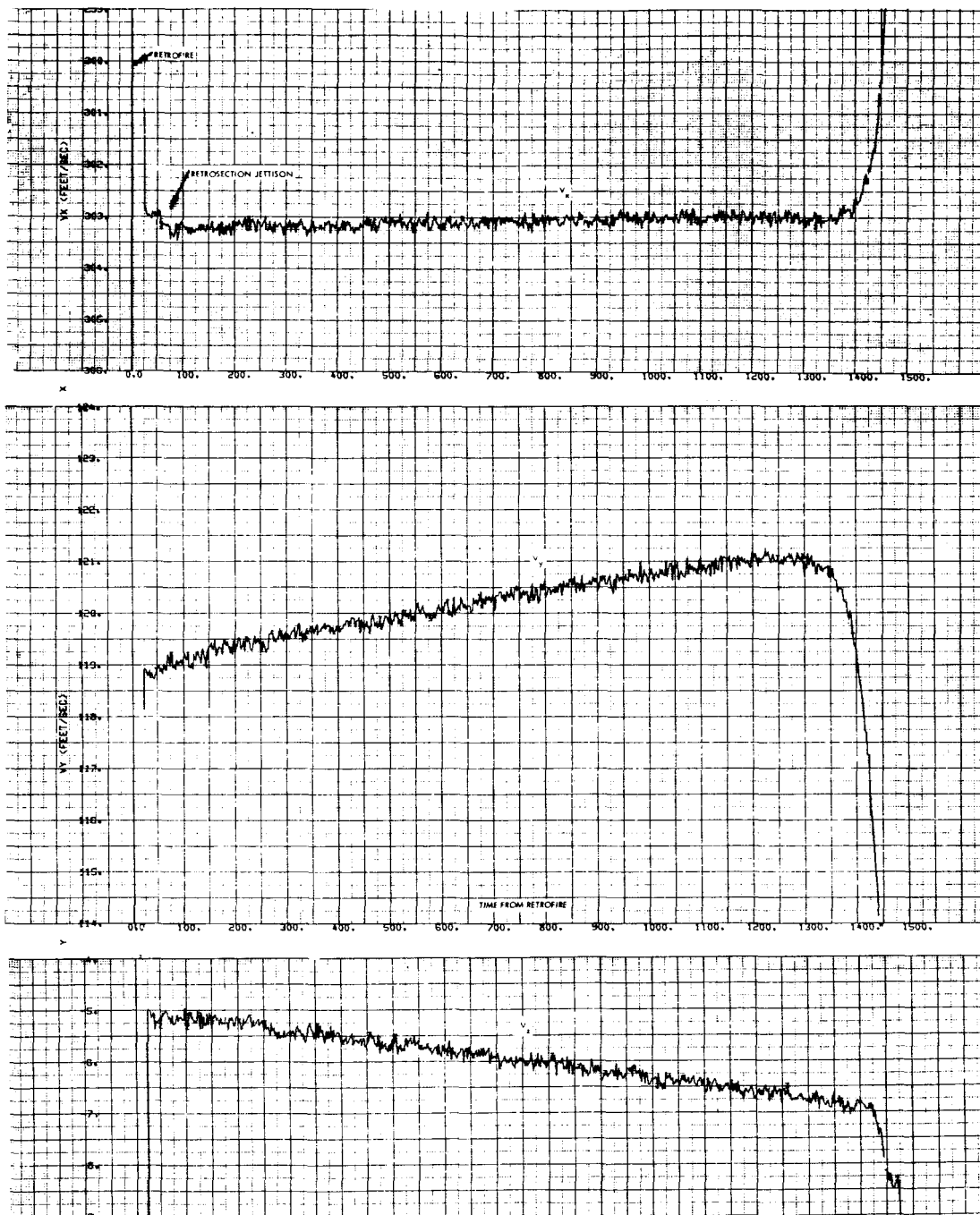


Figure 3-4. Post Retro IGS Indicated Sensed Velocity

CONFIDENTIAL

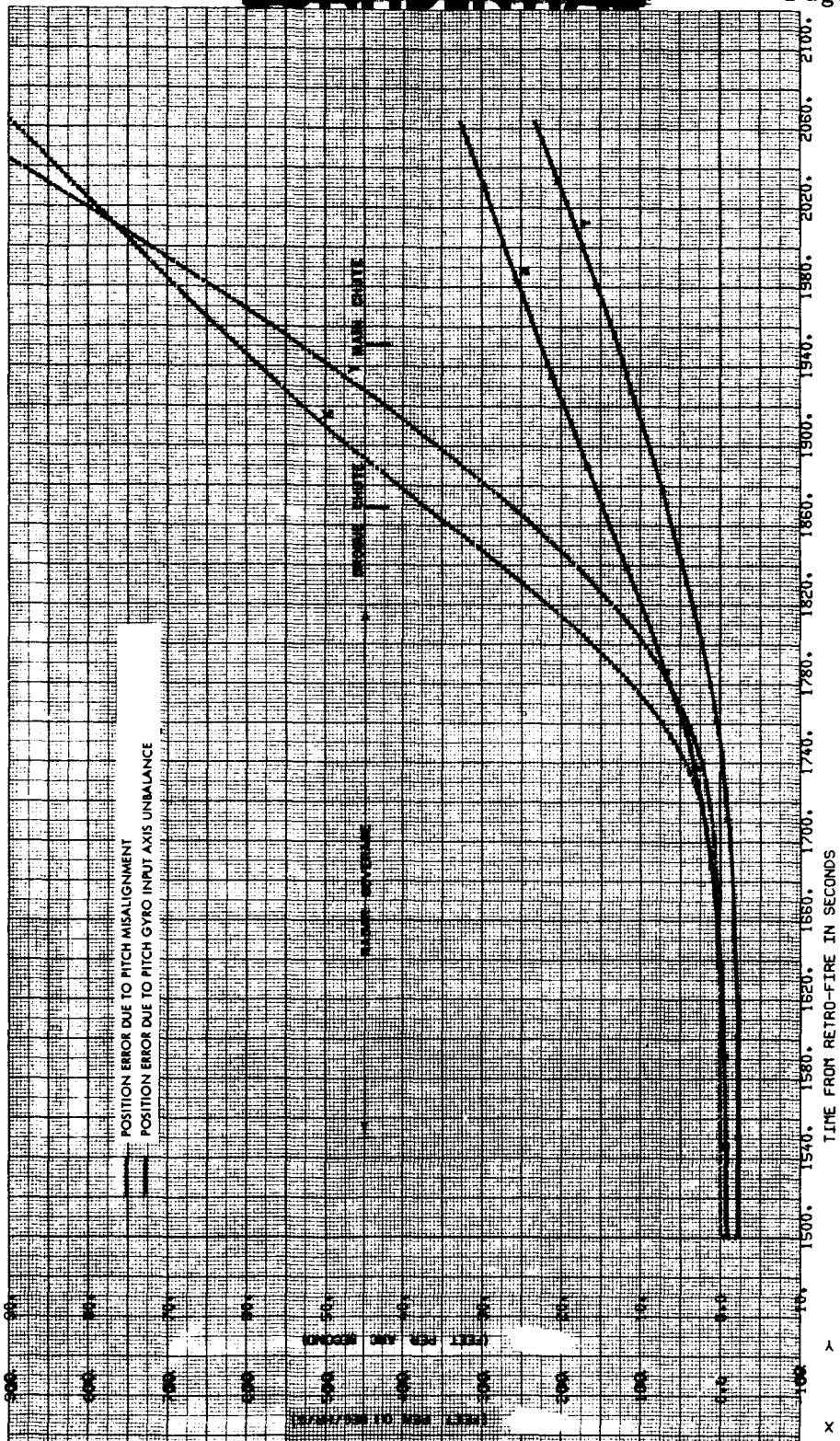


Figure 3-5. Reentry Error Functions

CONFIDENTIAL

CONFIDENTIAL

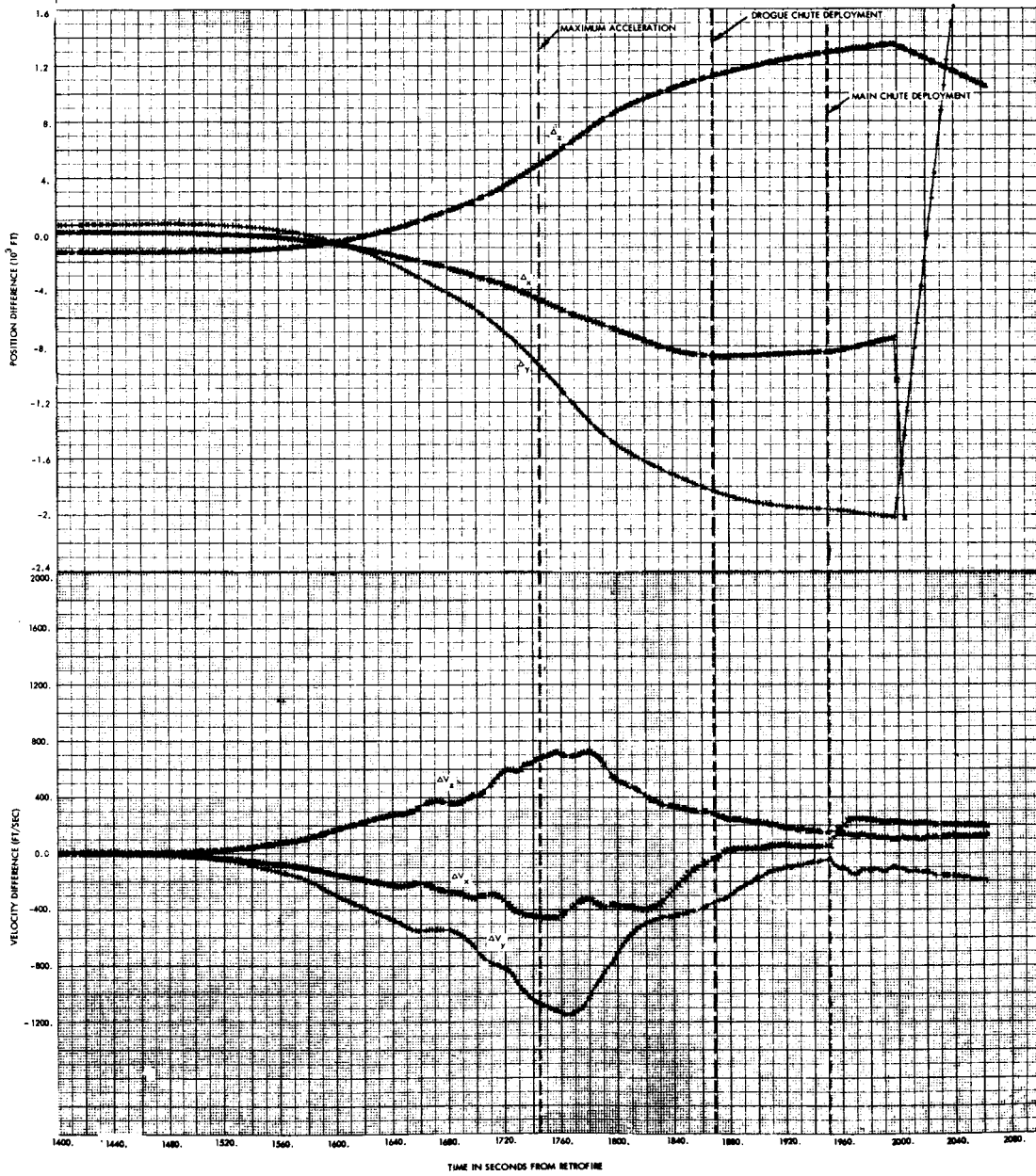


Figure 3-6. TRW BET - McDonnell Simulation Differences (IGS Coordinates)

CONFIDENTIAL

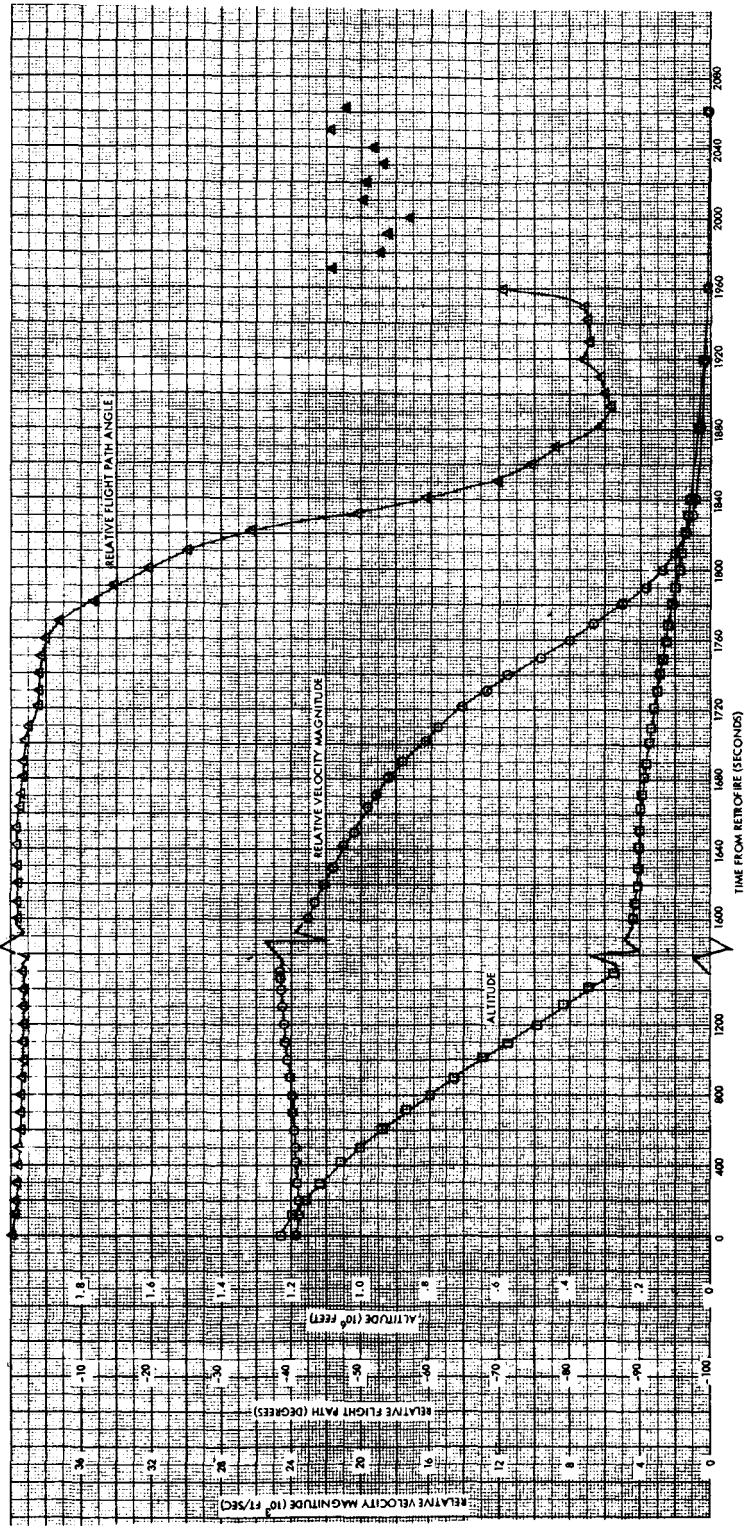


Figure 3-7. Reentry Trajectory Parameters

CONFIDENTIAL

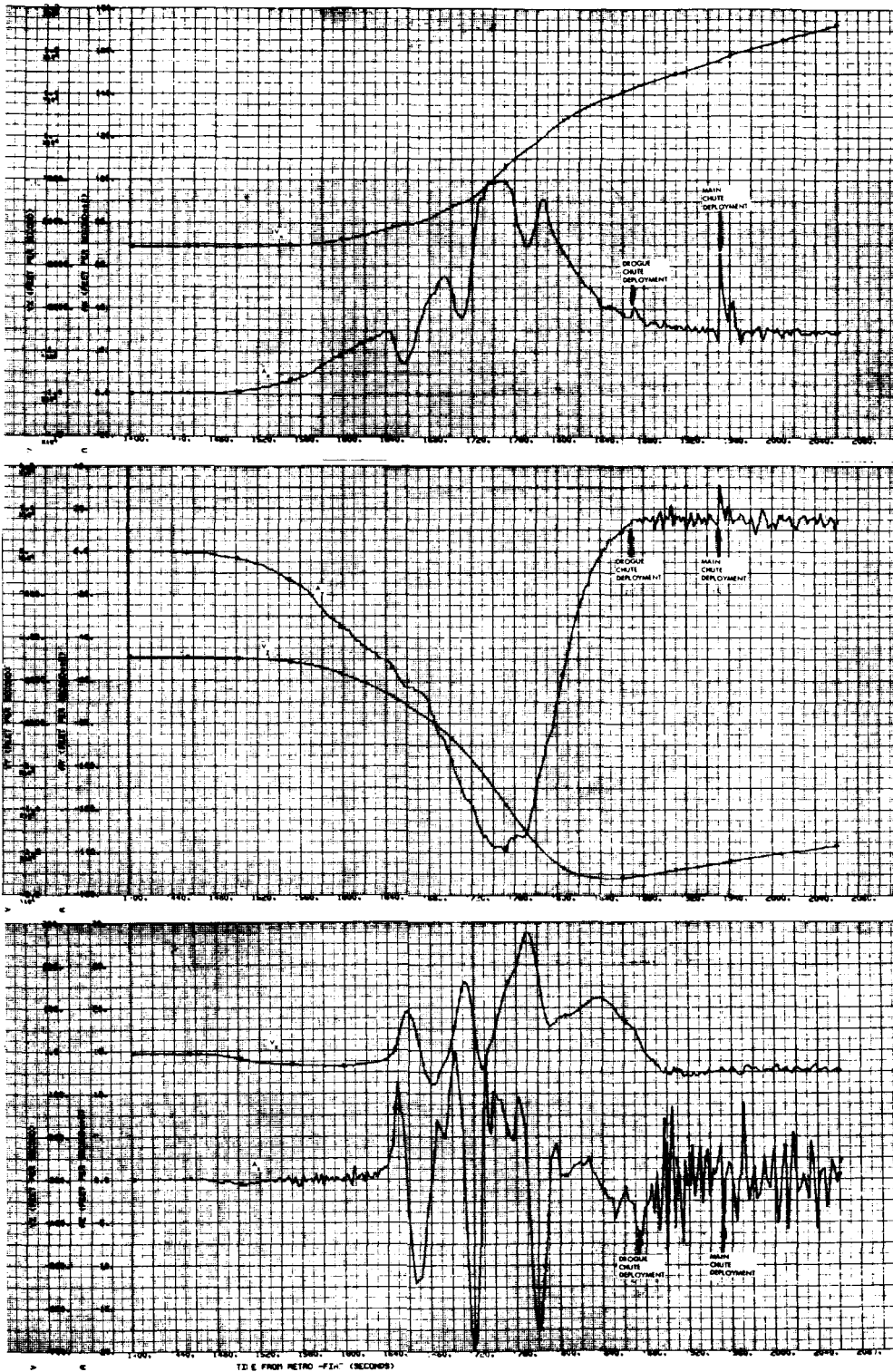


Figure 3-8. IGS Measured Sensed Velocities and Accelerations

CONFIDENTIAL

4. TRACKING SYSTEM PERFORMANCE

This section provides an evaluation of the ascent phase tracking data which included the following:

- a) GE MOD III Burroughs (TRW reduction)
- b) GE MOD III Burroughs (GE reduction)
- c) MISTRAM I quick-look 10K and 100K
- d) AFETR MISTRAM - only BET (Glad reduction)
- e) Air Force Eastern Test Range (AFETR) BET

Each of the above sets was used for position and velocity comparisons as described in Section 2. The TRW reduced GE MOD III Burroughs data were used for quick-look analysis, and the MISTRAM I and GE reduced MOD III Burroughs data were used for detailed analysis. The two AFETR BET's were also used to help substantiate the analysis.

Tracker error sources recovered from the ensemble IMU/tracking system analysis discussed in Section 2 are presented in Table 4-1. MISTRAM bias errors recovered from the AFETR BET programs are also presented for comparison purposes. The table shows that MISTRAM and GE errors were small on this flight and that there is good agreement among the error sources obtained from the separate analyses.

Figures 4-1 through 4-6 are comparisons of tracking data with inertial guidance data which had been corrected for IGS error sources derived from the IGS analysis (see Section 2). These are provided to give a clear indication of tracking data quality.

4.1 GE MOD III

4.1.1 GE MOD III Burroughs (TRW Reduction)

The GE/MOD III data, which consisted of raw counts recorded at a 2-per-second rate on punched paper tape, were transferred to magnetic tape at TRW and processed in the data reduction programs.

Figures 4-1 and 4-2 show comparisons of this data with compensated IGS data in IGS coordinates. The comparisons indicate that there

CONFIDENTIAL

CONFIDENTIAL

Table 4-1. Recovered Tracking Error Coefficients

System error	Units	TRW analysis		AFETR MISTRAM - Only BET		AFETR Final BET	
		Estimated bias	1 σ uncertainty	Estimated bias	1 σ uncertainty	Estimated bias	1 σ uncertainty
R SUM	ft	- 5.0	1.0	-11.0	1.85	2.82	1.519
P 10K	ft	- 0.12	0.02	- 0.16	0.0075	-0.14	0.0006
Q 10K	ft	- 0.19	0.17	- 0.098	0.011	-0.08	0.008
P 100K	ft	- 0.50	0.10	- 0.75	0.077	-0.57	0.065
Q 100K	ft	**		- 0.62	0.10	-0.45	0.076
Refraction	n-unit	- 0.48	2.0				
R	ft	-23	3.8	N/U		N/U	
A	mrad	- 0.0027	0.016	N/U		N/U	
E	mrad	+ 0.044	0.011	N/U		N/U	
Refraction	n-unit	- 4.44	2.22	*		*	
Timing	sec	- 0.00061	0.00022	*		*	

* Not included in error model Note: AFETR bias estimates were obtained from References 4 and 5.

** Could not be reliably extracted

N/U-GE MOD III position data not included in AFETR BET

CONFIDENTIAL

CONFIDENTIAL

is negligible tracking data position bias error, and the random and low frequency noise amplitude is large late in flight.

4. 1. 2 GE MOD III Burroughs (GE Processed)

The General Electric Company processes essentially the same 2-per-second MOD III Burroughs data; however more filtering and a refraction correction incorporating actual atmospheric conditions are applied. The GE processed data were available smoothed in both tracker natural measurement coordinates ($R, A, E, \dot{R}, \dot{P}, \dot{Q}$) and in ECI cartesian coordinates. The natural measurement coordinate data were used in the computer regression analysis and for plots included in this report.

Figures 4-1 and 4-2 also show the GE processed MOD III/compensated IGS differences. Comparisons with the TRW reduced MOD III clearly show the noise reduction resulting from the increased filtering incorporated in the GE data reduction. However, there are residual trends in the comparisons. The residuals of the GE processed data are for the most part attributed to errors in the tracking data which are partially explained by the GE MOD III errors presented in Table 4-1. From the error sources recovered, only the 4.4 n. unit refraction error contributes significantly to the observed IGS/tracker differences (0.08, +4.8 and +0.02 ft/sec in \dot{x} , \dot{y} , \dot{z} respectively). The TRW processed data also show a refraction type error, but of opposite sign to the GE processed data.

4. 2 MISTRAM

The MISTRAM I data received at TRW were fully scaled and corrected but unsmoothed Range Sum, P, and Q measurements. The data were processed in the usual manner to obtain IGS/MISTRAM I position and velocity comparisons.

Figures 4-3 and 4-4 show the MISTRAM I 10K and 100K/compensated IGS comparisons. The MISTRAM I 10K/IGS comparisons show no significant trends; however the MISTRAM 100K/IGS comparisons show trends resulting in approximately 0, +6.5, and +1 ft/sec \dot{x} , \dot{y} and \dot{z} errors respectively at SECO +20 seconds ($t = 360$). The TRW recovered MISTRAM I error sources presented in Table 4-1 contribute to the

CONFIDENTIAL

CONFIDENTIAL

explanation of these apparent velocity errors. The 6.5 ft/sec \dot{y} residual is attributable to the $-0.5 \text{ ft } P_{100K}$ bias error which was the most significant error on this flight, but was much less than those observed on previous Gemini flights.

4.3 AFETR BEST ESTIMATE OF TRAJECTORY

The MISTRAM-only BET is computed by means of the AFETR GLAD program using MISTRAM I (10K and 100K) and MISTRAM II measurements. The solution is obtained from a least-squares adjustment of measurement biases and trajectory values. No refraction errors are solved.

The AFETR Final BET is a weighted least squares adjustment of measurements obtained from MISTRAM I and II, GE MOD III (\dot{P} , \dot{Q} , \dot{R}), and available FPQ-6 radar data.

Figures 4-5 through 4-6 show the AFETR MISTRAM only and Final BET's compared with compensated IGS data which is in fact the TRW BET (see Section 2). The comparisons show only small differences between the respective AFETR BETS. This is consistent with the essentially equivalent recovered MISTRAM error sources listed in Table 4-1. The AFETR MISTRAM-only and final BET's generally have agreed on Gemini flights. This is most likely because of relatively heavy weighting of MISTRAM I data in both BET solutions.

4.4 CONCLUSIONS

The tracking system performance was satisfactory, and MISTRAM I bias errors were small relative to previous flights. The GE MOD III data was of expected quality; however, there was an apparent 4 n. unit refraction error in the GE processed MOD III data.

CONFIDENTIAL

CONFIDENTIAL

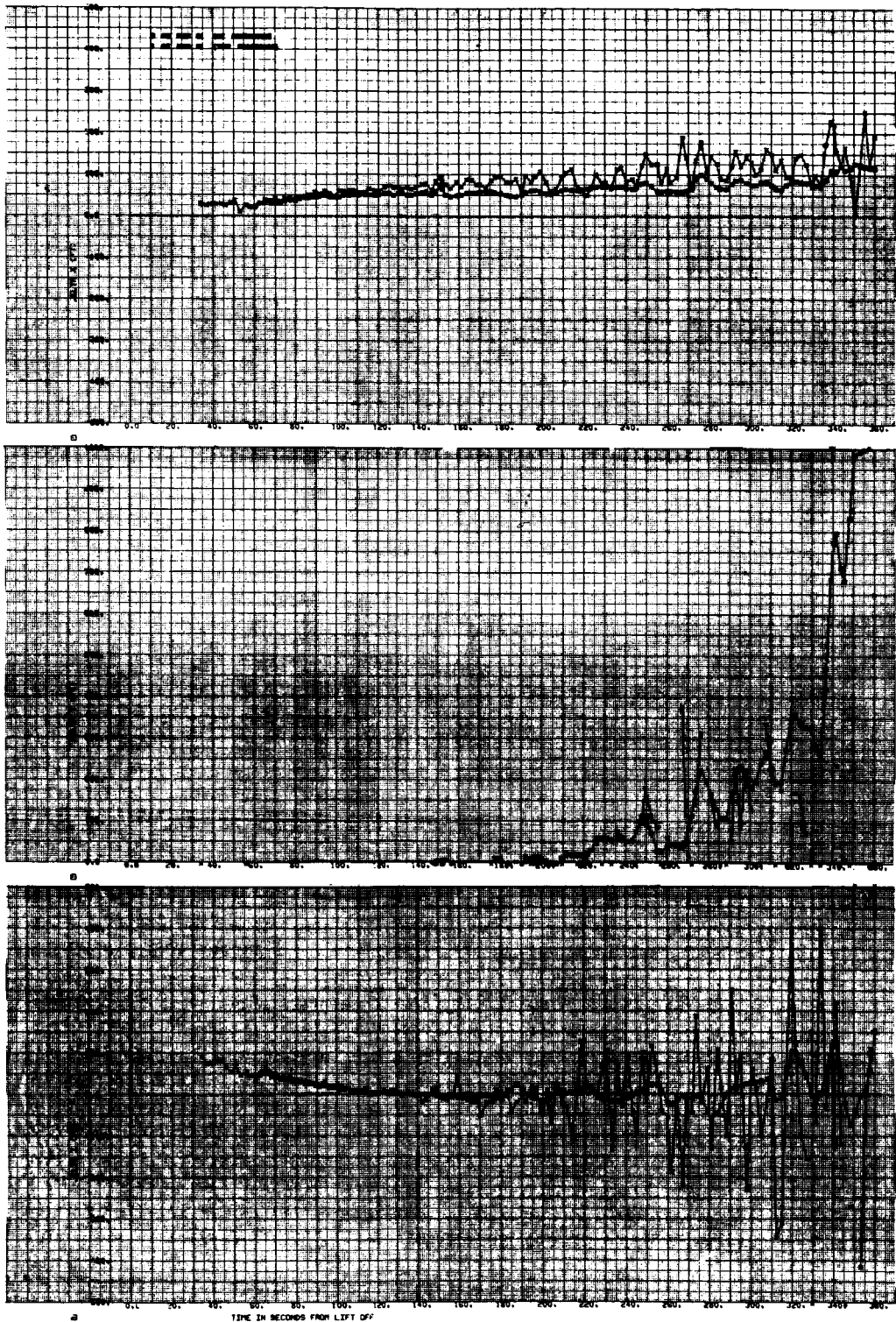


Figure 4-1. Sensed Position Comparison in Computer Coordinates (GE/Compensated IGS)

CONFIDENTIAL

CONFIDENTIAL

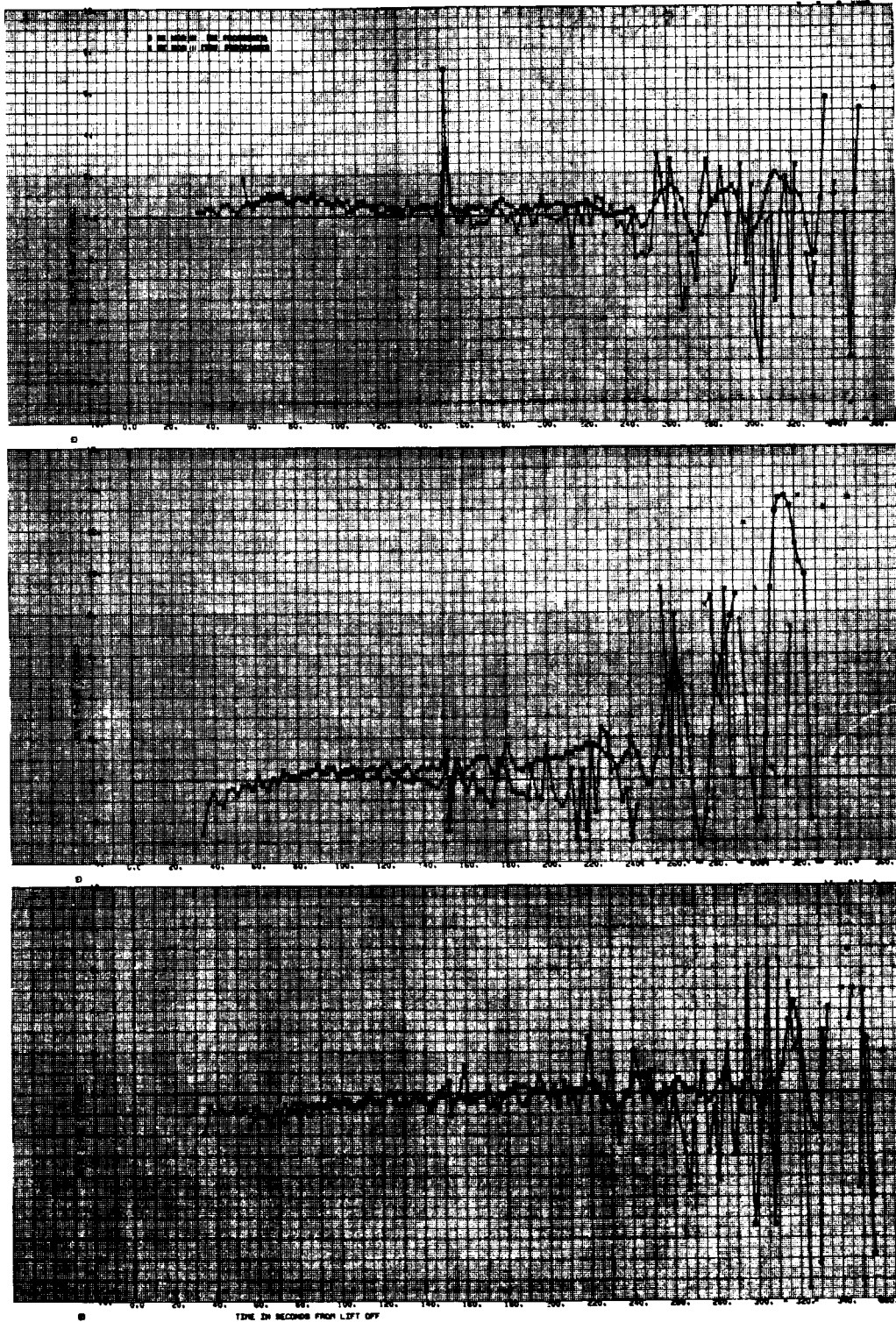


Figure 4-2. Sensed Velocity Comparison in Computer Coordinates (Mod III/Compensated IGS)

CONFIDENTIAL

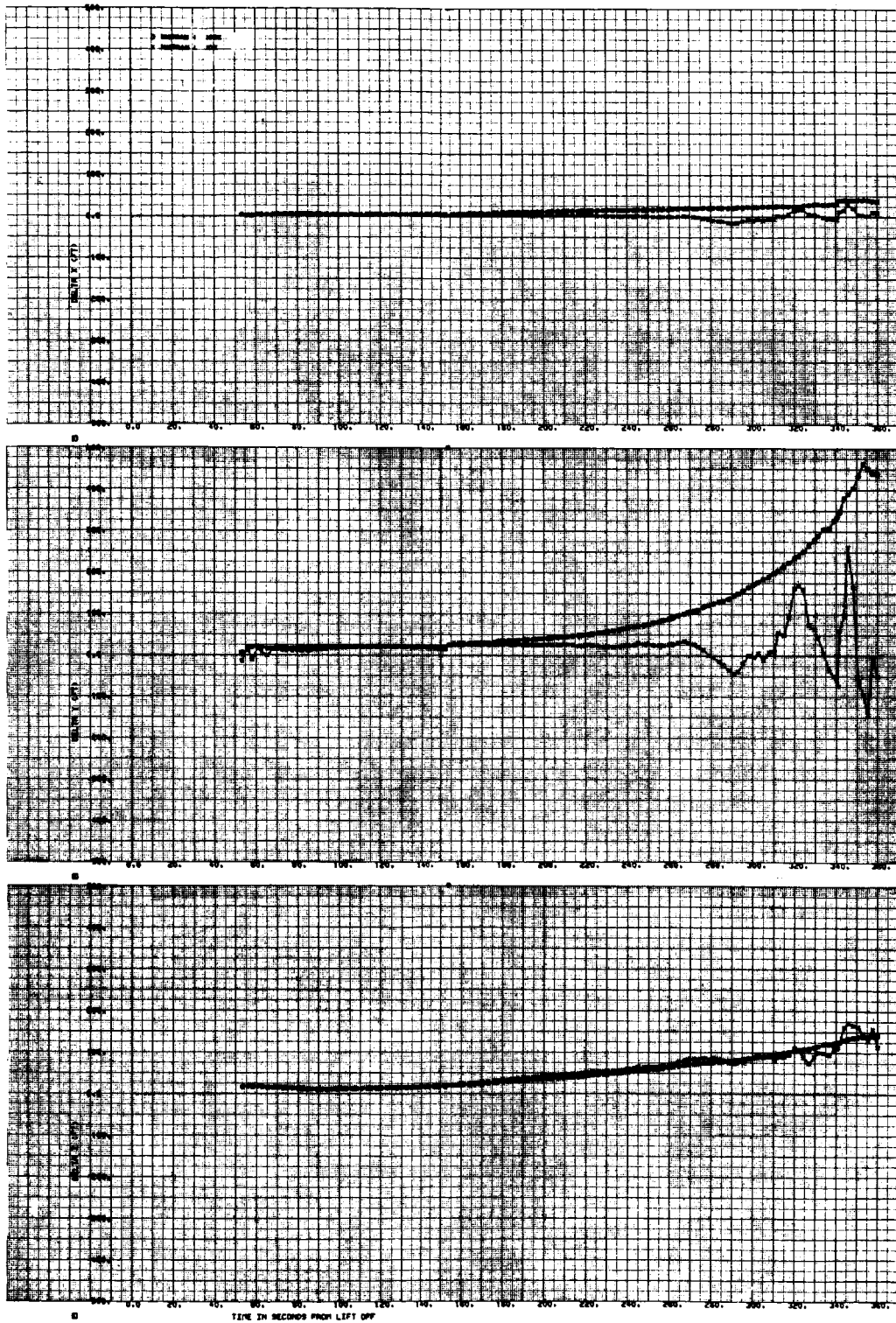


Figure 4-3. Sensed Position Comparison in Computer Coordinates (MISTRAM/Compensated IGS)

CONFIDENTIAL

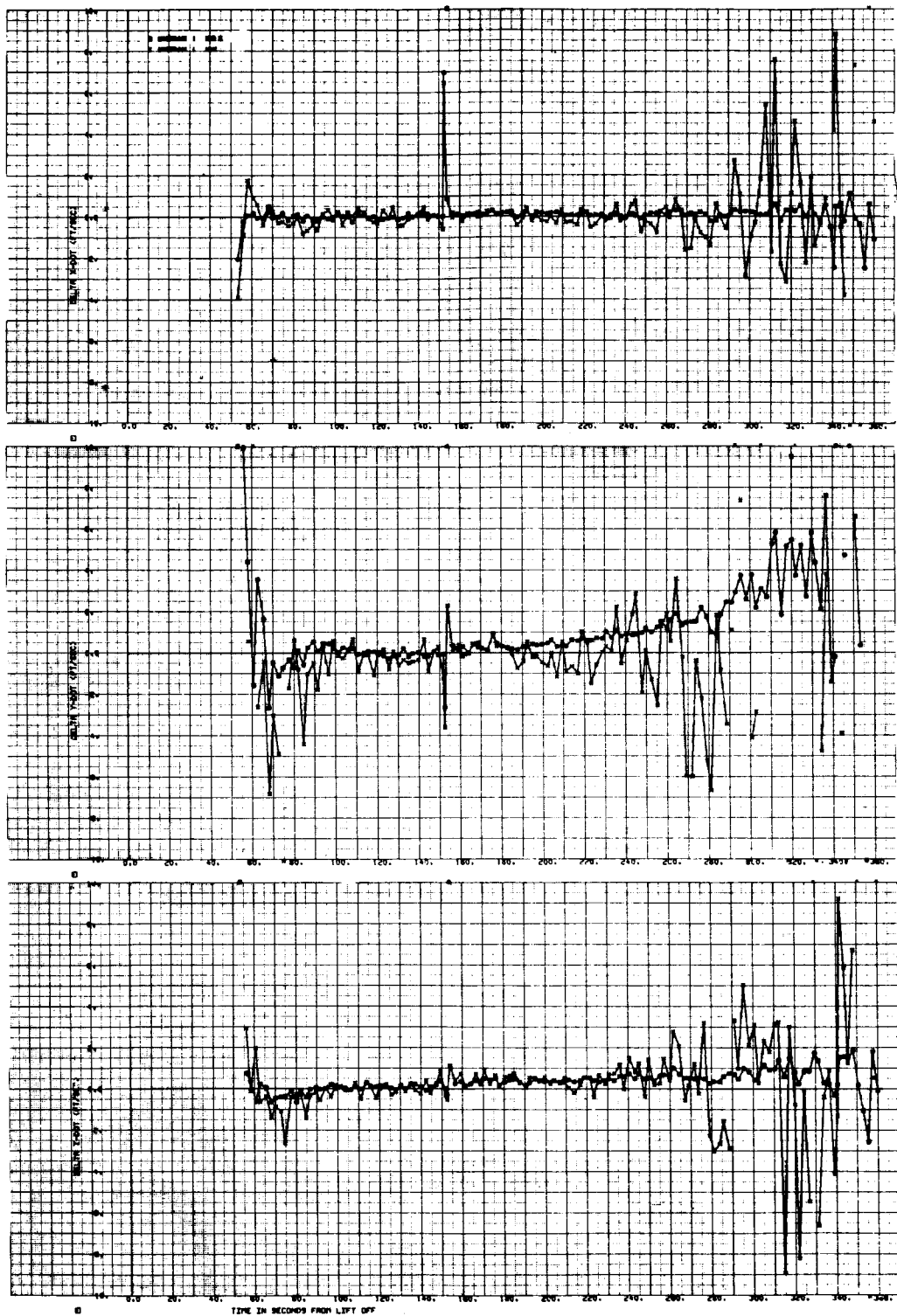


Figure 4-4. Sensed Velocity Comparison in Computer Coordinates (MISTRAM/Compensated IGS)

CONFIDENTIAL

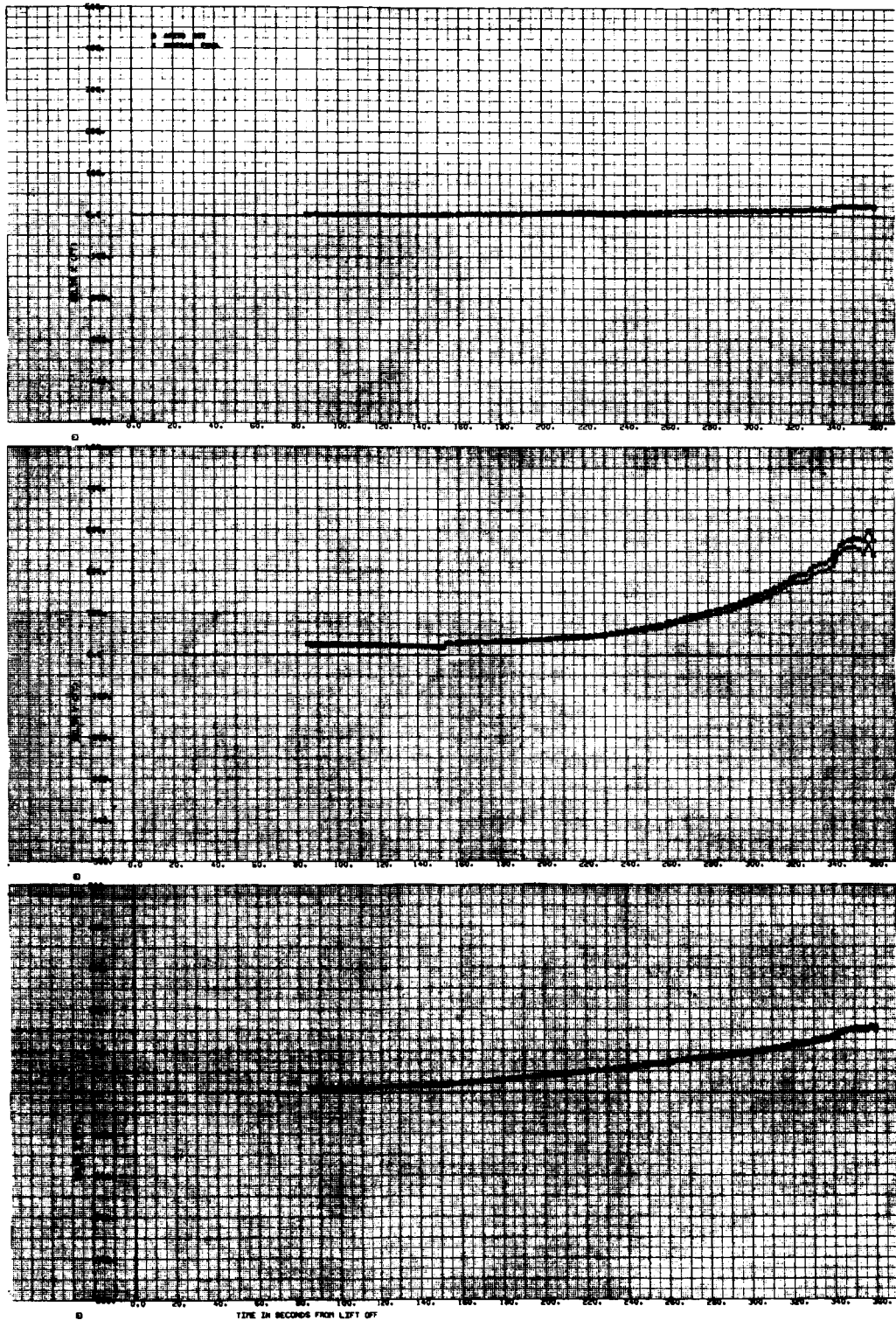


Figure 4-5. Sensed Position Comparison in Computer Coordinates
Coordinates (BET and MF/Compensated IGS)

CONFIDENTIAL

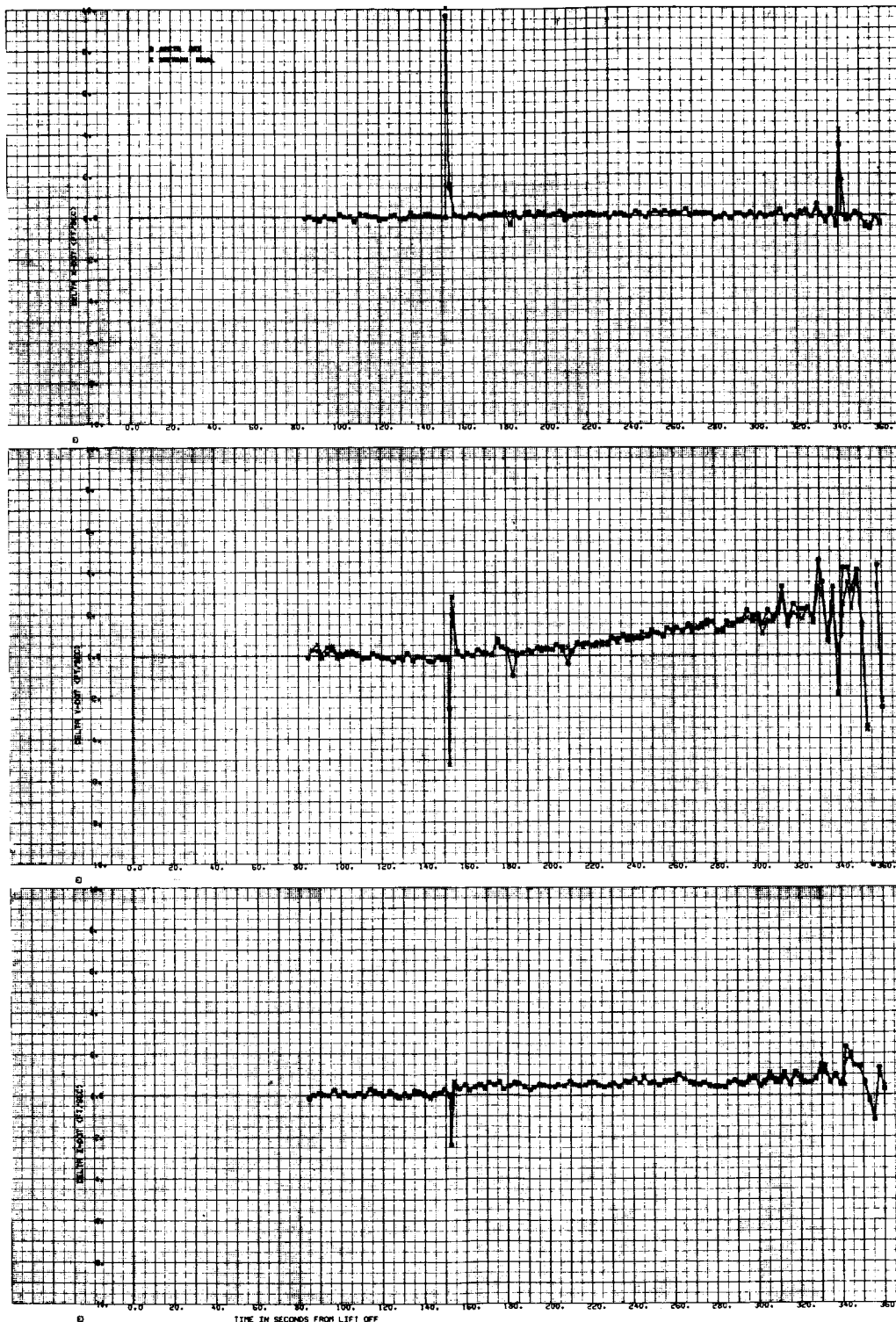


Figure 4-6. Sensed Velocity Comparison in Computer Coordinates (BET and MF/Compensated IGS)

CONFIDENTIAL

5. RENDEZVOUS RADAR EVALUATION

5.1 INTRODUCTION

This section presents the results of the analysis of the Gemini 10 rendezvous radar. The radar evaluation was made by comparing the telemetered onboard radar measurements (range, azimuth, elevation) to values obtained by reconstructing the relative trajectories of the Gemini 10 spacecraft and the Agena 10 target vehicle (ATV). The comparisons were made over the interval of time from radar acquisition through the terminal phase maneuvers preceding the first rendezvous. Refer to Figure 5-1 for help in interpreting the directional sense of the radar angular measurements and the IGS platform gimbals angles. It should be remembered that the radar is hard-mounted to the Gemini spacecraft. Details of the orbit reconstruction of both the Agena and Gemini BET can be found in the TRW Gemini 10 Orbit Report (Reference 3).

5.2 TELEMETRY DATA

The telemetered radar parameters are plotted in Figures 5-2, 5-3, and 5-4. A cursory explanation of the data follows. Before 220 minutes GET, the spacecraft appears to be drifting within $\pm 10^\circ$ of the local horizontal. After this time but prior to platform alignment (238 minutes GET), the angular radar measurements were relatively constant at -7° in elevation and $+1^\circ$ in azimuth; the relative range was between 120 and 100 n mi for this latter period. During alignment (238 to 253 minutes GET), the spacecraft must be held in the local horizontal; thus the elevation angle is offset by the angle between the Agena and the local horizontal and has a trend equal to the relative line-of-sight rate of the Agena. The azimuth measurements during alignment show a sinusoidal trend between plus and minus 3 degrees.

From the end of alignment to terminal phase finalization (TPF), the Agena was maintained near the spacecraft's boresight; i. e., the azimuth and elevation angles were near zero, as they should be for optimal radar accuracy.

CONFIDENTIAL

5.3 TRAJECTORY RECONSTRUCTION

5.3.1 Agna 10 Trajectory

The Agna 10 trajectory was reconstructed using the TRW orbit determination program (ESPOD) to fit all ground tracking data from Agna insertion to rendezvous. Since there were no Agna maneuvers, the reconstructed trajectory was estimated to be accurate to within 1000 feet.

5.3.2 Gemini 10 Trajectory Reconstruction

For the Gemini 10 spacecraft, two trajectories were generated.

- a) Gemini BET. This trajectory was made by fitting all ground tracking data over the interval of time from just after GT-10 insertion to TPF. IGS telemetric data were used to reconstruct the coelliptical (NSR) and the terminal phase maneuvers.

Prior to the end of platform alignment there was heavy ground radar coverage of the spacecraft. After platform alignment, there was very little ground tracking data - HAW 03 ($E_{MAX} = 15.6^\circ$) and CAL 03 ($E_{MAX} = 5.4^\circ$) - occurring just prior to and immediately following TPI, respectively. Coupled with the fact that there were four maneuvers to be reconstructed, the lack of ground radar coverage decreases the accuracy of the GEMINI trajectory reconstruction as the terminal phase progresses. The following are estimates of the accuracy of the BET:

Prior to the end of alignment	1000 feet
Prior to TPI	1500 feet
After TPF	3000 feet

- b) HAW 03 short arc fit. The ESPOD program was used to make a single station curve fit on the HAW 03 radar data which were collected just prior to TPI. This fit was made to check the accuracy of the BET during the interval of time that the spacecraft passed over Hawaii. The short arc fit agreed with the BET to within 1500 feet and this discrepancy was most likely caused by an apparent -0.03 degree elevation bias in this station.

5.4 ANALYSIS OF RENDEZVOUS RADAR OUTPUT

The Tracking Radar Analysis Program (TRAP) was used to compare the onboard radar data with the TRW calculated trajectories. The

CONFIDENTIAL

comparison was made in radar coordinates using telemetered gimbal angles to transform from IGS to body coordinates. The results are plotted in Figures 5-5, 5-6, and 5-7. Also annotated on these plots are the maneuver initiation times, the period of platform alignment, and the relative range of the Agena with respect to the spacecraft. The analysis was divided into four segments:

- Prior to platform alignment
- During alignment
- End of alignment to TPI
- TPI through TPF.

Table 5-1 gives the average residual magnitudes in range, azimuth, elevation, and total position, as well as an estimate of the uncertainty of the TRW relative trajectory for each of the above time intervals.

Prior to the platform alignment, it was estimated that the TRW reconstructed relative trajectory was accurate to approximately 1500 feet.

The elevation angle residuals (Figure 5-7) show a relatively constant offset of 2.5 degrees from 208 to 219 minutes GET, and then a shift to a much smaller difference of approximately 0.3 degree, which is then maintained nearly constant until alignment. During approximately the same period the azimuth residual (Figure 5-6) grows from a small value to a peak at 3 degrees and back to 0.5 degree, which is then nearly the same until alignment. Since the relative range was greater than 100 miles, these radar angle excursions represent total position differences of greater than 4 n. mi. Therefore, the error is clearly in the radar/platform measurements. An error of this shape is difficult to imagine in the platform alignment and, therefore, it was concluded to be a radar angle error. As seen in Figure 5-4, the target vehicle was considerably off the spacecraft's boresight, and it may be partially due to this fact that the radar angular measurements were relatively inaccurate.

~~CONFIDENTIAL~~

During the period of platform alignment, the azimuth residuals show the same ± 3 degree variations as noted in the total azimuth measurement (see Figures 5-3 and 5-6). These relatively abrupt changes must be due to onboard measurement error, since any bias error in the TRW-calculated azimuth is smooth. [MSC analyses of the horizon scanner/platform servo loop outputs indicate that the platform was momentarily torqued out of alignment. Approximately 80 percent of the misalignment was due to a spacecraft roll error which resulted in the platform misalignment. MSC also noted that some period of valid alignment mode remained even after the perturbation. This being the case, it would be expected that the major alignment error would be in the yaw direction. This error must be corrected by relatively slow gyrocompassing. The horizontal (pitch and roll) error would be more rapidly corrected by the horizon scanner.]

In any case, between the end of platform alignment and TPI, the azimuth residuals average -1.8° and the elevation residuals -0.5° , representing a total position residual of greater than 2 miles. The TRW calculated trajectory is, with good probability, accurate to within 2000 feet. It is therefore most likely that there was an error in either the platform alignment or the radar, or both. Since there is no evidence of this size radar azimuth bias prior to alignment and the error is closely correlated with alignment, it appears that a platform misalignment of $-1.9 \pm 0.5^\circ$ in the yaw direction (platform oriented left of the true down-range direction) was the cause of the large total position error. Similarly, the estimated post alignment error in the pitch (elevation) alignment, Figure 5-7, is $-0.6 \pm 0.5^\circ$ (the platform is pitched down from true horizontal).

Assuming the platform was misaligned in yaw, the error will appear in azimuth in the comparison, but decreasing in magnitude as the initial yaw direction is transformed to roll due to the orbit rate. If an initial yaw misalignment were the only error in the compared quantities, the azimuth error (Figure 5-6) should change as $\cos(\omega\Delta t)$, $\omega\Delta t$ being the angular travel of the spacecraft after "alignment." The curve, $\Delta A = 1.9^\circ \cos(\omega\Delta t)$, is shown in Figure 5-6. There is some indication that the observed error curve is decreasing as postulated before TPI. There is

~~CONFIDENTIAL~~

no agreement with the curve after TPI, which could be due to one or a combination of the following causes:

- a) The unknown initial roll misalignment is coupling into the azimuth comparison as initial roll becomes yaw with orbital travel
- b) The onboard radar has an azimuth bias error (though this is not completely consistent with the prealignment ΔA which shows a "bias" in the opposite direction)
- c) The trajectory reconstruction error is distorting the comparison.

The last cause is very likely, since the relative range at 280 minutes GET has decreased to 150,000 feet and the assumed trajectory uncertainty of 3,000 feet during this period represents a 1 degree angle uncertainty.

The range comparison, Figure 5-5, shows a sinusoidal trend suggestive of a trajectory reconstruction error. However, it is noted that over the entire comparison range, from 150 miles to a few thousand feet, the difference is within 1,000 feet. This comparison adds considerable confidence both to the accuracy of the reconstruction and the radar range measurement.

5.5 CONCLUSIONS

- a) During the radar tracking interval preceding platform alignment (208 to 224 minutes GET) radar/platform angle error trends of up to 3 degrees were evident. The error was most likely in the radar measurement.
- b) During platform alignment, the azimuth angle residuals showed excursions of ± 3 degrees, indicating possible problems in alignment. [MSC analysis indicated the platform was momentarily torqued out of alignment due to a spacecraft roll error.]
- c) After platform alignment, there is an indicated radar platform system misalignment: yaw/azimuth misalignment = $-1.9 \pm 0.5^\circ$, pitch/elevation misalignment = $0.6 \pm 0.5^\circ$.
- d) No radar range error is evident to within the accuracy of the trajectory reconstruction, 1000 to 3000 feet.

~~CONFIDENTIAL~~

Table 5-1. Average Magnitude of Residuals (Radar—Calculated)

Time	$ \Delta R $ (ft)	$ \Delta A $ (deg)	$ \Delta E $ (deg)	Δ Position (n. mi.)	Estimated Accuracy of Calculated Trajectory
Prior to alignment	497	0.8	1.3	4.0	0.25
During alignment	476	1.4	0.7	2.4	0.25
Alignment - TPI	277	1.8	0.6	2.3	0.33
TPI - TPF	721	0.7	0.4	0.2	0.50

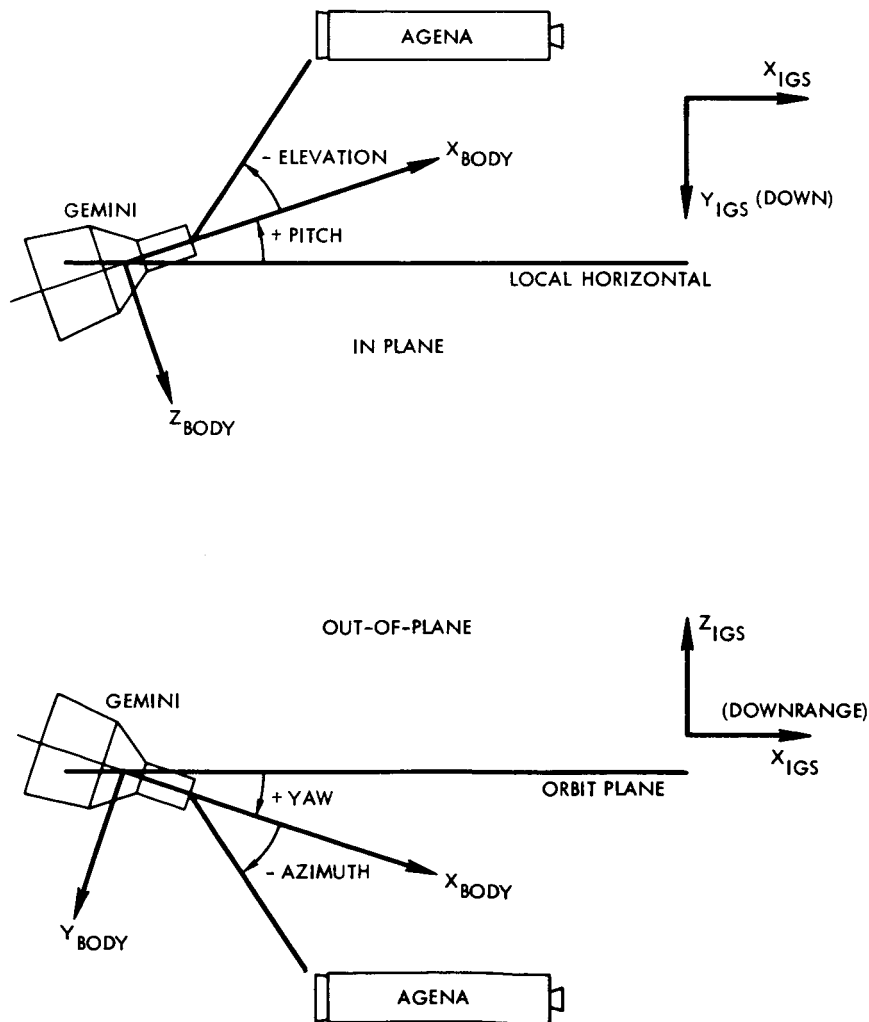


Figure 5-1. Rendezvous Geometry

~~CONFIDENTIAL~~

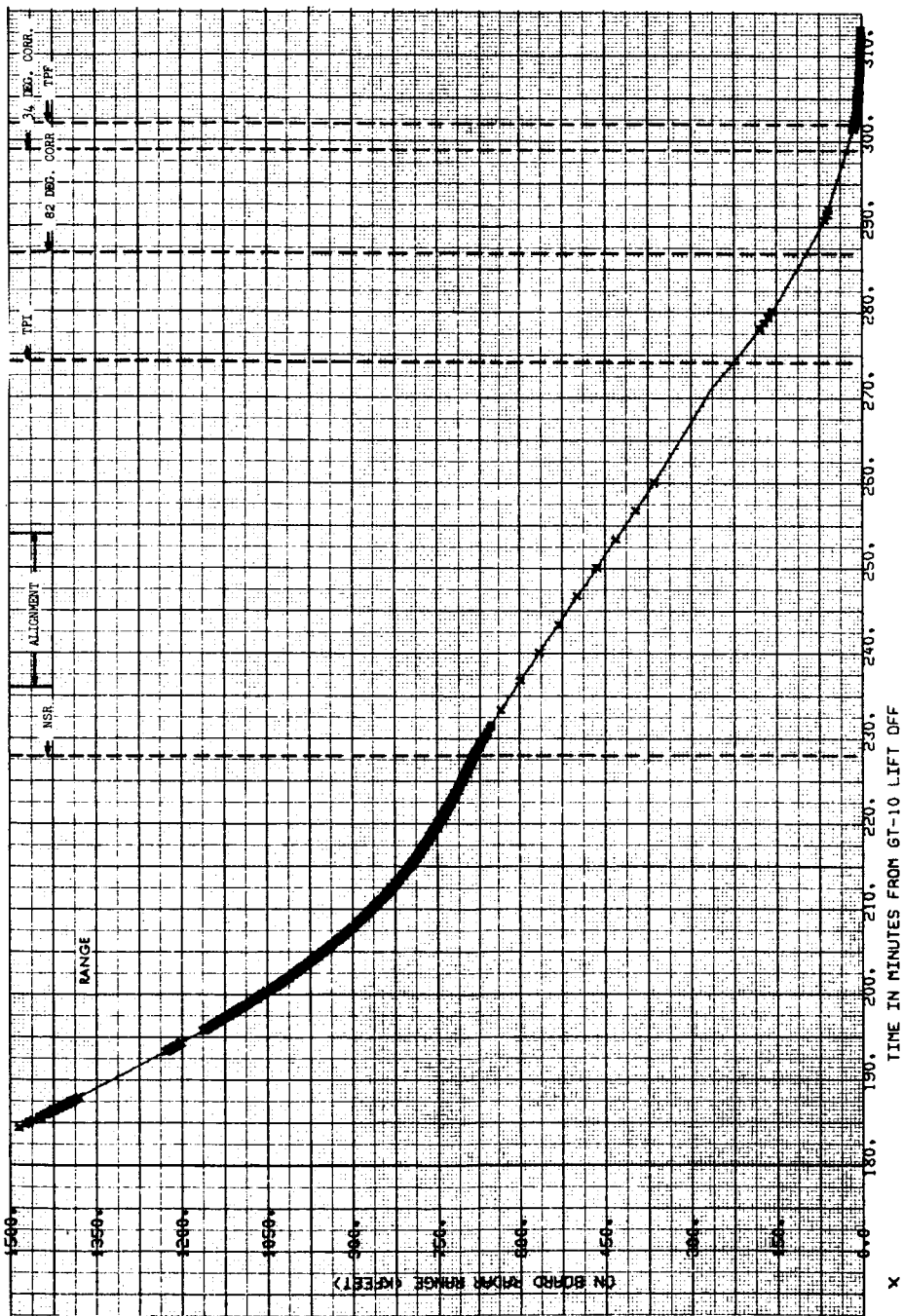


Figure 5-2. Radar Telemetered Parameters (On Board Radar Range)

CONFIDENTIAL

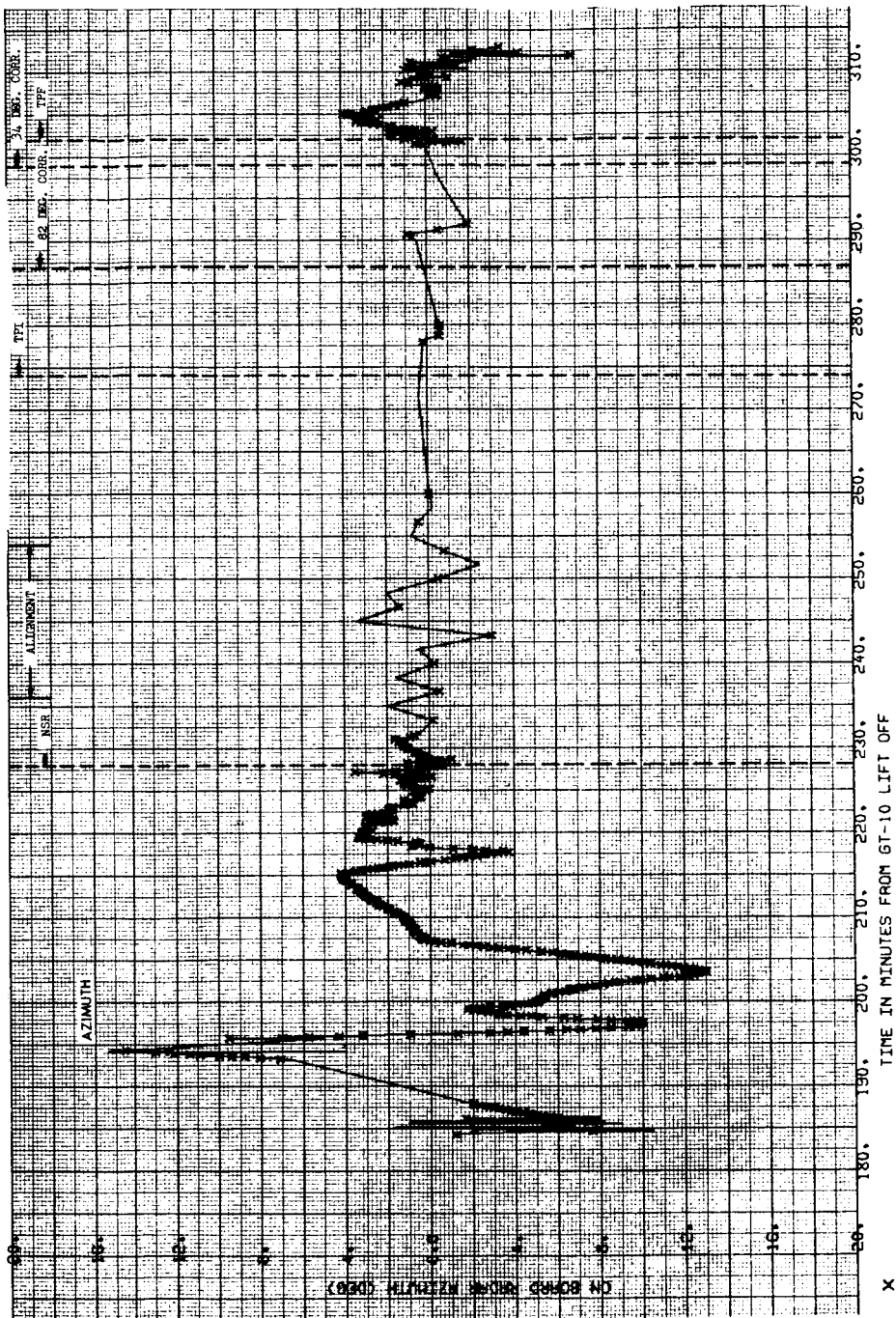


Figure 5-3. Radar Telemetered Parameters (On Board Azimuth)

CONFIDENTIAL

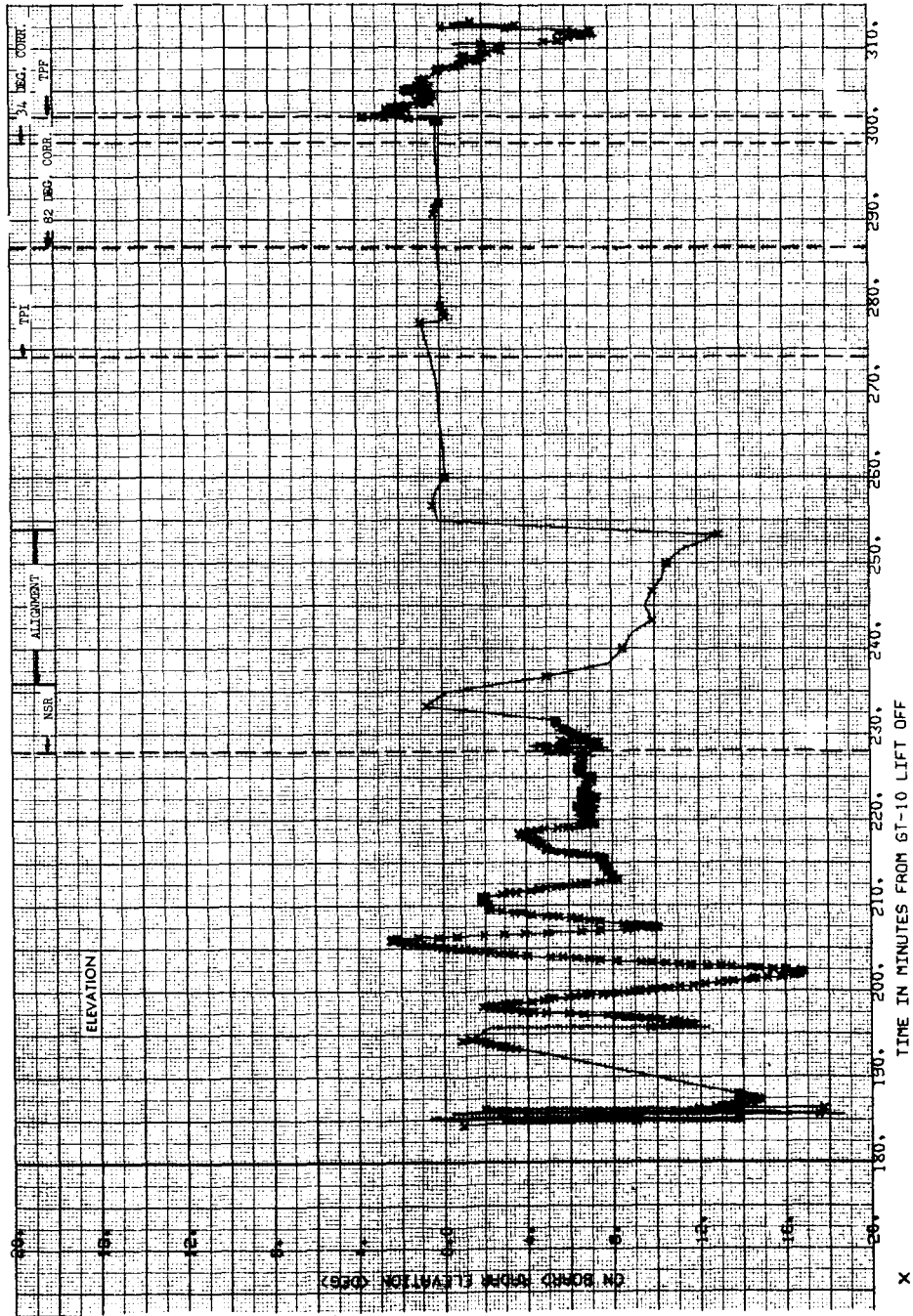


Figure 5-4. Radar Telemetered Parameters (On Board Radar Elevation)

CONFIDENTIAL

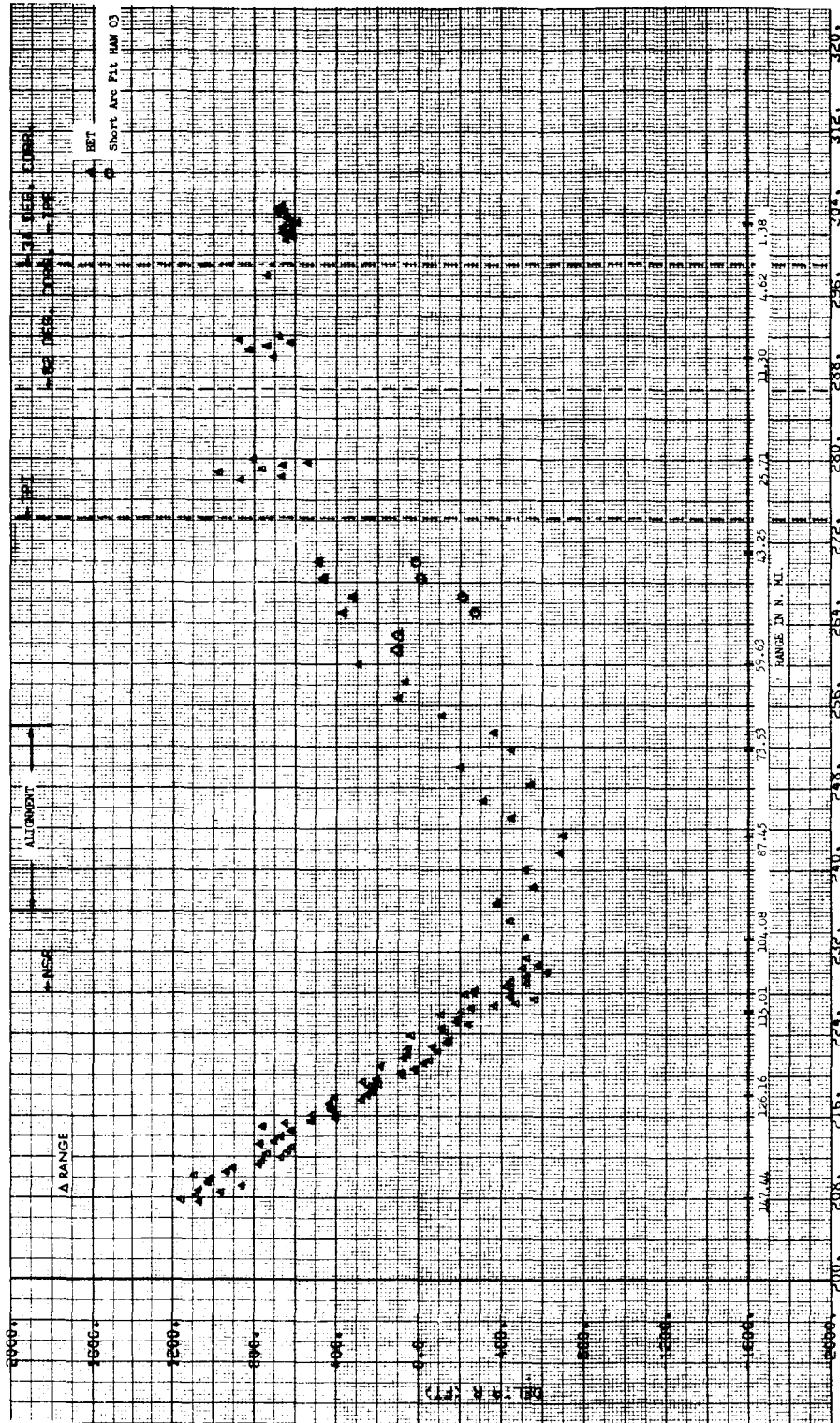


Figure 5-5. Radar Residuals (Telemetered Range Minus TRW Calculated Range)

CONFIDENTIAL

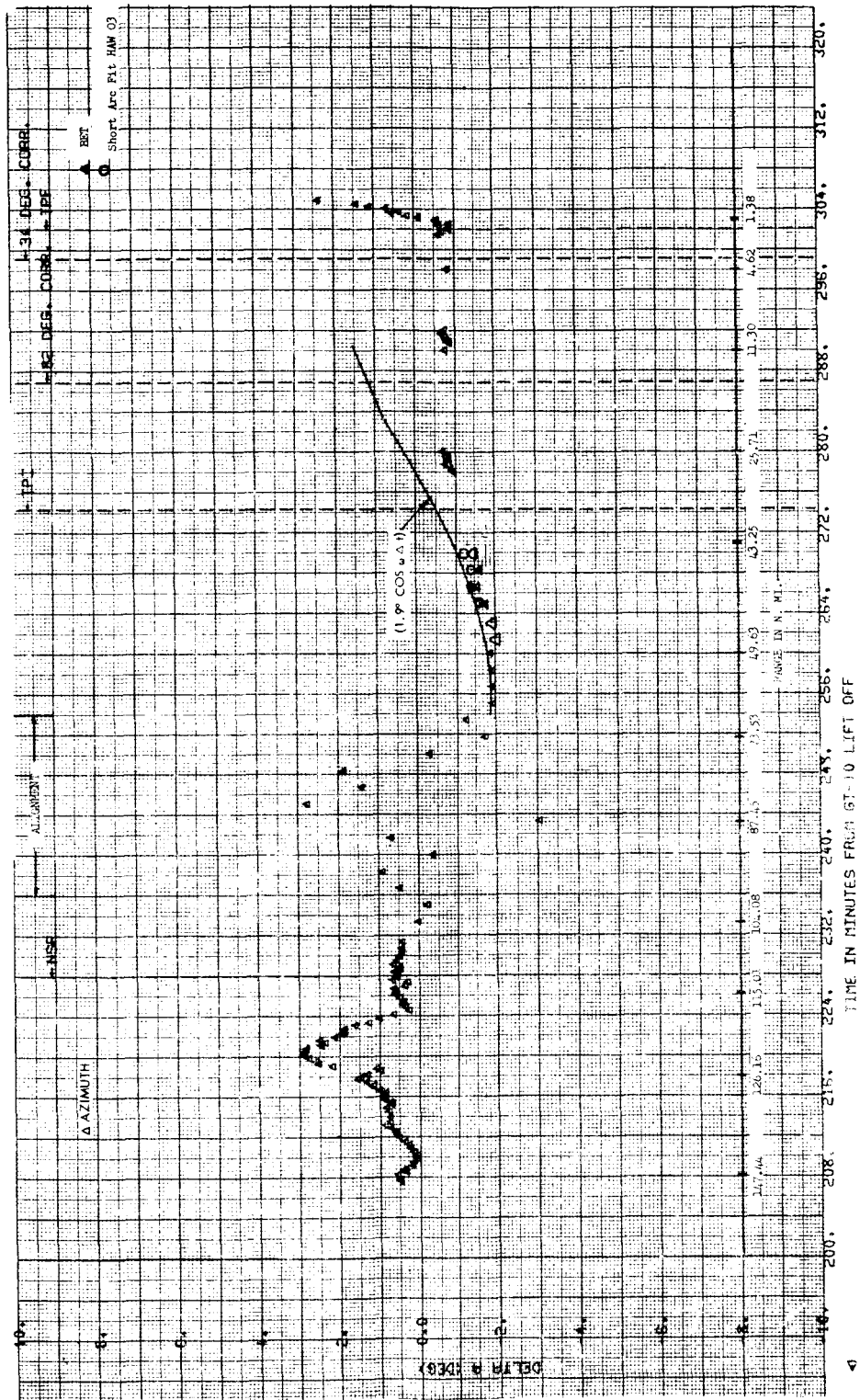


Figure 5-6. Radar Residuals (Telemetered Azimuth Minus TRW Calculated Azimuth)

CONFIDENTIAL

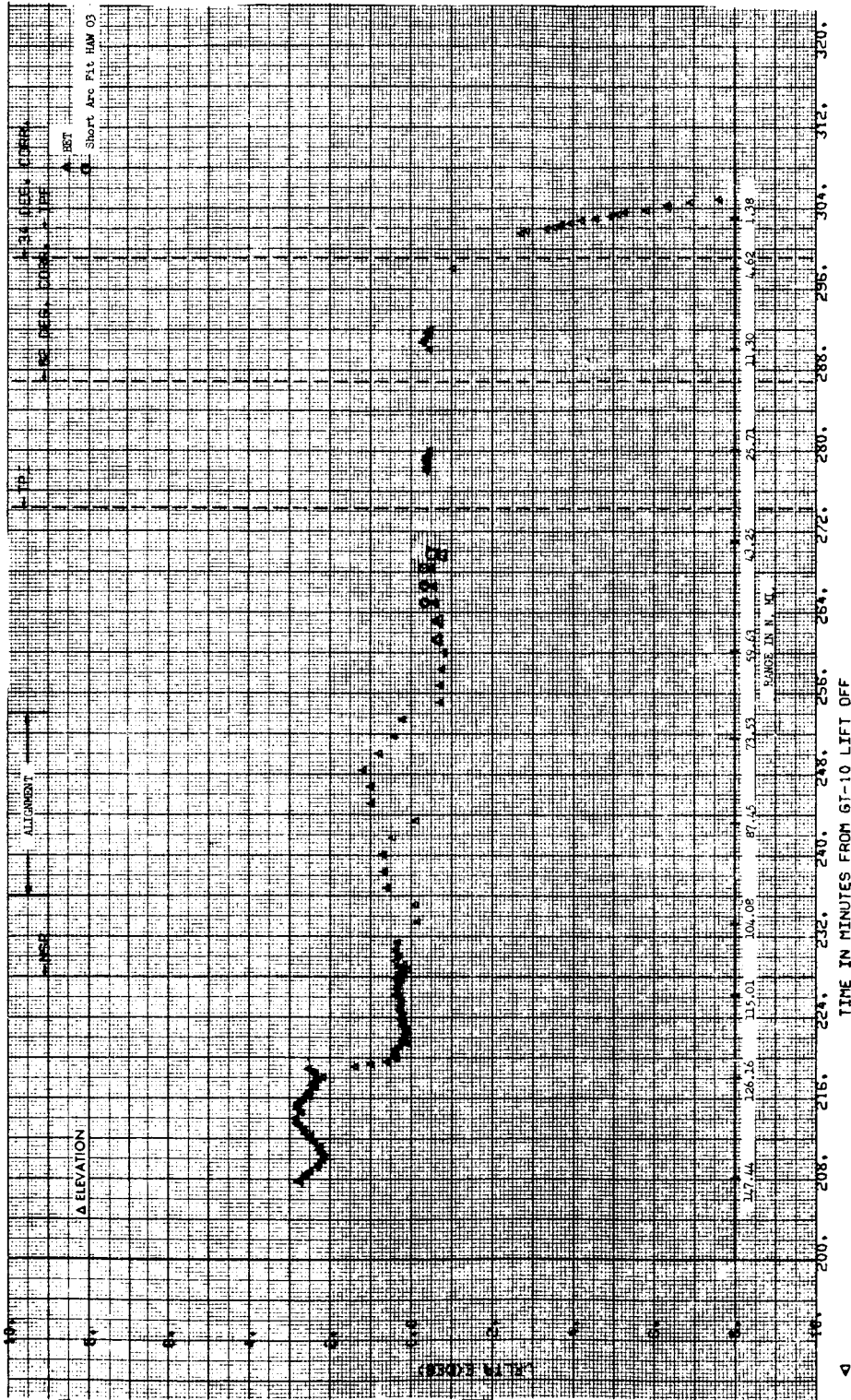


Figure 5-7. Radar Residuals (Telemetered Elevation Minus TRW Calculated Elevation)

CONFIDENTIAL

~~CONFIDENTIAL~~

6. ANALYSIS OF SEXTANT SIGHTINGS ON GEMINI 10

6.1 INTRODUCTION

During the flight interval between $0^{\text{h}} 7^{\text{m}} 25^{\text{s}}$ and 2^{h} GET, the celestial altitudes of six stars were measured by the astronaut with a hand-held sextant. This section presents comparisons of these sextant sightings with calculated values derived from a TRW-reconstructed Gemini 10 trajectory. The TRW reconstruction (TRW BET) was obtained by fitting a best orbit in a minimum variance sense to the ground radar tracking data on the first two Gemini orbits. The estimated accuracy of this trajectory is ± 1500 feet.

6.2 HORIZON BIAS

Table 6-1 shows results of six calibration measurements made on the star Schedar to establish the difference between the earth's hard crust horizon and a horizon determinable by visual means. Calculated altitudes using the TRW BET are shown for comparison. Onboard computations using this data resulted in a value of 27,500 yards for the horizon bias, and this value was used in the onboard computer to correct the other measured star altitudes. MSC postflight analysis of the bias computation indicated that 32,000 yards was a better estimate of the bias. The 4500-yard altitude difference results in a star angle bias of approximately 0.14 degrees in all onboard measurements. The TRW estimate of 31,500 yards was obtained by eliminating the first and last observation as wild points and averaging the four remaining differences.

6.3 SEXTANT MEASUREMENTS

The results of four-star altitude measurements made for trajectory updating are presented in Table 6-2 and compared with the TRW BET calculated values. The comparison was made assuming that a horizon bias of 32,000 yards was included in the measurement. Therefore, the last column in the table represents unexplained measurement error.

~~CONFIDENTIAL~~

CONFIDENTIAL

Table 6-1. Horizon Bias

Ground elapsed time (sec)	Measured Schedar altitude (deg)	TRW BET calculated Schedar altitude (deg)	Difference (measured minus TRW) (deg)
1509.500	4.446	6.56	-2.11
1626.875	8.749	7.60	1.15
1685.875	9.087	8.16	0.93
1760.000	9.849	8.90	0.95
1822.625	10.399	9.51	0.89
1892.375	10.842	10.24	0.60
Onboard bias		27,500 yards	
MSC bias		32,000 yards	
TRW bias		31,500 yards	

Table 6-2. Star Altitude Measurement Comparison

Star	Ground elapsed time (sec)	Star altitude (deg)		
		Measured	TRW BET calculated*	Difference (measured - TRW)
Hamel	2424	32.67	32.63	0.04
Vega	2654.5	8.44	7.58	0.86
Fomalhaut	6451.875	9.09	8.83	0.26
Arcturus	7112.125	18.02	17.71	0.31

* Bias = 32,000 yards

CONFIDENTIAL

6.4 ONBOARD COMPUTATIONS

These sextant sightings were used to update an onboard reference trajectory. This reference trajectory was propagated from the state vector stored in the IGS at insertion, which resulted from the IGS navigation throughout ascent. The error in this insertion vector was determined as part of the ascent IGS error analysis summarized in Table 2-8 of Section 2.

A comparison between the onboard reference trajectory and the TRW postflight reconstructed trajectory resulted in the following average differences in classical orbital elements.

Right ascension of ascending node	= 0.0225 degrees
Inclination	= 0.00308 degrees
Argument of perigee	= 3.6 degrees
Semimajor axis	= -280 feet
Eccentricity	= 0.0001
Period	= -0.0018 minutes

The relatively large error in the argument of perigee reflects the 13 feet per second IGS error in the vertical direction (\dot{y}) at insertion. This IGS ascent phase navigation error causes the onboard reference orbit to be rotated inplane from the true trajectory. The Cartesian coordinate differences, therefore, vary considerably as the calculated and true trajectory come into agreement periodically. The range of error over the period of interest is

$$\overline{\Delta P} = 5000 - 50,000 \text{ feet}$$

$$\overline{\Delta V} = 19 - 50 \text{ feet per second}$$

The residual between the observed, bias corrected altitude and the onboard calculated altitude is also a telemetry quantity. Table 6-3 shows this telemetry quantity along with the TRW simulation of the residual.

CONFIDENTIAL

Table 6-3. Star Altitude Residual Comparison

	Altitude (deg)		Residuals (deg)		
	Measured	TRW-simulated IGS value*	Measured minus TRW simulated	Measured minus IGS (telemetered)	$\Delta\Delta$
Hamel	32.67	32.69	-0.02	-0.02	0.00
Vega	8.44	7.54	0.90	-	-
Fomalhaut	9.09	9.04	0.05	-0.15	-0.20
Arcturus	18.02	17.67	0.35	0.35	0.00

*Bias = 27,500

The "TRW-simulated IGS value" was derived by propagating the onboard, IGS initial state vector by means of the integration of the TRW orbit determination program ESPOD. This TRW/IGS trajectory was used to calculate the respective star altitudes and the results differenced with the telemetered star altitude measurements. For comparative purposes the altitude bias was assumed to be 27,500 yards for the TRW-simulated values. The TRW calculated residuals, therefore, are a simulation of the onboard computations, but using a different trajectory propagation model. The TRW simulation also used the oblate earth radius at the horizon point, where the onboard computations assume a constant earth radius in the calculation of the star altitudes. There are perhaps other minor differences in the simulation, but collectively the onboard calculations are expected to have an accuracy of better than 0.01 degree. The last column of Table 6-3 is a comparison of the TRW-simulation and onboard results and indicates internal consistency to better than 0.01 degree for Hamel and Arcturus. The large difference for Fomalhaut may indicate that an incorrect time was associated with this telemetered angle reading as the result of a data reduction error.

If it is assumed that the onboard computer computations are accurate, which is the case for Hamel and Arcturus, and that the residual difference for Fomalhaut reflects a systematic error in the

CONFIDENTIAL

CONFIDENTIAL

TRW-simulation due perhaps to a time mismatch, then the sign sense of the residual difference is such that the TRW-simulated altitude will read larger by 0.20 degrees. The TRW calculated altitude for Fomalhaut in Table 6-2 should then also be increased by 0.20 degree. This adjustment would reduce the unexplained error in the astronaut measurement of Fomalhaut to 0.06 degree.

(Reverse of this page is intentionally blank.)

CONFIDENTIAL

CONFIDENTIAL

APPENDIX A

ASCENT TRAJECTORY

The ascent trajectory is provided in three separate forms: a) guidance coordinates as sensed by the accelerometers (these data are uncorrected for errors determined during flight); b) an earth-centered inertial coordinate set; and c) various special earth-referenced parameters. The latter two have been corrected for apparent IGS errors and therefore represent the TRW best estimate of the ascent trajectory.

The earth-centered inertial coordinate system has the z axis aligned with the earth's rotational axis, positive north, and the x-y plane is in the equatorial plane with the x-z plane containing the Greenwich meridian at platform release time (18 July 22^h20^m 26.648 GMT). Time is referenced to liftoff, which occurred 3.260 seconds after platform release.

<u>Figure</u>		<u>Page</u>
A-1	Sensed Acceleration in Computer Coordinates-Ascent ...	A-2
 <u>Tables</u>		
A-1	Sensed Trajectory for the Ascent Flight Phase	A-3
A-2	Reconstructed Ascent Trajectory, ECI Coordinates	A-5
A-3 a,b	Reconstructed Ascent Trajectory, Special Parameters	A-7

CONFIDENTIAL

CONFIDENTIAL



Figure A-1. Sensed Acceleration in Computer Coordinates - Ascent

CONFIDENTIAL

CONFIDENTIAL

Table A-1. Sensed Trajectory for the Ascent Flight Phase

Table with columns: TIME (SECS), X (FT), Y (FT), Z (FT), XDOT (FT/SEC), YDOT (FT/SEC), ZDOT (FT/SEC), XDDOT (FT/SEC^2), YDDOT (FT/SEC^2), ZDDOT (FT/SEC^2). Rows contain numerical data for trajectory points.

CONFIDENTIAL

Table A-3a. Reconstructed Ascent Trajectory,
Special Parameters (Continued)

GEMINI 10 TPM ASCENT BFT							
TIME FROM LIFTOFF (SECONDS)	INERTIAL VEL. MAGNITUDE (FT/SEC)	RELATIVE VEL. MAGNITUDE (FT/SEC)	INERTIAL FLT. PATH ANGLE (DEGREES)	INERTIAL HEADING ANGLE (DEGREES)	ALTITUDE (FEET)	GEODETTIC LAT. (DEGREES)	GEODETTIC LONG. (DEGREES)
399.767	25713.1	24346.2	.163	102.690	526843.7	26.324	-67.801
401.366	25712.8	24345.9	.165	102.765	526996.7	26.294	-67.618
403.943	25712.6	24345.8	.166	102.849	527146.7	26.245	-67.436
405.697	25712.6	24345.7	.166	102.907	527254.5	26.218	-67.312
408.291	25713.2	24346.3	.167	102.991	527409.2	26.178	-67.131
410.863	25715.0	24348.1	.168	103.076	527564.7	26.138	-66.949
413.442	25716.5	24349.7	.170	103.160	527722.0	26.097	-66.768

CONFIDENTIAL

Table A-3b. Reconstructed Ascent Trajectory,
Special Parameters (Continued)

GEMINI 10 TRW ASCENT BET

14

TIME (SEC)	RELATIVE FLT. PATH ANGLE (DEGREES)	RELATIVE HEADING ANGLE (DEGREES)	INERTIAL LONG. (DEGREES)	GEOCENTRIC LAT. (DEGREES)	RADIUS TO EARTH CENTER (FEET)
402.027	.173	103.405	-66.121	26.171	21438883.5
404.626	.174	103.495	-65.927	26.132	21439074.7
407.203	.175	103.584	-65.735	26.092	21439266.0
408.957	.175	103.646	-65.604	26.066	21439396.7
411.541	.177	103.735	-65.411	26.026	21439590.0
414.123	.178	103.825	-65.219	25.986	21439784.2
416.702	.180	103.914	-65.027	25.946	21439980.5

CONFIDENTIAL

APPENDIX B
REENTRY TRAJECTORY

The reentry trajectory is provided in two sets, the earth-centered inertial coordinates and the special earth-referenced coordinates. The inertial set has the z axis aligned with the earth's rotational axis, positive north, and the x-y plane is in the equatorial plane with the x-z plane containing the Greenwich meridian at the time of retrofire (21 July 20^h 30^m 51.0^s).

<u>Tables</u>		<u>Page</u>
B-1	Reconstructed Reentry Trajectory, ECI Coordinates	B-2
B-2a, b	Reconstructed Reentry Trajectory, Special Parameters	B-6

Table B-1. Reconstructed Reentry Trajectory,
ECI Coordinates (Continued)

TIME (SEC)	X (FT)	Y (FT)	Z (FT)	XDOT (FT/SEC)	YDOT (FT/SEC)	ZDOT (FT/SEC)	GEMINI IC ENTRY TRW BFT V		
							EARTH CENTERED INERTIAL GREENWICH COORDINATE SYSTEM		
1539.0990	3521414.72	-18270710.75	10076235.25	25239.24	4314.60	-2287.22			
1541.2460	3575566.31	-18261392.00	10071264.62	25205.36	4366.11	-2315.20			
1543.3910	3629594.37	-18251973.00	10066268.25	25170.00	4416.23	-2343.36			
1546.5650	3709398.84	-18237841.25	10058757.00	25116.67	4488.39	-2383.37			
1548.7130	3753307.91	-18228147.00	10053619.00	25077.67	4537.94	-2409.92			
1550.8610	3817131.16	-18218346.75	10048413.12	25036.93	4586.95	-2437.24			
1553.0040	3870741.16	-18208466.50	10043161.87	24995.59	4634.10	-2463.62			
1556.1770	3949951.20	-18193652.75	10035285.87	24932.42	4733.35	-2500.76			
1558.3270	4003507.84	-18183490.75	10029879.75	24887.08	4749.56	-2528.10			
1560.4750	4056914.23	-18173239.75	10024421.62	24839.81	4795.21	-2554.05			
1562.6220	4110194.20	-18162896.00	10018912.75	24792.14	4840.34	-2577.61			
1564.7640	4163245.59	-18152480.50	10013364.75	24742.55	4884.76	-2602.66			
1567.9450	4241828.31	-18136837.75	10005028.75	24665.33	4950.26	-2638.42			
1570.0880	4294628.50	-18126184.50	9999350.25	24610.98	4992.21	-2661.13			
1572.2300	4347283.19	-18115446.50	9993625.12	24553.05	5033.82	-2684.52			
1574.3730	4399835.50	-18104614.50	9987849.62	24492.41	5075.28	-2705.54			
1577.5450	4477374.19	-18088427.25	9979217.25	24397.08	5131.16	-2737.30			
1579.6960	4529776.50	-18077349.00	9973300.50	24326.59	5169.79	-2756.73			
1581.8390	4581832.81	-18066234.00	9967379.00	24255.94	5203.94	-2777.10			
1583.9840	4633781.19	-18055033.50	9961432.62	24181.03	5239.43	-2795.23			
1587.1590	4710373.06	-18038319.75	9952484.87	24065.53	5288.83	-2822.26			
1589.3060	4761453.62	-18026930.50	9946408.00	23983.37	5320.67	-2838.51			
1591.4480	4813235.81	-18015500.25	9940309.75	23899.19	5351.74	-2855.50			
1593.5940	4864432.12	-18003984.25	9934165.87	23814.17	5380.90	-2870.40			
1596.7710	4939881.75	-17986920.75	9925010.00	23683.20	5423.87	-2893.45			
1598.9200	4990680.25	-17975136.50	9918776.50	23593.51	5450.47	-2907.85			
1601.0630	5041141.19	-17963426.50	9912529.50	23500.11	5478.05	-2922.28			
1603.2010	5091284.81	-17951687.25	9906268.87	23406.89	5503.38	-2934.24			
1606.3730	5155302.94	-17934171.25	9896931.37	23262.83	5540.86	-2953.23			
1608.5190	5215119.37	-17922257.00	9890580.25	23164.53	5562.79	-2965.83			
1610.6570	5264534.75	-17910338.00	9884229.50	23061.29	5586.95	-2974.95			
1612.7960	5313750.62	-17898365.75	9877855.12	22956.18	5607.17	-2985.23			
1615.9690	5388334.50	-17880427.25	9868360.75	22794.69	5636.74	-2999.19			
1618.1160	5435156.37	-17868406.00	9861913.62	22688.88	5654.64	-3006.57			
1620.2570	5483661.75	-17856280.75	9855466.75	22569.80	5672.03	-3015.68			
1622.4010	5531967.25	-17844103.00	9848995.00	22455.25	5687.82	-3021.47			
1625.5750	5607863.37	-178262013.00	9839388.12	22278.67	5711.01	-3032.00			
1627.7210	5690549.50	-17813743.00	9832874.87	22161.32	5724.45	-3038.10			
1629.8640	5697910.81	-17801460.00	9826358.75	22039.48	5738.86	-3043.29			
1632.0070	5745510.44	-17789149.00	9819831.62	21917.11	5750.63	-3048.21			
1635.1810	5814262.44	-17770867.75	9810148.87	21732.37	5768.59	-3053.10			
1637.3270	5863781.56	-17758476.25	9803594.37	21603.35	5779.95	-3055.51			
1639.4710	5906361.70	-17746074.25	9797042.62	21474.84	5789.29	-3056.17			
1641.6130	5952862.06	-17733650.75	9790489.62	21343.07	5799.57	-3056.70			
1644.7700	6018623.25	-17716788.75	9781034.75	21152.03	5813.99	-3053.03			
1646.9030	6060654.37	-17704019.50	9774954.37	21027.11	5826.29	-3048.86			
1649.0490	6122320.94	-17686867.75	9765989.87	20837.31	5858.47	-3036.94			
1651.1950	6163780.25	-17675141.25	9759936.00	20705.01	5891.46	-3029.09			
1653.3400	6204908.50	-17663365.75	9753899.25	20568.17	5925.42	-3028.93			
1656.5860	6265240.94	-17645810.00	9744960.12	20362.51	5984.76	-3035.51			
1658.7300	6305679.56	-17633847.50	9738897.62	20218.54	6020.02	-3048.33			
1663.7800	6409841.31	-17602328.50	9722878.87	19835.82	6100.32	-3111.52			
1665.9370	6452454.94	-17589153.25	9716133.87	19676.40	6116.05	-3142.58			
1668.0900	6494743.12	-17575966.50	9709316.87	19515.81	6123.68	-3175.42			
1671.2440	6556592.33	-17556429.00	9699131.50	19272.77	6116.79	-3212.34			
1673.3940	6598042.56	-17543230.50	9692171.87	18821.34	6103.81	-3231.70			
1675.5410	6639974.12	-17530080.25	9685188.25	18939.81	6089.41	-3243.68			
1680.9460	6739185.12	-17497653.75	9667853.25	18519.11	6043.95	-3242.76			
1683.2220	6781117.56	-17483922.25	9660490.00	18328.40	6022.41	-3227.54			
1685.4240	6821262.44	-17470683.50	9653407.12	18133.83	6001.84	-3205.57			
1687.5640	6859862.69	-17457858.75	9646577.87	17940.93	5983.94	-3176.91			
1689.7030	6898119.87	-17445085.75	9639815.50	17737.07	5959.08	-3146.08			
1692.8670	6953649.56	-17426290.00	9629936.00	17527.07	5916.30	-3098.90			
1695.0170	6990888.70	-17413613.25	9623337.50	17212.94	5886.18	-3067.01			
1697.1590	7027525.50	-17401041.25	9616776.87	16999.75	5856.42	-3030.64			
1702.4670	7116266.50	-17377119.75	9603958.25	16641.06	5796.54	-2929.66			
1704.5610	7157451.25	-17357985.75	9594864.12	16209.21	5792.85	-2890.92			
1709.5700	7232203.19	-17328929.75	9580560.12	15634.24	5808.62	-2820.43			
1711.5630	7261122.56	-17317368.25	9574949.87	15393.52	5813.38	-2809.50			
1716.5080	7345918.56	-17300235.25	9566670.00	15028.18	5808.43	-2813.50			
1718.5320	7386072.94	-17288499.75	9560963.50	14768.80	5788.08	-2825.36			
1721.6130	7366526.59	-17276494.25	9555065.12	14499.69	5750.10	-2843.38			
1723.6750	7415311.56	-17259924.50	9546334.75	14099.05	5680.57	-2859.01			
1725.7470	7439237.31	-17243811.00	9540415.50	13821.72	5578.33	-2854.55			
1725.8920	7468570.44	-17235518.00	9534318.75	13528.25	5482.85	-2830.09			
1728.0490	7497366.12	-17223824.50	9528275.62	13221.00	5378.10	-2783.60			
1731.2250	7538676.56	-17206951.25	9519592.87	12760.18	5235.37	-2677.21			
1733.3680	7565680.50	-17195826.00	9513947.50	12441.29	5147.57	-2591.51			
1735.5150	7592749.12	-17184887.25	9508466.00	12122.36	5042.16	-2514.66			
1737.6600	7617703.44	-17174190.25	9503156.12	11797.66	4931.80	-2436.32			
1740.8290	7654374.37	-17158804.00	9495636.37	11314.08	4778.66	-2309.43			
1742.9720	7682158.75	-17148675.25	9490778.12	10982.96	4674.16	-2224.64			
1745.1120	7711367.00	-17138785.00	9486107.37	10653.60	4569.08	-2140.58			
1747.2460	7741367.59	-17129146.75	9481629.12	10324.82	4463.87	-2056.48			
1750.4170	7757116.50	-17115244.50	9475300.37	9936.40	4364.57	-1935.12			
1752.5610	7764447.44	-17104333.25	9471237.12	9502.35	4194.75	-1855.28			
1754.7040	7796455.06	-17097261.00	9467343.50	9170.09	4085.39	-1778.48			

UNCLASSIFIED

Table B-1. Reconstructed Reentry Trajectory,
ECI Coordinates (Continued)

TIME (SEC)	X (FT)	Y (FT)	Z (FT)	XDOT (FT/SEC)	YDOT (FT/SEC)	ZDOT (FT/SEC)	GEMINI 1C ENTRY TRW BET V		
							EARTH CENTERED INERTIAL GREENWICH COORDINATE SYSTEM		
1756.8450	7815740.50	-17088627.75	9463614.87	8845.38	3979.32	-1704.61			
1760.0140	7843019.75	-17076262.00	9458383.12	8570.87	3824.94	-1597.26			
1762.1610	7860645.69	-17068141.25	9455031.37	8048.25	3759.77	-1524.97			
1767.1700	7899164.31	-17049823.00	9447774.37	7307.56	3574.31	-1372.58			
1769.1630	7913373.44	-17042756.75	9445086.62	7011.60	3516.74	-1324.62			
1772.1090	7933381.06	-17032522.25	9441260.25	6575.36	3433.73	-1274.00			
1774.1050	7946219.44	-17025727.75	9438739.50	6283.24	3371.05	-1250.52			
1776.0960	7958446.44	-17019085.00	9436265.75	5999.05	3301.76	-1234.41			
1779.0460	7975545.62	-17009519.50	9432652.75	5593.55	3183.19	-1215.10			
1781.0440	7986458.25	-17003251.50	9430238.00	5330.08	3091.27	-1202.01			
1784.0740	8002037.00	-16994117.75	9426639.25	4952.92	2937.62	-1173.46			
1786.2240	8012410.56	-16987925.50	9424153.87	4696.82	2822.38	-1138.41			
1788.3690	8022220.12	-16981993.50	9421760.12	4449.67	2708.89	-1093.59			
1790.5140	8031506.37	-16976296.75	9419470.37	4210.73	2602.67	-1041.40			
1795.8290	8052400.96	-16963051.25	9414308.37	3651.01	2381.58	-901.03			
1797.9590	8059954.50	-16958752.75	9412443.00	3441.52	2311.71	-850.42			
1800.0910	8067087.94	-16953198.75	9410679.00	3245.60	2241.85	-804.38			
1803.3180	8077114.06	-16946133.50	9408183.12	2971.36	2136.99	-742.48			
1805.5250	8083481.37	-16941490.50	9406588.25	2798.78	2070.42	-702.80			
1807.6730	8089325.94	-16937109.25	9405118.00	2643.12	2008.95	-666.24			
1809.8020	8094799.12	-16932894.75	9403737.00	2498.47	1950.35	-630.99			
1812.9490	8102354.37	-16926885.50	9401831.50	2303.07	1868.64	-579.99			
1815.0790	8107130.62	-16922959.00	9400631.25	2181.67	1818.17	-547.03			
1819.2580	8115804.69	-16915951.00	9398471.50	1969.56	1727.23	-486.59			
1822.3350	8121658.56	-16910332.00	9397040.25	1835.38	1664.91	-443.75			
1824.4150	8125392.55	-16906309.00	9396144.12	1754.97	1626.54	-417.86			
1826.4960	8128463.69	-16903584.00	9395301.37	1680.50	1591.44	-392.95			
1829.5710	8133484.87	-16898740.50	9394148.12	1583.19	1543.67	-356.63			
1831.6530	8137217.19	-16895561.25	9393427.25	1521.82	1510.39	-335.79			
1836.8570	8144804.31	-16887906.75	9391807.50	1394.04	1431.42	-286.75			
1838.9410	8147666.62	-16884952.25	9391224.37	1352.92	1403.98	-272.84			
1841.0870	8153529.50	-16881963.50	9390649.62	1315.21	1381.32	-262.74			
1843.2450	8153329.75	-16879006.00	9390092.75	1279.98	1359.73	-253.35			
1846.3660	8157245.19	-16874826.50	9389321.25	1237.20	1327.11	-242.67			
1848.4310	8157885.44	-16872096.50	9388825.62	1211.18	1304.31	-234.99			
1850.4670	8162260.13	-16869413.25	9388345.62	1192.23	1280.70	-227.51			
1853.5780	8165898.94	-16865536.50	9387654.12	1164.52	1263.98	-222.82			
1855.6560	8168301.56	-16862975.50	9387196.12	1147.94	1221.11	-217.95			
1860.7940	8174111.75	-16856824.00	9386107.37	1113.73	1173.35	-205.69			
1862.8690	8176412.06	-16854405.75	9385686.37	1103.38	1157.44	-199.83			
1866.0110	8182045.50	-16848549.75	9384675.25	1087.76	1120.32	-193.48			
1870.0920	8184303.87	-16846237.50	9384274.37	1084.81	1103.96	-192.13			
1872.1620	8186952.31	-16843976.25	9383876.37	1085.48	1078.81	-192.04			
1875.2320	8189887.06	-16840725.00	9383288.62	1087.02	1039.27	-190.86			
1877.3110	8192147.12	-16838585.50	9382887.75	1087.16	1018.86	-194.73			
1879.3860	8194402.69	-16836489.50	9382483.87	1088.99	1003.29	-195.01			
1882.4510	8197359.12	-16833443.00	9381885.00	1086.69	983.42	-195.47			
1884.4890	8201001.37	-16831467.75	9381477.75	1090.62	975.01	-196.47			
1886.4620	8202263.69	-16829394.25	9381072.37	1092.00	967.96	-194.64			
1889.4710	8205613.69	-16826452.00	9380470.62	1091.05	949.47	-197.50			
1891.7560	8207892.19	-16824481.00	9380064.12	1094.61	941.21	-192.46			
1893.8390	8210164.37	-16822535.00	9379656.87	1087.00	927.24	-198.53			
1896.9140	8213516.69	-16819698.75	9379044.00	1093.40	917.40	-200.09			
1898.9960	8215802.12	-16817788.25	9378641.00	1102.00	917.97	-187.04			
1901.0720	8218083.25	-16815900.25	9378243.75	1095.62	900.91	-195.68			
1904.1450	8221461.00	-16813142.50	9377649.50	1102.69	893.93	-191.06			
1906.2300	8223762.56	-16811277.00	9377267.87	1105.11	895.49	-175.07			
1908.3070	8226772.25	-16809426.50	9376897.00	1118.94	896.48	-182.02			
1913.4830	8228391.91	-16807589.00	9376525.62	1115.68	883.68	-175.79			
1915.5660	8231834.56	-16804879.25	9375989.12	1120.61	876.40	-172.72			
1917.6160	8234163.31	-16803074.50	9375621.87	1125.01	863.98	-181.44			
1919.6610	8236503.56	-16801279.50	9375250.12	1125.21	862.07	-175.99			
1921.6910	8239972.75	-16798634.00	9374707.50	1131.18	858.56	-176.96			
1922.7700	8242316.31	-16796855.25	9374342.00	1123.37	852.51	-174.59			
1924.8480	8244649.94	-16795083.50	9373987.25	1122.62	852.72	-166.90			
1927.9230	8248119.06	-16792468.25	9373467.50	1133.75	848.33	-171.14			
1930.0030	8250472.12	-16790706.75	9373116.75	1128.78	845.37	-166.09			
1932.0810	8252816.87	-16788948.75	9372778.62	1127.98	846.75	-159.35			
1935.1560	8256361.12	-16786351.00	9372277.87	1138.22	842.79	-166.33			
1937.2350	8258665.35	-16784600.25	9371939.25	1135.83	841.43	-159.45			
1939.3150	8261300.81	-16782847.25	9371613.12	1138.95	844.22	-154.18			
1942.3870	8264523.69	-16780266.00	9371136.00	1135.06	836.23	-156.38			
1944.4670	8266891.75	-16778527.00	9370813.37	1141.91	835.97	-153.85			
1949.6200	8272787.31	-16774236.12	9370039.25	1146.21	829.41	-146.61			
1951.7000	8275172.12	-16772507.00	9369739.50	1146.80	833.24	-141.67			
1953.7740	8277581.19	-16770851.00	9369474.12	1176.25	763.70	-114.22			
1956.8460	8281227.75	-16768586.00	9369168.62	1197.85	710.93	-84.64			
1958.9270	8283721.37	-16767121.00	9369005.25	1198.69	696.97	-72.42			
1961.0030	8286223.56	-16765589.75	9368863.50	1211.89	686.77	-64.14			
1964.0750	8289961.52	-16763628.37	9368699.25	1221.75	652.00	-49.28			
1966.1550	8292498.87	-16762302.00	9368592.00	1217.89	623.37	-44.28			
1968.2320	8295294.42	-16761011.25	9368500.75	1219.02	619.95	-43.55			
1971.3100	8298773.69	-16759107.62	9368372.62	1221.72	621.38	-39.96			
1973.3840	8301427.37	-16757794.50	9368299.00	1229.05	638.88	-30.68			
1975.4540	8303175.74	-16756470.75	9368235.62	1233.34	640.01	-30.55			
1978.5250	8307657.50	-16754513.62	9368132.75	1229.41	634.59	-36.45			
1980.6110	8310220.00	-16753190.00	9368056.25	1227.43	634.49	-36.93			

UNCLASSIFIED

Table B-1. Reconstructed Reentry Trajectory,
ECI Coordinates (Continued)

GEMINI 1C ENTRY TRM BET V						
EARTH CENTERED INERTIAL GREENWICH COORDINATE SYSTEM						
TIME (SEC)	X (FT)	Y (FT)	Z (FT)	XDOT (FT/SEC)	YDOT (FT/SEC)	ZDOT (FT/SEC)
1982.685C	8312769.87	-16751870.62	9367980.25	1231.44	637.85	-36.36
1985.749D	8316537.12	-16749923.37	936786C.25	1227.62	633.16	-41.95
1987.832C	8319081.44	-16746609.50	9367771.37	1215.34	628.42	-43.48
1989.910C	8321604.37	-16747396.75	9367683.87	1212.89	625.43	-40.75
1991.986D	8324132.20	-16746000.00	936760C.37	1222.21	633.46	-39.66
1995.055D	8327906.19	-16744245.87	9367472.25	1237.34	640.02	-43.84
1997.125C	8330467.44	-16742726.25	9367382.25	1237.28	635.01	-43.13
1999.204U	8333032.75	-16741405.00	9367296.87	1230.55	636.00	-38.92
2002.284D	8336814.37	-16739440.87	9367188.75	1225.04	639.37	-31.32
2004.358D	8339352.06	-16738120.00	9367114.25	1222.13	634.38	-40.55
2006.439D	8341888.31	-16736805.25	9367026.37	1215.35	629.18	-43.86
2009.510C	8345637.44	-16734865.87	9366893.50	1223.05	633.89	-42.65
2011.591D	8348181.26	-16733540.62	9366808.12	1226.40	639.77	-39.45
2013.666C	8350726.56	-16732220.37	9366716.75	1227.04	632.79	-48.65
2016.742C	8354501.50	-16730275.25	9366565.50	1227.42	631.87	-49.67
2018.820C	8357056.12	-16728954.75	9366470.37	1231.31	639.09	-41.87
2020.899D	8359615.56	-16727627.12	9366386.37	1226.05	638.05	-38.88
2023.967D	8363362.44	-16725676.25	9366262.50	1219.77	633.69	-41.93
2026.048D	8365892.87	-16724361.00	9366175.12	1212.21	630.39	-41.99
2031.199D	8372149.37	-16721103.25	9365958.25	1217.02	634.51	-42.22
2033.279C	8374685.75	-16719784.12	9365866.62	1221.81	633.85	-45.84
2035.356C	8377221.06	-16718461.62	9365778.37	1219.48	639.70	-39.21
2038.429D	8380973.75	-16716490.50	9365662.50	1222.92	643.11	-36.23
2040.510C	8383520.56	-16715159.37	9365577.75	1224.76	636.25	-45.16
2042.585C	8386066.10	-16713837.25	9365481.50	1228.63	638.03	-47.60
2045.659D	8388637.75	-16711875.62	9365338.87	1225.38	638.24	-45.18
2047.735C	8392388.12	-16710549.25	9365245.75	1231.66	639.60	-44.53
2049.812D	8394944.62	-16709224.00	9365147.12	1230.01	636.31	-50.47
2052.8929	8398722.12	-16707269.12	9364988.75	1222.11	632.54	-52.30
2054.982D	8401273.50	-16705945.50	9364883.37	1220.56	634.65	-48.64
2057.063C	8403817.37	-16704622.75	9364783.62	1224.39	636.62	-47.18
2060.145D	8407592.00	-16702660.75	9364635.50	1225.08	636.52	-49.00
2062.226D	8410136.00	-16701335.75	9364534.62	1219.80	636.98	-47.86

UNCLASSIFIED

Table B-2a. Reconstructed Reentry Trajectory,
Special Parameters

GEMINI 1C ENTRY			TRW BET		V		51	
TIME FROM RETROFIRE (SECONDS)	INERTIAL VEL. MAGNITUDE (FT/SEC)	RELATIVE VEL. MAGNITUDE (FT/SEC)	INERTIAL FLT. PATH ANGLE (DEGREES)	INERTIAL HEADING ANGLE (DEGREES)	ALTITUDE (FEET)	GEODETTIC LAT. (DEGREES)	GEODETTIC LONG. (DEGREES)	
1347.366	25864.6	2455.1	-1.635	87.658	383719.0	28.917	-99.989	
1349.356	25866.4	2457.1	-1.633	87.731	382293.5	28.922	-99.843	
1352.163	25868.8	2459.5	-1.631	87.841	380196.5	28.930	-99.628	
1354.15	25870.6	24511.5	-1.630	87.915	378772.2	28.935	-99.482	
1356.966	25873.0	24513.9	-1.627	88.025	376680.5	28.942	-99.268	
1358.900	25874.6	24515.7	-1.626	88.099	375260.5	28.946	-99.122	
1361.766	25877.1	24518.3	-1.624	88.209	373189.2	28.953	-98.907	
1363.659	25878.6	24519.9	-1.622	88.283	371752.5	28.957	-98.761	
1366.556	25881.2	24522.6	-1.619	88.393	369667.2	28.963	-98.546	
1368.494	25882.9	24524.4	-1.618	88.468	368254.5	28.966	-98.400	
1371.354	25885.4	24527.0	-1.615	88.577	366171.5	28.972	-98.184	
1373.296	25887.1	24528.7	-1.614	88.652	364758.7	28.975	-98.038	
1376.166	25889.4	24531.2	-1.611	88.761	362677.2	28.979	-97.822	
1378.107	25891.1	24532.9	-1.609	88.836	361263.7	28.982	-97.676	
1380.969	25893.5	24535.5	-1.607	88.947	359186.5	28.986	-97.460	
1382.914	25895.1	24537.1	-1.605	89.021	357779.5	28.989	-97.313	
1385.778	25897.4	24539.6	-1.603	89.132	355706.5	28.992	-97.097	
1387.722	25899.2	24541.5	-1.601	89.207	354301.2	28.994	-96.951	
1390.568	25901.5	24544.0	-1.599	89.317	352231.5	28.996	-96.734	
1392.534	25903.1	24545.5	-1.597	89.392	350827.5	28.998	-96.587	
1394.474	25904.6	24547.2	-1.595	89.466	349429.2	28.999	-96.441	
1397.346	25906.9	24549.6	-1.592	89.577	347362.0	29.001	-96.224	
1399.286	25908.5	24551.3	-1.590	89.651	345967.6	29.002	-96.078	
1402.161	25910.8	24553.8	-1.588	89.762	343902.5	29.003	-95.861	
1404.111	25912.2	24555.3	-1.586	89.837	342510.7	29.003	-95.714	
1406.972	25914.5	24557.7	-1.584	89.948	340453.5	29.004	-95.497	
1411.785	25918.3	24561.7	-1.579	90.133	337011.5	29.003	-95.133	
1416.662	25921.7	24565.4	-1.574	90.319	333575.5	29.002	-94.769	

GEMINI 1C ENTRY			TRW BET		V		52	
TIME FROM RETROFIRE (SECONDS)	INERTIAL VEL. MAGNITUDE (FT/SEC)	RELATIVE VEL. MAGNITUDE (FT/SEC)	INERTIAL FLT. PATH ANGLE (DEGREES)	INERTIAL HEADING ANGLE (DEGREES)	ALTITUDE (FEET)	GEODETTIC LAT. (DEGREES)	GEODETTIC LONG. (DEGREES)	
1418.542	25923.3	24567.0	-1.572	90.394	332194.2	29.001	-94.623	
1421.417	25925.4	24569.3	-1.570	90.505	330149.7	29.000	-94.405	
1423.356	25927.0	24570.9	-1.567	90.580	328772.2	28.998	-94.258	
1426.230	25928.9	24573.0	-1.565	90.691	326733.7	28.996	-94.041	
1428.161	25930.0	24574.2	-1.563	90.765	325365.7	28.994	-93.895	
1431.034	25932.1	24576.4	-1.560	90.877	323332.2	28.992	-93.678	
1432.974	25933.4	24577.8	-1.558	90.952	321962.2	28.989	-93.531	
1435.849	25935.4	24579.9	-1.555	91.063	319933.2	28.986	-93.313	
1437.797	25936.7	24581.3	-1.553	91.137	318565.5	28.983	-93.166	
1440.664	25938.5	24583.2	-1.550	91.249	316543.0	28.979	-92.949	
1442.608	25939.5	24584.3	-1.547	91.324	315177.2	28.976	-92.802	
1445.481	25940.9	24585.8	-1.544	91.435	313161.7	28.971	-92.584	
1447.425	25941.6	24586.7	-1.542	91.511	311800.0	28.968	-92.437	
1450.330	25942.8	24587.9	-1.539	91.622	309789.7	28.962	-92.220	
1452.243	25943.5	24589.7	-1.536	91.697	308431.2	28.958	-92.072	
1455.117	25944.4	24589.8	-1.533	91.808	306430.0	28.952	-91.855	
1457.066	25944.9	24590.3	-1.530	91.883	305078.0	28.948	-91.708	
1459.933	25945.5	24591.0	-1.527	91.994	303000.5	28.941	-91.490	
1461.875	25945.7	24591.4	-1.525	92.069	301735.7	28.936	-91.343	
1464.748	25945.8	24591.6	-1.521	92.179	299747.0	28.928	-91.126	
1466.692	25945.8	24591.7	-1.519	92.254	298403.5	28.923	-90.979	
1469.565	25945.8	24591.7	-1.516	92.364	296421.5	28.915	-90.761	
1471.510	25945.4	24591.5	-1.512	92.459	295022.5	28.909	-90.614	
1474.594	25944.4	24590.6	-1.508	92.559	292964.0	28.900	-90.381	
1476.762	25943.9	24590.3	-1.505	92.643	291479.5	28.893	-90.217	
1478.922	25942.9	24589.3	-1.502	92.727	290000.2	28.886	-90.053	
1481.081	25941.6	24588.1	-1.500	92.812	288525.7	28.878	-89.890	
1483.242	25940.1	24586.7	-1.497	92.896	287052.2	28.871	-89.726	

GEMINI 1C ENTRY			TRW BET		V		53	
TIME FROM RETROFIRE (SECONDS)	INERTIAL VEL. MAGNITUDE (FT/SEC)	RELATIVE VEL. MAGNITUDE (FT/SEC)	INERTIAL FLT. PATH ANGLE (DEGREES)	INERTIAL HEADING ANGLE (DEGREES)	ALTITUDE (FEET)	GEODETTIC LAT. (DEGREES)	GEODETTIC LONG. (DEGREES)	
1486.446	25937.5	24584.3	-1.493	93.022	284876.2	28.859	-89.485	
1488.666	25934.7	24581.6	-1.490	93.107	283405.7	28.851	-89.321	
1490.765	25931.7	24578.7	-1.487	93.192	281943.0	28.843	-89.158	
1492.926	25928.3	24575.4	-1.484	93.275	280481.0	28.834	-88.994	
1496.122	25922.7	24570.0	-1.479	93.400	278325.5	28.821	-88.753	
1498.285	25918.5	24565.8	-1.475	93.485	276707.5	28.812	-88.589	
1500.444	25913.8	24561.2	-1.471	93.571	275421.5	28.803	-88.426	
1502.606	25908.8	24556.4	-1.468	93.656	273975.0	28.793	-88.263	
1504.766	25903.1	24550.8	-1.465	93.741	272534.5	28.783	-88.100	
1507.968	25897.7	24544.5	-1.461	93.867	270402.5	28.768	-87.859	
1510.130	25892.6	24534.5	-1.457	93.952	268966.2	28.758	-87.696	
1512.289	25887.5	24526.5	-1.452	94.036	267536.7	28.747	-87.533	
1514.450	25880.9	24518.0	-1.446	94.121	266112.0	28.737	-87.370	
1517.648	25885.9	24504.2	-1.437	94.246	264014.2	28.720	-87.130	
1519.814	25884.9	24493.3	-1.433	94.330	262400.0	28.709	-86.967	
1521.969	25883.2	24481.6	-1.428	94.413	261198.5	28.697	-86.805	
1524.124	25881.0	24469.5	-1.421	94.495	259803.0	28.686	-86.643	
1527.314	25881.9	24450.5	-1.416	94.616	257750.7	28.668	-86.403	
1529.468	25878.5	24436.2	-1.403	94.699	256374.5	28.656	-86.242	
1531.625	25877.4	24420.2	-1.397	94.780	255003.2	28.643	-86.080	
1533.777	25875.9	24402.8	-1.391	94.862	253641.7	28.630	-85.919	
1536.949	25872.2	24370.3	-1.378	94.983	251650.0	28.611	-85.682	
1539.099	25870.3	24356.5	-1.369	95.064	250311.0	28.598	-85.521	
1541.246	25868.3	24334.5	-1.363	95.143	248982.2	28.585	-85.361	
1543.391	25866.1	24311.0	-1.355	95.224	247662.5	28.571	-85.201	
1546.565	25865.6	24275.1	-1.339	95.343	245725.7	28.551	-84.965	
1548.713	25869.6	24248.2	-1.330	95.422	244433.5	28.537	-84.805	
1550.861	25871.1	24214.7	-1.323	95.502	243146.2	28.523	-84.646	

UNCLASSIFIED

Table B-2a. Reconstructed Reentry Trajectory, Special Parameters (Continued)

TIME FROM RETROFIRE (SECONDS)	GEMINI 10 ENTRY		TRW BET	V		ALTITUDE (FEET)	GEODEIC LAT. (DEGREES)	GEODEIC LONG. (DEGREES)
	INERTIAL VEL. MAGNITUDE (FT/SEC)	RELATIVE VEL. MAGNITUDE (FT/SEC)		INERTIAL FLT. PATH ANGLE (DEGREES)	INERTIAL HEADING ANGLE (DEGREES)			
1553.004	25540.6	24190.4	-1.312	95.582	241872.5	28.508	-84.487	
1556.177	25495.1	24145.0	-1.295	95.697	240009.7	28.487	-84.253	
1558.327	25462.1	24112.0	-1.286	95.780	238760.2	28.472	-84.094	
1560.475	25427.0	24077.0	-1.276	95.861	237522.7	28.457	-83.936	
1562.622	25391.4	24041.5	-1.263	95.937	236298.2	28.442	-83.778	
1564.764	25354.1	24004.2	-1.253	96.017	235089.5	28.426	-83.620	
1567.945	25319.2	23965.4	-1.238	96.132	233915.0	28.403	-83.387	
1570.088	25282.4	23923.2	-1.224	96.209	232735.7	28.387	-83.231	
1572.230	25247.1	23887.6	-1.213	96.288	231597.0	28.371	-83.074	
1574.373	25215.6	23849.1	-1.201	96.362	230481.2	28.355	-82.918	
1577.545	25080.7	23731.3	-1.178	96.478	228139.2	28.331	-82.688	
1579.696	25022.1	23672.8	-1.164	96.552	227020.7	28.314	-82.533	
1581.839	24962.8	23613.0	-1.147	96.631	225924.0	28.297	-82.378	
1583.984	24899.5	23555.4	-1.132	96.705	224843.5	28.281	-82.224	
1587.159	24800.9	23491.9	-1.118	96.817	223276.2	28.255	-81.996	
1589.306	24720.9	23381.9	-1.090	96.890	222239.2	28.238	-81.843	
1591.448	24657.0	23308.0	-1.074	96.965	221223.0	28.221	-81.691	
1593.594	24582.7	23233.8	-1.053	97.038	220224.5	28.203	-81.539	
1596.771	24468.0	23119.3	-1.029	97.147	218782.2	28.177	-81.314	
1598.927	24388.9	23040.2	-1.008	97.221	217831.0	28.159	-81.163	
1601.063	24306.5	22957.8	-0.994	97.293	216901.2	28.141	-81.013	
1603.201	24223.5	22874.9	-0.973	97.362	215992.7	28.123	-80.864	
1606.373	24095.3	22746.8	-0.950	97.467	214680.5	28.096	-80.644	
1608.519	24007.0	22658.5	-0.929	97.541	213815.2	28.078	-80.469	
1610.657	23914.2	22565.5	-0.915	97.604	212972.5	28.059	-80.346	
1612.796	23818.9	22470.5	-0.896	97.674	212147.5	28.041	-80.203	
1615.969	23672.1	22323.8	-0.872	97.775	210958.0	28.013	-79.987	
1618.116	23571.1	22222.8	-0.851	97.840	210177.0	27.995	-79.842	

TIME FROM RETROFIRE (SECONDS)	GEMINI 10 ENTRY		TRW BET	V		ALTITUDE (FEET)	GEODEIC LAT. (DEGREES)	GEODEIC LONG. (DEGREES)
	INERTIAL VEL. MAGNITUDE (FT/SEC)	RELATIVE VEL. MAGNITUDE (FT/SEC)		INERTIAL FLT. PATH ANGLE (DEGREES)	INERTIAL HEADING ANGLE (DEGREES)			
1620.257	23466.2	22118.0	-0.837	97.910	209416.0	27.976	-79.698	
1622.401	23360.6	22017.4	-0.817	97.973	208672.7	27.957	-79.555	
1625.575	23249.9	21891.8	-0.795	98.071	207605.0	27.929	-79.343	
1627.721	23049.5	21791.4	-0.778	98.137	206904.2	27.910	-79.202	
1629.864	22976.8	21628.8	-0.766	98.200	206219.7	27.891	-79.061	
1632.007	22863.1	21515.1	-0.750	98.264	205551.0	27.872	-78.921	
1635.181	22769.1	21343.3	-0.730	98.353	204589.2	27.843	-78.715	
1637.327	22571.0	21223.0	-0.720	98.411	203955.2	27.824	-78.577	
1639.471	22450.5	21102.6	-0.704	98.467	203336.2	27.805	-78.439	
1641.615	22327.2	20979.3	-0.695	98.521	202730.7	27.785	-78.303	
1644.710	22147.9	20800.0	-0.681	98.589	202187.2	27.757	-78.107	
1646.703	22031.4	20683.3	-0.679	98.624	201336.2	27.739	-77.982	
1649.649	21857.7	20509.0	-0.708	98.643	200527.2	27.713	-77.799	
1651.645	21739.4	20390.6	-0.758	98.642	199952.7	27.695	-77.676	
1653.638	21617.9	20269.5	-0.827	98.655	199337.5	27.677	-77.553	
1656.586	21430.8	20091.2	-0.964	98.678	198320.7	27.651	-77.374	
1658.579	21314.8	19966.3	-1.064	98.718	197549.7	27.634	-77.253	
1663.780	20986.0	19636.6	-1.357	98.906	195185.0	27.588	-76.942	
1665.937	20743.3	19495.6	-1.452	99.018	194060.5	27.569	-76.815	
1668.095	20699.7	19391.8	-1.536	99.116	192872.5	27.550	-76.693	
1671.285	20672.7	19312.1	-1.610	99.331	191030.2	27.521	-76.504	
1673.444	20617.3	18971.0	-1.649	99.454	189765.0	27.501	-76.380	
1675.601	20557.4	18811.4	-1.673	99.562	188480.2	27.482	-76.258	
1680.946	19748.5	18403.1	-1.692	99.764	185302.7	27.433	-75.959	
1683.222	19560.6	18215.2	-1.693	99.815	183961.2	27.412	-75.834	
1685.424	19368.4	18023.0	-1.698	99.844	182673.5	27.392	-75.714	
1687.564	19177.5	17832.1	-1.706	99.849	181429.7	27.373	-75.599	
1689.703	18974.0	17628.4	-1.709	99.856	180195.5	27.354	-75.485	

TIME FROM RETROFIRE (SECONDS)	GEMINI 10 ENTRY		TRW BET	V		ALTITUDE (FEET)	GEODEIC LAT. (DEGREES)	GEODEIC LONG. (DEGREES)
	INERTIAL VEL. MAGNITUDE (FT/SEC)	RELATIVE VEL. MAGNITUDE (FT/SEC)		INERTIAL FLT. PATH ANGLE (DEGREES)	INERTIAL HEADING ANGLE (DEGREES)			
1692.867	18663.0	17317.3	-1.712	99.868	178391.2	27.326	-75.319	
1695.017	18447.6	17101.9	-1.715	99.879	177179.7	27.307	-75.208	
1697.159	18229.5	16883.6	-1.726	99.872	175982.2	27.289	-75.099	
1702.467	17577.4	16330.9	-1.817	99.789	172997.0	27.245	-74.835	
1704.561	17494.3	16107.5	-1.929	99.724	171778.2	27.228	-74.733	
1709.570	16915.2	15588.0	-2.336	99.577	168531.2	27.188	-74.495	
1711.563	16862.8	15509.7	-2.374	99.547	167077.2	27.173	-74.403	
1714.578	16355.4	15028.9	-2.928	99.628	164722.2	27.151	-74.269	
1716.532	16112.2	14766.4	-3.163	99.726	162962.5	27.136	-74.179	
1718.613	14955.3	14510.5	-3.380	99.876	161049.5	27.121	-74.088	
1721.675	15459.6	14116.3	-3.610	100.125	158106.2	27.098	-73.957	
1723.747	15175.8	13833.4	-3.698	100.287	156068.7	27.083	-73.870	
1725.892	14868.6	13527.0	-3.742	100.411	153963.0	27.067	-73.783	
1728.045	14542.2	13200.7	-3.749	100.478	151879.2	27.051	-73.697	
1731.225	14049.9	12568.2	-3.755	100.418	148863.2	27.029	-73.603	
1733.368	13711.3	12369.1	-3.782	100.303	146914.2	27.014	-73.494	
1735.515	13367.8	12075.4	-3.774	100.248	144985.2	27.000	-73.416	
1737.660	13017.2	11674.6	-3.761	100.192	143112.5	26.986	-73.340	
1740.829	12497.1	11153.8	-3.776	100.030	140437.2	26.967	-73.232	
1742.972	12141.7	10798.0	-3.800	99.914	138681.0	26.954	-73.162	
1745.112	11788.0	10443.0	-3.829	99.793	136966.2	26.942	-73.094	
1747.246	11434.9	10090.3	-3.863	99.661	135293.5	26.931	-73.029	
1750.417	10911.0	9564.8	-3.926	99.668	132872.5	26.915	-72.876	
1752.561	10551.4	9205.0	-3.986	99.338	131275.5	26.905	-72.876	
1754.704	10195.3	8849.3	-4.061	99.210	129706.7	26.895	-72.818	
1756.845	9847.9	8511.7	-4.151	99.077	128161.5	26.886	-72.763	
1760.014	9340.9	7994.3	-4.311	98.861	125907.5	26.873	-72.684	
1762.161	9004.8	7657.8	-4.537	98.641	124381.0	26.865	-72.634	

UNCLASSIFIED

Table B-2a. Reconstructed Reentry Trajectory, Special Parameters (Continued)

TIME FROM RETROFIRE (SECONDS)	GEMINI IC ENTRY		TRW BET	V		ALTITUDE (FEET)	GEODETIC LAT. (DEGREES)	GEODETIC LONG. (DEGREES)
	INERTIAL VEL. MAGNITUDE (FT/SEC)	RELATIVE VEL. MAGNITUDE (FT/SEC)	INERTIAL FLT. PATH ANGLE (DEGREES)	INERTIAL HEADING ANGLE (DEGREES)	INERTIAL HEADING ANGLE (DEGREES)			
1767.17C	8249.9	6922.8	-5.353	98.044	98.044	120654.5	26.847	-72.525
1769.163	7995.2	6608.8	-5.819	97.923	97.923	119078.2	26.841	-72.485
1772.10B	7522.5	6182.2	-6.277	97.589	97.589	116598.0	26.833	-72.429
1774.165	7239.3	5897.1	-7.273	97.514	97.514	114806.7	26.828	-72.393
1776.096	6958.0	5618.6	-7.897	97.514	97.514	112937.7	26.823	-72.359
1779.046	6549.6	5214.9	-8.771	97.619	97.619	110048.0	26.816	-72.312
1781.044	6277.8	4946.6	-9.362	97.751	97.751	108032.2	26.811	-72.282
1784.074	5876.9	4551.9	-9.954	97.975	97.975	104949.5	26.804	-72.240
1786.224	5599.6	4273.5	-10.307	98.052	98.052	102778.2	26.800	-72.212
1788.369	5322.9	4027.4	-10.618	98.037	98.037	100646.5	26.795	-72.186
1790.514	5058.5	3740.4	-10.943	97.909	97.909	98560.7	26.791	-72.162
1795.829	4451.3	3140.0	-12.027	97.164	97.164	93536.5	26.782	-72.109
1797.959	4232.2	2925.2	-12.651	96.768	96.768	91558.2	26.779	-72.091
1800.091	4025.8	2723.8	-13.261	96.402	96.402	89583.2	26.776	-72.074
1803.318	3734.6	2441.3	-14.172	95.901	95.901	86614.7	26.773	-72.050
1805.525	3551.6	2265.3	-14.812	95.534	95.534	84601.7	26.771	-72.036
1807.673	3386.1	2117.2	-15.427	95.167	95.167	82557.5	26.769	-72.023
1809.802	3231.8	1964.8	-16.130	94.776	94.776	80474.0	26.767	-72.011
1812.949	3022.0	1763.9	-16.885	94.144	94.144	77960.0	26.765	-71.996
1815.079	2892.2	1644.2	-17.472	93.675	93.675	76099.2	26.764	-71.986
1819.258	2664.5	1438.0	-18.570	92.704	92.704	72510.5	26.762	-71.970
1822.335	2517.4	1307.8	-19.254	91.940	91.940	69926.7	26.762	-71.960
1824.415	2429.0	1231.4	-19.685	91.440	91.440	68212.2	26.761	-71.954
1826.494	2347.6	1162.9	-20.109	90.955	90.955	66522.7	26.761	-71.948
1828.571	2272.8	1074.2	-20.528	90.489	90.489	64868.0	26.761	-71.941
1831.653	2171.2	1019.6	-20.949	89.619	89.619	62435.7	26.761	-71.936
1836.857	2018.5	900.7	-21.498	88.479	88.479	58490.7	26.761	-71.927
1838.941	1968.4	863.2	-21.672	88.151	88.151	56962.5	26.762	-71.924

TIME FROM RETROFIRE (SECONDS)	GEMINI IC ENTRY		TRW BET	V		ALTITUDE (FEET)	GEODETIC LAT. (DEGREES)	GEODETIC LONG. (DEGREES)
	INERTIAL VEL. MAGNITUDE (FT/SEC)	RELATIVE VEL. MAGNITUDE (FT/SEC)	INERTIAL FLT. PATH ANGLE (DEGREES)	INERTIAL HEADING ANGLE (DEGREES)	INERTIAL HEADING ANGLE (DEGREES)			
1841.087	1925.3	833.9	-21.916	87.879	87.879	55411.7	26.762	-71.921
1843.245	1894.5	807.5	-22.146	87.619	87.619	53870.0	26.762	-71.919
1846.356	1936.2	771.5	-22.332	87.363	87.363	51683.7	26.763	-71.915
1848.431	1795.4	747.8	-22.481	87.251	87.251	50253.5	26.763	-71.913
1850.507	1764.5	723.3	-22.259	87.179	87.179	48850.5	26.764	-71.911
1853.578	1718.5	688.8	-22.121	87.300	87.300	46831.2	26.765	-71.909
1855.656	1690.1	667.4	-21.987	87.321	87.321	45502.2	26.765	-71.908
1860.794	1636.0	623.7	-21.651	87.309	87.309	42331.5	26.766	-71.905
1862.869	1611.5	608.8	-21.475	87.245	87.245	41095.7	26.766	-71.904
1868.011	1573.5	575.8	-20.960	87.441	87.441	38132.7	26.767	-71.902
1870.090	1559.6	561.1	-20.650	87.349	87.349	36976.0	26.768	-71.902
1872.162	1529.4	536.0	-20.269	88.006	88.006	35858.2	26.768	-71.901
1875.232	1516.1	501.7	-19.100	88.597	88.597	34284.7	26.768	-71.901
1877.311	1502.6	485.1	-18.674	89.363	89.363	33269.2	26.769	-71.900
1879.384	1493.5	471.1	-18.254	89.342	89.342	32285.7	26.769	-71.900
1882.451	1478.6	454.7	-17.827	89.667	89.667	30874.2	26.769	-71.899
1884.529	1476.0	446.6	-17.531	89.876	89.876	29942.2	26.769	-71.899
1886.602	1472.2	439.2	-17.282	89.941	89.941	29028.0	26.769	-71.899
1889.671	1459.8	425.2	-16.881	90.349	90.349	27766.2	26.769	-71.898
1891.759	1450.4	414.7	-16.491	90.333	90.333	26833.2	26.769	-71.898
1893.839	1442.5	404.8	-16.418	90.736	90.736	25978.0	26.769	-71.898
1896.914	1441.2	399.0	-16.018	91.014	91.014	24739.5	26.769	-71.898
1898.996	1446.4	390.0	-15.591	90.593	90.593	23920.7	26.768	-71.898
1901.072	1431.9	382.5	-15.441	91.156	91.156	23121.5	26.768	-71.898
1904.145	1432.3	372.0	-14.991	91.162	91.162	21966.0	26.768	-71.897
1906.230	1433.1	364.3	-14.691	90.567	90.567	21201.0	26.768	-71.897
1908.307	1439.1	355.9	-14.227	91.083	91.083	20456.5	26.768	-71.897
1910.383	1434.1	351.4	-14.116	90.881	90.881	19725.7	26.768	-71.897

TIME FROM RETROFIRE (SECONDS)	GEMINI IC ENTRY		TRW BET	V		ALTITUDE (FEET)	GEODETIC LAT. (DEGREES)	GEODETIC LONG. (DEGREES)
	INERTIAL VEL. MAGNITUDE (FT/SEC)	RELATIVE VEL. MAGNITUDE (FT/SEC)	INERTIAL FLT. PATH ANGLE (DEGREES)	INERTIAL HEADING ANGLE (DEGREES)	INERTIAL HEADING ANGLE (DEGREES)			
1913.462	1433.1	342.1	-13.737	90.934	90.934	18663.2	26.767	-71.897
1915.536	1430.0	335.3	-13.437	91.501	91.501	17965.7	26.767	-71.897
1917.610	1428.4	330.6	-13.278	91.338	91.338	17278.7	26.767	-71.896
1920.691	1431.1	326.4	-13.246	91.483	91.483	16277.5	26.767	-71.896
1922.770	1421.0	322.5	-13.015	91.446	91.446	15608.5	26.767	-71.896
1924.848	1419.6	318.7	-12.897	91.157	91.157	14966.7	26.766	-71.896
1927.923	1426.3	313.8	-12.576	91.475	91.475	13981.7	26.766	-71.896
1930.003	1420.0	311.1	-12.514	91.307	91.307	13338.7	26.766	-71.896
1932.081	1419.4	307.7	-12.445	91.033	91.033	12771.2	26.766	-71.895
1935.156	1426.0	304.9	-12.207	91.438	91.438	11767.0	26.766	-71.895
1937.235	1422.5	300.7	-12.096	91.194	91.194	11153.5	26.765	-71.895
1939.315	1426.1	299.1	-12.002	90.911	90.911	10593.0	26.765	-71.895
1942.387	1418.5	294.7	-11.895	91.174	91.174	9620.2	26.765	-71.895
1944.467	1423.5	291.0	-11.678	91.139	91.139	9016.2	26.765	-71.894
1946.542	1422.5	280.3	-11.246	91.027	91.027	7558.5	26.764	-71.894
1951.711	1424.6	280.5	-11.248	90.789	90.789	6981.2	26.764	-71.894
1953.774	1407.1	282.1	-8.089	91.175	91.175	6487.7	26.764	-71.893
1956.846	1395.5	138.7	-5.494	91.144	91.144	5977.7	26.764	-71.893
1958.927	1389.5	120.2	-4.810	90.939	90.939	5717.7	26.764	-71.893
1961.003	1394.4	105.1	-4.076	90.910	90.910	5493.7	26.764	-71.893
1963.075	1385.7	68.4	-2.498	91.029	91.029	5248.7	26.764	-71.893
1966.154	1368.9	48.3	-1.537	91.307	91.307	5147.7	26.763	-71.893
1968.232	1368.1	46.1	-1.362	91.350	91.350	5075.7	26.763	-71.893
1971.300	1371.2	43.1	-1.297	91.218	91.218	4978.0	26.763	-71.893
1973.384	1385.5	46.0	-1.564	90.636	90.636	4906.2	26.763	-71.892
1975.454	1394.8	47.5	-1.516	90.650	90.650	4828.7	26.763	-71.892
1978.525	1384.0	47.1	-1.505	90.928	90.928	4716.5	26.763	-71.892
1980.611	1387.2	47.0	-1.537	90.942	90.942	4639.7	26.762	-71.892

UNCLASSIFIED

Table B-2a. Reconstructed Reentry Trajectory, Special Parameters (Continued)

TIME FROM RETROFIRE (SECONDS)	GEMINI 10 ENTRY		TRW BET		V		60°	
	INERTIAL VEL. MAGNITUDE (FT/SEC)	RELATIVE VEL. MAGNITUDE (FT/SEC)	INERTIAL FLT. PATH ANGLE (DEGREES)	INERTIAL HEADING ANGLE (DEGREES)	ALTITUDE (FEET)	GEODETIC LAT. (DEGREES)	GEODETIC LONG. (DEGREES)	
1982.685	1387.3	49.2	-1.558	90.899	4562.0	26.762	-71.892	
1985.749	1381.9	50.1	-1.564	91.163	4446.2	26.762	-71.892	
1987.832	1368.9	49.0	-1.645	91.212	4365.7	26.762	-71.892	
1989.910	1365.3	45.6	-1.531	91.146	4287.0	26.762	-71.892	
1991.986	1377.2	47.7	-1.603	91.043	4209.0	26.762	-71.892	
1995.055	1393.8	57.1	-1.617	91.207	4089.2	26.761	-71.891	
1997.125	1391.4	53.7	-1.435	91.268	4012.2	26.761	-71.891	
1999.204	1385.7	49.1	-1.498	91.050	3938.2	26.761	-71.891	
2002.284	1382.2	44.6	-1.552	90.675	3824.5	26.761	-71.891	
2004.358	1377.6	48.3	-1.604	91.084	3745.9	26.761	-71.891	
2006.439	1369.3	48.8	-1.607	91.249	3665.5	26.761	-71.891	
2009.510	1378.2	49.7	-1.591	91.187	3547.5	26.760	-71.891	
2011.591	1383.8	50.6	-1.657	93.997	3465.7	26.760	-71.890	
2013.666	1381.5	54.6	-1.581	91.466	3385.0	26.760	-71.890	
2016.742	1381.4	55.1	-1.551	91.528	3268.0	26.760	-71.890	
2018.820	1387.9	52.6	-1.566	91.149	3190.0	26.760	-71.890	
2020.899	1382.7	48.6	-1.561	91.021	3111.0	26.759	-71.890	
2023.967	1375.2	48.2	-1.574	91.106	2995.2	26.759	-71.890	
2026.048	1367.0	47.2	-1.593	91.171	2916.2	26.759	-71.890	
2031.199	1373.1	48.6	-1.629	91.155	2717.2	26.759	-71.890	
2033.275	1377.2	51.4	-1.581	91.342	2637.2	26.758	-71.890	
2035.356	1377.6	48.7	-1.683	90.981	2555.5	26.758	-71.890	
2038.429	1382.2	48.5	-1.666	90.846	2431.2	26.758	-71.889	
2040.511	1380.9	51.9	-1.568	91.311	2350.2	26.758	-71.889	
2042.585	1385.2	55.4	-1.595	91.404	2270.5	26.758	-71.889	
2045.659	1382.4	52.8	-1.603	91.292	2151.7	26.757	-71.889	
2047.735	1388.5	54.0	-1.517	91.296	2073.0	26.757	-71.889	
2049.812	1385.9	57.2	-1.547	91.560	1996.0	26.757	-71.889	
	GEMINI 10 ENTRY		TRW BET		V		61	
TIME FROM RETROFIRE (SECONDS)	INERTIAL VEL. MAGNITUDE (FT/SEC)	RELATIVE VEL. MAGNITUDE (FT/SEC)	INERTIAL FLT. PATH ANGLE (DEGREES)	INERTIAL HEADING ANGLE (DEGREES)	ALTITUDE (FEET)	GEODETIC LAT. (DEGREES)	GEODETIC LONG. (DEGREES)	
2052.893	1377.1	56.2	-1.579	91.644	1879.5	26.757	-71.889	
2054.982	1376.6	53.4	-1.600	91.464	1799.5	26.757	-71.888	
2057.063	1380.8	53.2	-1.561	91.408	1720.2	26.756	-71.888	
2060.145	1381.4	54.8	-1.568	91.488	1603.7	26.756	-71.888	
2062.221	1376.9	53.4	-1.648	91.403	1523.0	26.756	-71.888	

UNCLASSIFIED

Table B-2b. Reconstructed Reentry Trajectory,
Special Parameters

TIME (SEC)	GEMINI 10 ENTRY		TRW BET		V	82
	RELATIVE FLT. PATH ANGLE (DEGREES)	RELATIVE HEADING ANGLE (DEGREES)	INERTIAL LONG. (DEGREES)	GEOCENTRIC LAT. (DEGREES)		
1347.366	-1.726	87.523	-94.359	28.754	21293164.0	
1349.376	-1.724	87.601	-94.206	28.759	21291733.0	
1352.163	-1.721	87.716	-93.979	28.767	21289628.0	
1354.165	-1.720	87.795	-93.825	28.772	21288198.5	
1356.965	-1.718	87.910	-93.598	28.779	21286099.5	
1358.921	-1.716	87.989	-93.444	28.784	21284674.7	
1361.762	-1.714	88.105	-93.217	28.790	21282576.7	
1363.699	-1.712	88.183	-93.063	28.794	21281155.7	
1366.656	-1.709	88.299	-92.836	28.800	21279064.7	
1368.494	-1.707	88.378	-92.682	28.804	21277648.0	
1371.354	-1.705	88.493	-92.455	28.809	2127559.7	
1373.296	-1.703	88.572	-92.300	28.812	21274143.5	
1376.161	-1.700	88.688	-92.073	28.817	21272057.5	
1378.107	-1.699	88.767	-91.918	28.819	21270641.0	
1380.963	-1.696	88.884	-91.690	28.823	21268561.5	
1382.914	-1.694	88.962	-91.535	28.826	21267150.0	
1385.778	-1.691	89.079	-91.307	28.829	21265074.0	
1387.722	-1.689	89.158	-91.153	28.831	21263666.0	
1390.581	-1.687	89.274	-90.924	28.834	21261594.0	
1392.534	-1.685	89.353	-90.769	28.835	21260188.5	
1394.474	-1.683	89.432	-90.615	28.836	21258788.7	
1397.346	-1.680	89.548	-90.386	28.838	21256719.7	
1399.286	-1.678	89.627	-90.231	28.839	21255324.0	
1402.161	-1.676	89.744	-90.002	28.840	21253258.2	
1404.101	-1.674	89.823	-89.848	28.840	21251866.0	
1406.972	-1.671	89.942	-89.619	28.841	21249808.5	
1411.785	-1.666	90.136	-89.235	28.841	21246366.7	
1416.602	-1.661	90.332	-88.851	28.839	21242932.2	

TIME (SEC)	GEMINI 10 ENTRY		TRW BET		V	83
	RELATIVE FLT. PATH ANGLE (DEGREES)	RELATIVE HEADING ANGLE (DEGREES)	INERTIAL LONG. (DEGREES)	GEOCENTRIC LAT. (DEGREES)		
1418.542	-1.659	90.411	-88.696	28.838	21241551.7	
1421.417	-1.656	90.528	-88.466	28.837	21239509.0	
1423.355	-1.654	90.607	-88.312	28.836	21238132.7	
1426.230	-1.651	90.724	-88.082	28.833	21236096.5	
1428.161	-1.649	90.803	-87.928	28.832	21234730.2	
1431.034	-1.646	90.920	-87.699	28.829	21232700.2	
1432.974	-1.644	90.999	-87.544	28.827	21231332.0	
1435.849	-1.641	91.117	-87.314	28.823	21229366.7	
1437.792	-1.638	91.196	-87.159	28.820	21227941.7	
1440.664	-1.635	91.313	-86.930	28.816	21225923.5	
1442.608	-1.633	91.393	-86.774	28.813	21224561.0	
1445.481	-1.630	91.510	-86.545	28.808	21222556.5	
1447.425	-1.627	91.590	-86.390	28.805	21221152.5	
1450.301	-1.623	91.707	-86.160	28.799	21219187.7	
1452.243	-1.621	91.786	-86.005	28.795	21217835.2	
1455.117	-1.617	91.903	-85.775	28.789	21215838.5	
1457.060	-1.615	91.982	-85.620	28.785	21214491.0	
1459.933	-1.611	92.099	-85.391	28.778	21212502.5	
1461.875	-1.609	92.178	-85.236	28.773	21211160.7	
1464.749	-1.605	92.295	-85.006	28.766	21209179.7	
1466.692	-1.602	92.374	-84.851	28.761	21207841.7	
1469.565	-1.599	92.490	-84.621	28.752	21205868.2	
1471.510	-1.596	92.569	-84.466	28.747	21204535.0	
1474.594	-1.591	92.695	-84.220	28.737	21202426.2	
1476.760	-1.588	92.784	-84.047	28.730	21200949.0	
1478.922	-1.585	92.873	-83.874	28.723	21199477.0	
1481.081	-1.582	92.962	-83.702	28.716	21198010.0	
1483.242	-1.579	93.052	-83.529	28.708	21196544.5	

TIME (SEC)	GEMINI 10 ENTRY		TRW BET		V	84
	RELATIVE FLT. PATH ANGLE (DEGREES)	RELATIVE HEADING ANGLE (DEGREES)	INERTIAL LONG. (DEGREES)	GEOCENTRIC LAT. (DEGREES)		
1486.440	-1.575	93.185	-83.274	28.697	21194380.5	
1488.606	-1.572	93.274	-83.101	28.689	21192918.5	
1490.765	-1.569	93.363	-82.929	28.680	21191464.2	
1492.928	-1.566	93.451	-82.757	28.672	21190011.2	
1496.122	-1.561	93.583	-82.502	28.659	21187869.0	
1498.285	-1.556	93.673	-82.329	28.650	21186423.5	
1500.446	-1.552	93.763	-82.157	28.640	21184984.0	
1502.603	-1.549	93.853	-81.985	28.631	21183547.5	
1504.766	-1.545	93.943	-81.813	28.621	21182117.0	
1507.968	-1.541	94.074	-81.558	28.606	21180000.2	
1510.130	-1.538	94.164	-81.386	28.596	21178574.7	
1512.289	-1.532	94.255	-81.215	28.585	21177156.2	
1514.450	-1.526	94.344	-81.043	28.575	21175742.5	
1517.648	-1.517	94.476	-80.789	28.558	21173661.5	
1519.814	-1.512	94.565	-80.617	28.547	21172259.0	
1521.969	-1.507	94.653	-80.446	28.536	21170869.2	
1524.124	-1.500	94.739	-80.275	28.524	21169485.7	
1527.314	-1.488	94.868	-80.022	28.506	21167451.7	
1529.468	-1.480	94.959	-79.852	28.494	21166088.2	
1531.625	-1.474	95.041	-79.681	28.481	21164729.7	
1533.777	-1.468	95.128	-79.511	28.469	21163381.2	
1536.949	-1.454	95.256	-79.260	28.450	21161409.0	
1539.099	-1.445	95.341	-79.091	28.437	21160083.5	
1541.246	-1.438	95.426	-78.922	28.424	21158768.2	
1543.391	-1.430	95.512	-78.753	28.410	21157462.5	
1546.555	-1.413	95.638	-78.503	28.390	21155549.5	
1548.713	-1.404	95.721	-78.335	28.376	21154268.5	
1550.861	-1.397	95.806	-78.166	28.362	21152994.0	

UNCLASSIFIED

Table B-2b. Reconstructed Reentry Trajectory, Special Parameters (Continued)

TIME (SEC)	GEMINI IC ENTRY		INERTIAL LONG. (DEGREES)	GEOCENTRIC LAT. (DEGREES)	RADIUS TO EARTH CENTER (FEET)
	RELATIVE FLT. PATH ANGLE (DEGREES)	RELATIVE HEADING ANGLE (DEGREES)			
1553.004	-1.305	95.891	-77.999	28.347	21151737.0
1556.177	-1.267	96.013	-77.751	28.326	21149895.2
1558.327	-1.358	96.132	-77.583	28.311	21148661.7
1560.475	-1.348	96.187	-77.416	28.296	21147439.7
1562.622	-1.334	96.268	-77.249	28.281	21146231.0
1564.764	-1.323	96.353	-77.083	28.265	21145031.7
1567.945	-1.308	96.476	-76.836	28.242	21143287.0
1570.088	-1.293	96.558	-76.671	28.227	21142123.7
1572.233	-1.281	96.642	-76.506	28.211	21140974.5
1574.373	-1.269	96.721	-76.341	28.194	21139830.0
1577.545	-1.245	96.845	-76.097	28.170	21138184.7
1579.696	-1.231	96.924	-75.933	28.154	21137083.2
1581.839	-1.212	97.009	-75.769	28.137	21136033.5
1583.984	-1.196	97.088	-75.606	28.120	21134942.0
1587.153	-1.171	97.208	-75.365	28.095	21133398.5
1589.306	-1.153	97.287	-75.203	28.078	21132379.0
1591.448	-1.136	97.367	-75.042	28.061	21131380.5
1593.594	-1.115	97.446	-74.880	28.043	21130399.7
1596.771	-1.089	97.584	-74.643	28.017	21128984.0
1598.927	-1.067	97.643	-74.493	27.999	21128051.0
1601.063	-1.052	97.721	-74.324	27.981	21127139.5
1603.201	-1.030	97.796	-74.166	27.963	21126249.2
1606.373	-1.006	97.910	-73.933	27.937	21124963.7
1608.519	-0.985	97.990	-73.776	27.918	21124117.5
1610.657	-0.969	98.059	-73.620	27.900	21123293.2
1612.796	-0.949	98.135	-73.465	27.882	21122487.0
1615.969	-0.924	98.245	-73.236	27.854	21121325.5
1618.116	-0.903	98.317	-73.081	27.835	21120563.2

TIME (SEC)	GEMINI IC ENTRY		INERTIAL LONG. (DEGREES)	GEOCENTRIC LAT. (DEGREES)	RADIUS TO EARTH CENTER (FEET)
	RELATIVE FLT. PATH ANGLE (DEGREES)	RELATIVE HEADING ANGLE (DEGREES)			
1620.257	-0.888	98.393	-72.928	27.817	21119821.5
1622.401	-0.867	98.463	-72.770	27.798	21119097.0
1625.575	-0.845	98.571	-72.552	27.777	21118057.7
1627.721	-0.827	98.643	-72.401	27.751	21117376.2
1629.864	-0.814	98.712	-72.251	27.732	21116711.0
1632.007	-0.797	98.784	-72.102	27.713	21116061.5
1635.181	-0.776	98.883	-71.983	27.685	21115128.2
1637.327	-0.765	98.948	-71.736	27.665	21114513.7
1639.471	-0.749	99.011	-71.589	27.646	21113914.2
1641.615	-0.744	99.072	-71.444	27.627	21113328.0
1644.715	-0.725	99.148	-71.236	27.599	21112501.7
1646.703	-0.723	99.189	-71.102	27.581	21111979.7
1649.649	-0.755	99.214	-70.907	27.555	21111197.2
1651.645	-0.819	99.216	-70.775	27.537	21110640.5
1653.638	-0.892	99.234	-70.644	27.519	21110043.0
1656.586	-1.028	99.263	-70.452	27.494	21109052.5
1658.579	-1.135	99.309	-70.323	27.476	21108299.0
1663.787	-1.450	99.519	-69.991	27.430	21105980.2
1665.937	-1.553	99.644	-69.855	27.411	21104874.7
1668.095	-1.643	99.785	-69.719	27.392	21103706.0
1671.284	-1.730	99.990	-69.521	27.363	21101901.5
1673.444	-1.766	100.128	-69.389	27.344	21100646.7
1675.601	-1.793	100.249	-69.257	27.324	21099381.7
1680.946	-1.816	100.482	-68.936	27.276	21096252.7
1683.222	-1.818	100.544	-68.801	27.255	21094932.0
1685.424	-1.825	100.583	-68.672	27.235	21093664.0
1687.584	-1.835	100.596	-68.548	27.216	21092439.5
1689.703	-1.839	100.613	-68.425	27.197	21091224.0

TIME (SEC)	GEMINI IC ENTRY		INERTIAL LONG. (DEGREES)	GEOCENTRIC LAT. (DEGREES)	RADIUS TO EARTH CENTER (FEET)
	RELATIVE FLT. PATH ANGLE (DEGREES)	RELATIVE HEADING ANGLE (DEGREES)			
1697.867	-1.845	100.639	-68.246	27.169	21089447.5
1699.217	-1.850	100.661	-68.126	27.151	21088254.5
1697.153	-1.844	100.664	-68.008	27.133	21087075.2
1702.467	-1.966	100.601	-67.722	27.088	21084134.0
1704.561	-2.090	100.541	-67.611	27.071	21082932.2
1709.577	-2.557	100.410	-67.352	27.032	21079724.2
1711.533	-2.800	100.410	-67.252	27.017	21078785.2
1714.503	-3.191	100.405	-67.104	26.995	21077592.0
1716.532	-3.452	100.616	-67.007	26.980	21074217.2
1716.613	-3.694	100.795	-66.907	26.965	21072309.5
1721.675	-3.954	101.094	-66.763	26.942	21069388.7
1723.747	-4.058	101.292	-66.660	26.927	21067366.2
1725.892	-4.114	101.451	-66.572	26.911	21065276.0
1728.045	-4.131	101.551	-66.477	26.896	21063207.7
1731.225	-4.152	101.527	-66.341	26.873	21061234.0
1733.369	-4.193	101.429	-66.252	26.859	21058279.5
1735.515	-4.196	101.401	-66.165	26.845	21056384.2
1737.660	-4.195	101.373	-66.080	26.831	21054505.0
1740.829	-4.231	101.247	-65.999	26.812	21051848.7
1742.972	-4.274	101.158	-65.880	26.799	21050105.0
1745.112	-4.322	101.064	-65.803	26.787	21048402.0
1747.246	-4.379	100.959	-65.729	26.776	21046740.2
1750.417	-4.480	100.811	-65.622	26.760	21044935.0
1752.561	-4.570	100.714	-65.553	26.750	21042748.2
1754.704	-4.680	100.622	-65.487	26.746	21041189.0
1756.845	-4.810	100.526	-65.422	26.731	21039653.0
1760.014	-5.038	100.366	-65.331	26.718	21037411.7
1762.161	-5.338	100.174	-65.272	26.710	21035893.2

UNCLASSIFIED

Table B-2b. Reconstructed Reentry Trajectory,
Special Parameters (Continued)

GEMINI 10 ENTRY TRW BET V 88					
TIME (SEC)	RELATIVE FLT. PATH ANGLE (DEGREES)	RELATIVE HEADING ANGLE (DEGREES)	INERTIAL LONG. (DEGREES)	GEOCENTRIC LAT. (DEGREES)	RADIUS TO EARTH CENTER (FEET)
1767.172	-64.41	99.628	-65.162	26.693	21032183.5
1769.163	-7.079	99.433	-65.293	26.687	21030613.2
1772.169	-8.114	99.262	-65.025	26.678	21028161.2
1774.175	-8.941	99.252	-64.981	26.673	21026355.0
1776.096	-9.796	99.342	-64.938	26.668	21024491.0
1779.046	-11.041	99.623	-64.879	26.661	21022168.2
1781.044	-11.837	99.937	-64.860	26.656	21019597.0
1784.074	-12.894	100.396	-64.786	26.650	21016521.0
1786.224	-13.551	100.662	-64.749	26.645	21014352.2
1788.369	-14.185	100.827	-64.714	26.641	21012226.7
1790.514	-14.876	100.857	-64.681	26.637	21010145.0
1792.829	-17.181	100.380	-64.606	26.628	21005129.5
1797.959	-18.474	100.051	-64.579	26.625	21003154.2
1800.000	-19.818	99.762	-64.553	26.622	21001182.0
1803.018	-21.995	99.444	-64.516	26.618	20998217.0
1805.525	-23.629	99.114	-64.492	26.616	20996276.0
1807.673	-25.377	98.871	-64.470	26.614	20994263.5
1809.867	-27.073	98.446	-64.450	26.613	20992354.7
1812.949	-29.041	97.762	-64.421	26.611	20989569.5
1815.079	-31.892	97.192	-64.403	26.610	20987710.0
1819.258	-36.164	95.786	-64.369	26.608	20984122.7
1822.335	-39.474	94.446	-64.346	26.607	20981540.0
1824.415	-41.646	93.445	-64.331	26.607	20979286.0
1826.494	-43.953	92.261	-64.317	26.607	20978136.5
1829.571	-47.300	90.104	-64.297	26.606	20975680.0
1831.653	-49.686	88.647	-64.284	26.606	20974049.7
1836.857	-55.278	84.200	-64.253	26.607	20970104.2
1838.941	-57.383	82.470	-64.241	26.607	20968575.7

GEMINI 10 ENTRY TRW BET V 89					
TIME (SEC)	RELATIVE FLT. PATH ANGLE (DEGREES)	RELATIVE HEADING ANGLE (DEGREES)	INERTIAL LONG. (DEGREES)	GEOCENTRIC LAT. (DEGREES)	RADIUS TO EARTH CENTER (FEET)
1841.087	-59.509	80.753	-64.229	26.608	20967024.5
1843.245	-61.678	78.836	-64.217	26.608	20965482.5
1846.356	-64.349	76.343	-64.201	26.609	20963295.5
1848.431	-66.148	74.388	-64.190	26.609	20961865.0
1850.567	-67.534	72.738	-64.180	26.610	20960461.5
1853.574	-69.561	71.077	-64.165	26.610	20958441.5
1855.656	-71.465	69.375	-64.155	26.611	20957112.0
1860.794	-74.736	63.804	-64.131	26.612	20953940.5
1862.869	-75.777	60.811	-64.121	26.612	20952704.2
1868.011	-77.836	56.669	-64.098	26.613	20949740.2
1871.000	-78.633	56.070	-64.088	26.613	20948583.2
1872.162	-79.476	57.765	-64.079	26.614	20947465.2
1875.232	-81.381	61.293	-64.066	26.614	20945891.2
1877.311	-82.616	66.492	-64.057	26.614	20944875.5
1879.384	-83.263	71.614	-64.048	26.614	20943892.0
1882.451	-84.572	77.456	-64.034	26.614	20942480.5
1884.529	-84.563	84.273	-64.025	26.614	20941548.2
1886.662	-84.701	86.298	-64.016	26.614	20940394.0
1889.671	-85.573	100.687	-64.003	26.614	20939312.5
1891.786	-85.515	102.580	-63.994	26.614	20938439.5
1893.839	-86.397	131.968	-63.986	26.614	20937584.2
1896.914	-85.438	139.353	-63.972	26.614	20936346.0
1898.996	-85.241	115.352	-63.964	26.614	20935527.2
1901.072	-85.250	150.643	-63.955	26.614	20934728.0
1904.145	-84.814	145.616	-63.942	26.614	20933973.0
1906.232	-85.989	120.648	-63.933	26.614	20932808.0
1908.307	-83.652	130.230	-63.924	26.613	20932063.5
1910.383	-84.565	128.191	-63.915	26.613	20931333.0

GEMINI 10 ENTRY TRW BET V 90					
TIME (SEC)	RELATIVE FLT. PATH ANGLE (DEGREES)	RELATIVE HEADING ANGLE (DEGREES)	INERTIAL LONG. (DEGREES)	GEOCENTRIC LAT. (DEGREES)	RADIUS TO EARTH CENTER (FEET)
1913.462	-84.040	128.531	-63.902	26.613	20930270.7
1915.536	-82.338	143.912	-63.893	26.613	20929573.2
1917.616	-82.845	141.267	-63.884	26.613	20928886.5
1920.691	-81.817	140.259	-63.871	26.612	20927885.5
1922.771	-82.857	149.996	-63.863	26.612	20927216.7
1924.848	-83.496	144.681	-63.854	26.612	20926555.2
1927.923	-81.742	141.981	-63.841	26.612	20925590.0
1930.000	-82.898	144.959	-63.832	26.612	20924947.7
1932.081	-83.833	138.138	-63.823	26.611	20924310.2
1935.156	-81.407	139.475	-63.810	26.611	20923376.2
1937.235	-82.489	136.734	-63.801	26.611	20922753.0
1939.315	-82.537	126.988	-63.792	26.611	20922134.5
1942.387	-82.781	139.342	-63.779	26.611	20921230.0
1944.467	-81.954	132.082	-63.770	26.610	20920626.2
1949.627	-81.826	127.972	-63.748	26.610	20919169.0
1951.707	-82.175	119.050	-63.739	26.610	20918591.7
1953.774	-78.345	134.053	-63.730	26.610	20918098.2
1956.846	-74.373	137.545	-63.717	26.610	20917588.7
1958.927	-75.546	138.707	-63.709	26.609	20917326.7
1961.003	-77.613	128.951	-63.700	26.609	20917105.0
1964.075	-61.044	140.376	-63.687	26.609	20916860.0
1966.155	-49.235	172.133	-63.678	26.609	20916759.2
1968.232	-44.926	175.593	-63.669	26.609	20916667.5
1971.307	-40.738	166.715	-63.656	26.609	20916590.0
1973.384	-55.292	125.750	-63.648	26.608	20916518.2
1975.444	-50.767	121.487	-63.639	26.608	20916441.0
1978.525	-50.540	138.839	-63.626	26.608	20916328.7
1980.611	-52.077	141.759	-63.617	26.608	20916252.2

UNCLASSIFIED

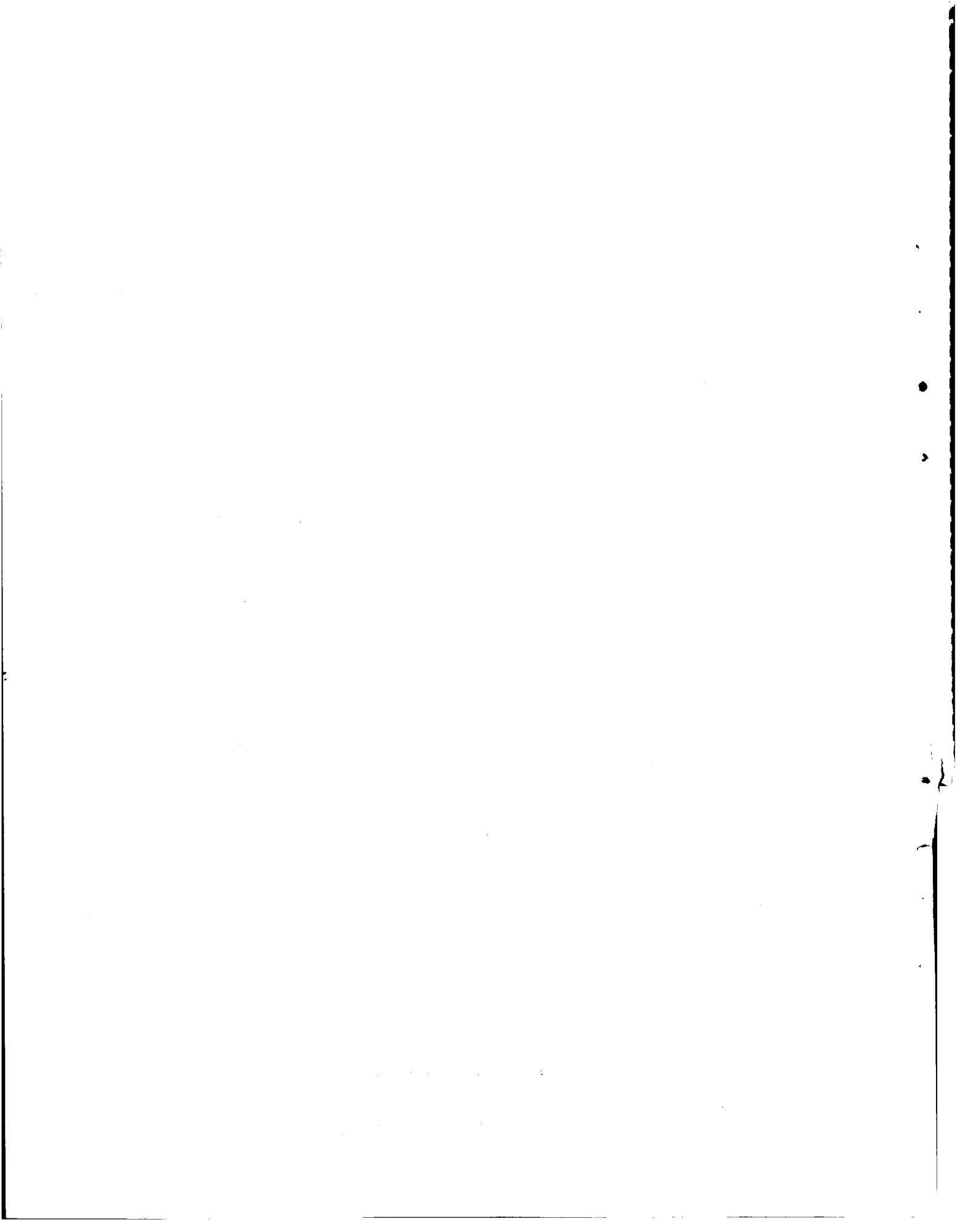
UNCLASSIFIED

Table B-2b. Reconstructed Reentry Trajectory,
Special Parameters (Continued)

TIME (SEC)	GENIIC ENTRY		TRM DET		V	RADIUS TO EARTH CENTER (FEET)
	RELATIVE FLT. PATH ANGLE (DEGREES)	RELATIVE HEADING ANGLE (DEGREES)	INERTIAL LONG. (DEGREES)	GEOCENTRIC LAT. (DEGREES)		
1982.685	-50.037	133.382	-63.668	26.608	20916174.5	
1985.749	-48.837	149.040	-63.595	26.608	20916059.0	
1987.832	-53.324	171.475	-63.586	26.608	20915978.7	
1989.911	-53.167	178.300	-63.578	26.607	20915900.0	
1991.986	-53.876	152.972	-63.569	26.607	20915822.2	
1995.055	-43.531	133.012	-63.556	26.607	20915762.7	
1997.125	-40.419	139.727	-63.547	26.607	20915626.0	
1999.204	-47.539	139.911	-63.538	26.607	20915552.0	
2002.284	-57.101	132.034	-63.525	26.606	20915438.5	
2004.354	-52.900	153.176	-63.516	26.606	20915359.7	
2006.439	-51.815	170.944	-63.508	26.606	20915279.7	
2009.511	-50.392	156.213	-63.495	26.606	20915162.0	
2011.591	-52.322	141.068	-63.488	26.606	20915080.5	
2013.666	-44.242	154.467	-63.477	26.606	20914999.7	
2016.742	-42.749	159.454	-63.464	26.605	20914883.2	
2018.821	-46.176	139.746	-63.455	26.605	20914805.2	
2020.899	-50.843	143.243	-63.446	26.605	20914726.5	
2023.967	-51.584	158.892	-63.436	26.605	20914610.7	
2026.048	-53.584	174.802	-63.425	26.605	20914532.0	
2031.199	-53.371	162.514	-63.403	26.604	20914333.5	
2033.279	-47.656	158.467	-63.394	26.604	20914253.5	
2035.356	-56.247	151.808	-63.386	26.604	20914172.0	
2038.429	-56.118	138.865	-63.373	26.604	20914048.0	
2042.517	-46.708	152.452	-63.364	26.604	20913967.0	
2045.585	-44.139	148.553	-63.355	26.603	20913887.5	
2048.659	-47.100	150.074	-63.342	26.603	20913769.0	
2047.735	-42.875	142.391	-63.333	26.603	20913690.5	
2049.812	-40.834	150.535	-63.324	26.603	20913613.7	
TIME (SEC)	GENIIC ENTRY		TRM DET		V	RADIUS TO EARTH CENTER (FEET)
	RELATIVE FLT. PATH ANGLE (DEGREES)	RELATIVE HEADING ANGLE (DEGREES)	INERTIAL LONG. (DEGREES)	GEOCENTRIC LAT. (DEGREES)		
2052.833	-42.514	162.501	-63.311	26.602	20913497.5	
2054.982	-45.979	161.124	-63.303	26.602	20913417.7	
2057.063	-44.992	154.265	-63.294	26.602	20913338.5	
2060.145	-43.638	156.736	-63.281	26.602	20913222.5	
2062.226	-47.798	159.771	-63.272	26.601	20913141.7	

(Reverse of this page is intentionally blank.)

UNCLASSIFIED



CONFIDENTIAL

APPENDIX C

TRACKER CALIBRATION DATA

1. GE MOD III

The following calibration data were used in the processing of the GE/MOD III tracking data. The values listed below are the parameters which vary from flight to flight; approximately 40 other scaling and calibration biases associated with the MOD III data reduction remain the same for each flight. A complete description of the use of each parameter in the data reduction is included in Section 4.4.2.2 of the TRW Gemini Analysis Plan, Reference 1.

Zero-Set Calibration Data

Range (J_1)	=	-1793.343 ft
Azimuth (J_3)	=	-130.72247°
Elevation (J_5)	=	-15.05196°
Squint Angle (J_4)	=	0.01511°

Refraction

Ground Index of Refraction (J_2) = 1.000380

The calibration values used by TRW and GE are, as far as known, identical. The General Electric Co. postflight report on the calibration procedures and flight constants used on this mission may be found in Reference 7. However, the refraction correction calculated by GE is based on the measured atmosphere while the TRW correction relies on an analytical model which is a function of the ground-measured index of refraction. This model is defined in Reference 1. Curves of the TRW refraction correction for a typical Gemini flight are shown in Figures C-1 and C-2.

2. MISTRAM

Responsibility for reduction of the MISTRAM data lies with RCA/PAA at the Eastern Test Range. Their analysis results are reported in the Gemini 10 "Red Book" of trajectory data, References 4 and 5. The following calibration data were extracted from these documents:

CONFIDENTIAL

~~CONFIDENTIAL~~

	<u>R</u> (ft)	<u>P1</u> (ft)	<u>Q1</u> (ft)	<u>P2</u> (ft)	<u>Q2</u> (ft)
Calibrations	211.6487	-79.4601	-38.2355	-77.0259	-45.1216
Accumulated transfers	0	-10140.3628	-7.6259	-3.2479	-1.4389
Transponder delay	-8.3700				
BIAS**	<u>-0.0540</u>	<u>-3.8897</u>	<u>1.8573</u>	<u>-2.8815</u>	<u>0.9605</u>
Total	203.2247	-10223.7126	-44.0041	-83.1553	-45.6000

Index of Refraction

Central Receiver = 1.000387

P₂ Site = 1.000387

Q₂ Site = 1.000387

Having corrected the raw measurements as well as possible, all the available MISTRAM as well as "C" band radar data were used by the ETR to form a minimum variance estimate of the spacecraft trajectory. Additional MISTRAM bias errors are solved for in this regression and are recorded in Table 4-1 of this report for comparison with TRW results. The "fully corrected" but unsmoothed measurement data were used by TRW in their simultaneous IGS/tracker error regression program.

<u>Figures</u>	<u>Page</u>
C-1 GE MOD III Refraction Corrections (Range and Elevation)	C-3
C-2 GE MOD III Refraction Corrections (Range Rate, P, and Q)	C-4

**Data prior to 153.55 sec were biased to agree with data after 153.55 sec. The bias was calculated by extrapolating from 153.55 sec backwards and agreement of the comparison between 10K and 100K base lines.

~~CONFIDENTIAL~~

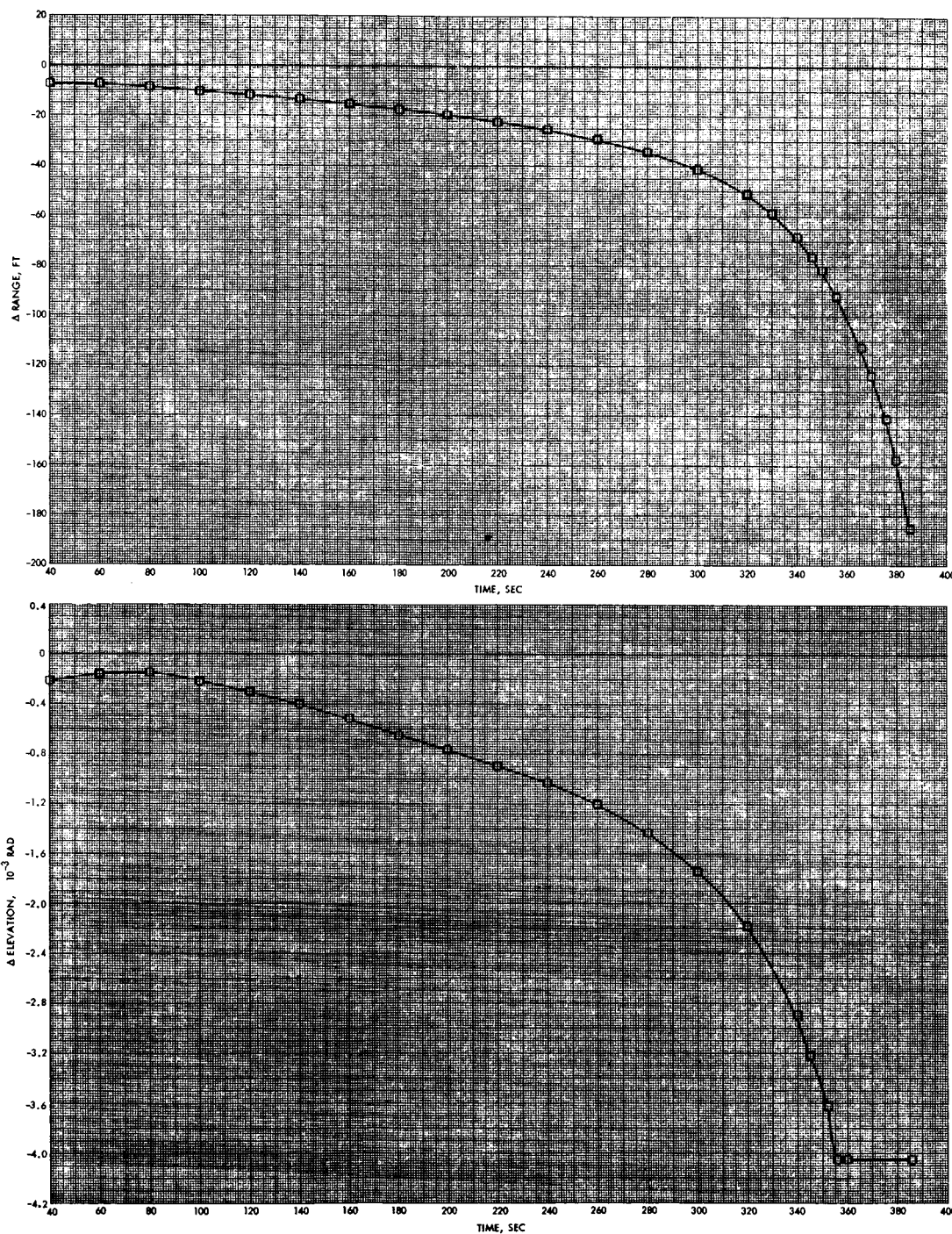


Figure C-1. GE MOD III Refraction Corrections (Range and Elevation)

CONFIDENTIAL

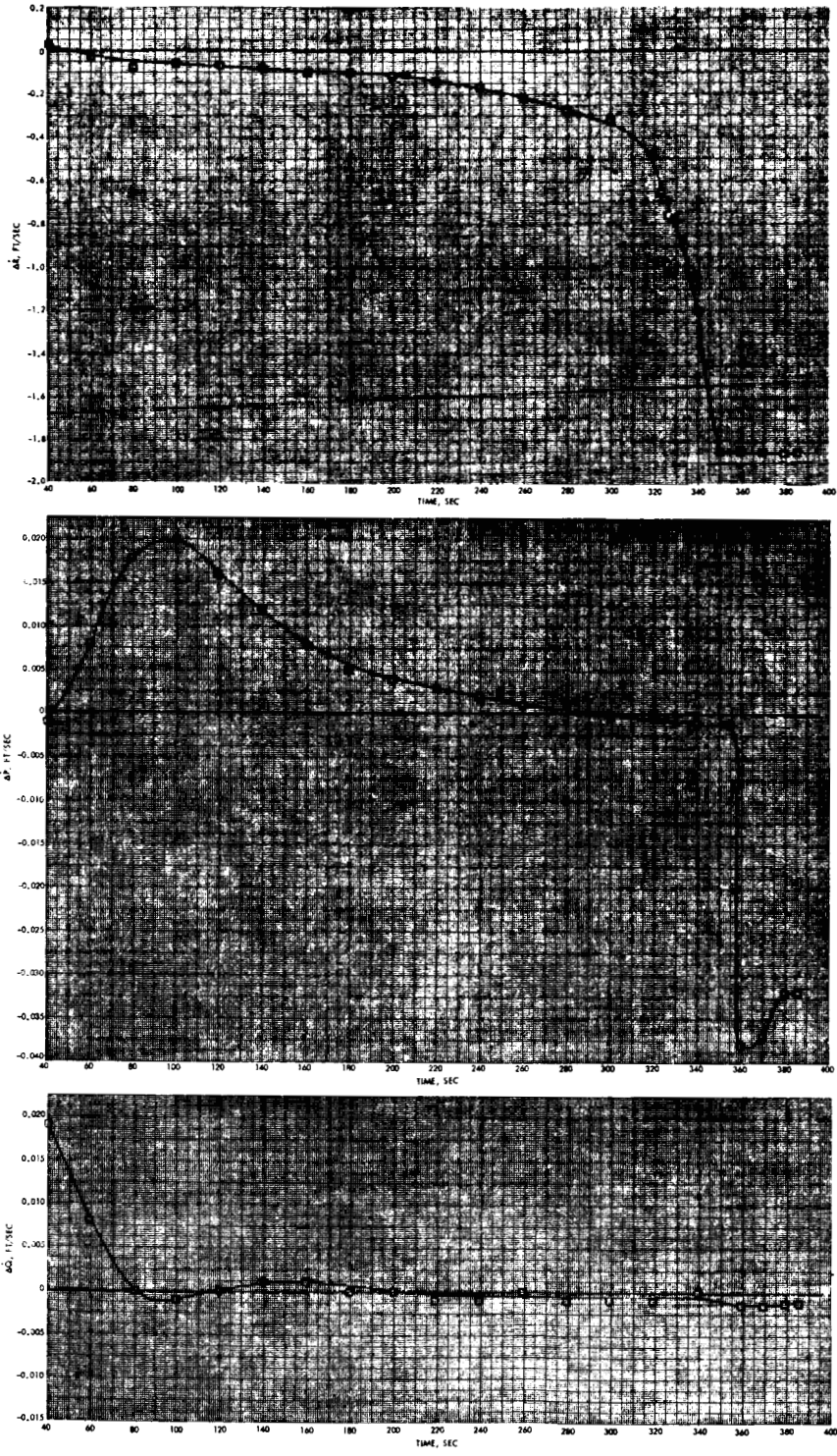


Figure C-2. GE MOD III Refraction Corrections
(Range Rate, P, and Q)

CONFIDENTIAL

REFERENCES

1. F. B. Lavenhar, "Preliminary Gemini G and C Data Reduction and Analysis Plan, " Technical Report 4160-6009-TU-000, TRW Systems, 30 October 1964.
2. R. Sansom, "Gemini Inertia Measurement Unit Accuracy Prediction Study (U), " Technical Report 4160-6016-TW000, TRW Systems, 8 February 1965 (Confidential).
3. "Gemini 10 Orbit and Reentry Trajectory Reconstruction, " Technical Report 05952-6061-R000, TRW Systems, 14 November 1966.
4. "Final Flight Test Data MISTRAM Coordinate Systems No. 1 and 3, AFETR Test No. 3287," Gemini Missile No. GT-11, OD Item 9.2.1.3-20, AFETR Data Reduction, no date.
5. "Final Flight Test Data Best Estimate of Trajectory Coordinate Systems No. 1 and 3, AFETR Test No. 3287," Gemini Missile No. GT-11, OD Item No. 9.2.1.3-26.
6. "NASA Gemini Mission Program Report, Gemini 11 (U) MSC-G-R-66-8, November 1966 (Confidential).
7. "Flight Test Report MOD III Guidance System With Gemini Launch Vehicle 10" Range Test No. 6833 Gemini Titan 10 (U), dated 18 July 1966, General Electric Company.

(Reverse of this page is intentionally blank.)